UNIVERSITY OF INSUBRIA

Doctoral School of Biological and Medical sciences
Ph.D. Program in Neurobiology
XXV Cycle

PARKINSON'S DISEASE BIOMARKERS IN PERIPHERAL BLOOD T LYMPHOCYTES: IDENTIFICATION THROUGH A PROTEOMIC APPROACH

Tutor:
Prof. Mauro Fasano

Coordinator:
Prof. Daniela Parolaro

Ph.D. thesis of:
Agnese Chiara Pippione

Table of contents:

Abstract

Parkinson's disease (PD) is a progressive movement disorder characterized by degeneration of dopaminergic neurons of the substantia nigra pars compacta (SNpc). The mean age of PD patients at the onset of motor signs is in the seventh decade of life (prevalence is about 1% at age 65, 5% at age 85), but an estimated 3% of cases are initially recognized in individuals younger than age 50. PD is mostly sporadic, although genetic forms of the disease are known. In particular, 20% of PD cases are genetic forms, and are found more frequently in patients with onset before 50 years.

The diagnosis is currently based on clinical manifestations of the disease, but 70% of nigral neurons are lost when symptoms appear. Late diagnosis hampers clinical development of new disease-modifying therapies; only alleviating symptoms is possible at present. For this reason, great interest in developing peripheral biomarker for PD has increased. In particular, such biomarker should be: (1) specific for PD, (2) able to monitor the progression of the disease, (3) providing no discomfort for the -potential- patients, (4) available at an accessible cost for a population screening.

The immune system may possibly reflect specific mechanisms of PD pathogenesis occurring at the central level. In fact, peripheral blood cells have been shown to share some of the changes exhibited by nigral neurons. In particular, T-lymphocytes express some features of the dopaminergic system: they express dopamine receptors, membrane and vesicular transporters, they store catecholamines into vesicles and - only the T regulatory subset - release it as co-stimulatory signal for other immune cells.

On this basis, our group proposed that T-lymphocytes may constitute an amenable and easily accessible source of peripheral biomarkers for PD, where the dopaminergic system is impaired. In particular, patients affected by familial forms of PD (about 20% of all PD cases) may express, also at the peripheral level, genetic alterations that mirror the pathogenic process at the central level.

To investigate differences between patients and people not affected by PD, we used a global and unbiased approach: the proteomic approach permitted us to gain a view of T lymphocytes' proteome and to compare cells from patients and control subjects (healthy people or people affected by other disorders).

We enrolled 15 PD patients and 17 control subjects (14 healthy subjects and 3 affected by atypical parkinsonisms). The group of patients was enriched with Early Onset PD patients, who have a greater probability to be affected by a genetic form of the disease, in order to highlight possible effects due to the genetic background. All subjects underwent a venous blood sampling, then T-lymphocytes were collected and isolated. Protein expression differences were evaluated using two-dimensional electrophoresis (2-DE).

A statistical analysis was conducted in order to (1) find significant differences between patients and control subjects, (2) calculate a function that, taking into account contributes of changing spots, was able to rightly predict patients and controls, (3) identify spots correlating with other parameters of disease: duration, gravity of symptoms, age at onset.

Wilcoxon test was applied on spots from maps of PD patients and control subjects, after elimination of spots correlating with confounding factors such as therapy and age; we found 20 proteins whose level was significantly different in PD patients and controls ($p<0.05$): their relative volumes were combined by Linear Discriminant Analysis so to obtain a likelihood score (PD Score) for each subject. PD scores were significantly different in PD patients with respect to control subjects (Wilcoxon test, $p < 10^{-8}$); performance of the model was tested with the leave-one-out method (87% sensitivity, 81% specificity). We eliminated from the dataset those spots whose contribution to the LDA function was lower and we obtained a better model with 100% sensitivity and 94% specificity. A third model with a lower number of spots has been proposed (100% sensitivity and 88% specificity).

These 20 spots were also evaluated for the occurrence of correlation with time or disease severity, in order to propose biomarkers of PD progression. Correlation with the Hoehn and Yahr score (parameter used to assess gravity of symptoms) was observed for 8 spots; 4 spots correlate with duration (years of disease). Both the correlations were evaluated as Pearson linear correlation ($r = 0.603$, $p < 0.0005$ and $r = 0.548$, $p = 0.001$, respectively).

Also the parameter “age at onset” was evaluated: we divided patients into two groups: early onset PD patients (EOPD, age at onset before 45 years) and late onset PD patients (LOPD, age at onset after 45 years), than we compared the two groups: we found 7 quantitative protein differences (Wilcoxon test, $p = 0.006$).

All the spots of the models or showing correlation with one of the mentioned parameters were excised from the gels and identified by LC-MS/MS fragmentation: some of the most important and recurring identification were beta fibrinogen and transaldolase; in particular,

4 spots correspond to beta fibrinogen and 2 spots correspond to transaldolase; all together, these 6 spots contribute to the prediction model in a very remarkable way.

For this reason, we validated by Western blot total beta fibrinogen and transaldolase changes to verify their proper identification and confirm the differences observed by 2-DE with another technique (Western blotting).

Worth of note, the level of some proteins was modified by levodopa and dopamine agonists therapy in T lymphocytes: this is a demonstration that these cells are sensitive to long term dopaminergic stimulation and that they are a valid tool to investigate dopaminergic imbalance at a peripheral level.

Additional experiments were conducted in order to deepen the role of fibrinogen in T cells, and the reason why its volume is reduced in PD patients: this study is currently going on, but preliminary results indicate that it is internalized by T cells from plasma.

In conclusion, in this thesis T lymphocyte proteome changes have been shown to be a valid tool to recognize and classify PD patients. It has been proposed a model using a rationale of similarity between affected cells (dopaminergic neurons) and probed system (T lymphocytes): we expect that our system will reasonably provide information on the effectiveness of future (or under development) drugs designed to interfere with specific cell death mechanisms targeting nigral neurons. Moreover, our system possess most features required for candidate PD biomarkers (specificity, indication of progression, accessibility).

Next step of this research is leading the current finding to the clinical practice. This objective will be reached only through large collaborative networks, that will allow us to select large cohorts of subjects with high heterogeneity in terms of gender, age, ethnicity, clinical phenotype; the use of a different and less time consuming technique in the clinical phase is advisable.

1. INTRODUCTION

1.1 PARKINSON'S DISEASE

Parkinson's Disease (PD) is the second most common movement disorder after Alzheimer's disease, affecting about 6 million people worldwide (Shulman et al., 2011).

PD is typically a chronic and slowly progressive disorder. Cardinal manifestations include resting tremor, bradykinesia (slowed movements), rigidity (increased muscular tone), postural instability, and gait impairment. They are attributable to dopaminergic cell loss within the substantia nigra pars compacta (SNpc) and resultant dysfunction of the basal ganglia, a cluster of deep nuclei that participate in the initiation and execution of movements (Shulman et al., 2011).

In the later stages of the disease the symptoms are accompanied by postural instability and, in some cases, by cognitive impairment. As PD progresses, other symptoms like pain, sensory complaints, autonomic dysfunction, neuropsychiatric manifestations (depression, hallucinations, and dementia) become prominent: these features are probably due to the spread of pathology beyond the basal ganglia (Jankovic 2008).The progression of the disease is evaluated through clinical parameters. The Unified Parkinson's Disease Rating Scale (UPDRS) was developed as an effort to incorporate different elements of PD impairment and disability. It is divided into four components: Part I, mentation, behavior and mood; Part II, activities of daily living; Part III, motor; Part IV, complications (Goetz et al., 2007). A simplified way to clinically evaluate PD stages is the Hoehn and Yahr scale, modified by the Movement Disorder Society Task Force for Rating Scales for Parkinson's disease (Goetz et al., 2004) (Table 1).

Table 1: Modified Hoehn and Yahr scale. Point 1.5 and 2.5 were inserted in revision of 2004 with respect to the original scale published in 1967 (Goetz et al., 2004).

Modified Hoehn and Yahr scale	
1.0	Unilateral involvement only
1.5	Unilateral and axial involvement
2.0	Bilateral involvement without impairment of balance
2.5	Mild bilateral disease with recovery on pull test
3.0	Mild to moderate bilateral disease; some postural instability; physically independent
4.0	Severe disability; still able to walk or stand unassisted
5.0	Wheelchair bound or bedridden unless aided

1.1.1 Epidemiology

With a prevalence of approximately 1% at age 65, which rises to nearly 5% at age 85, PD is the second most common neurodegenerative disorder after Alzheimer's disease (Shulman et al., 2011).

A number of epidemiological factors have been proposed to increase PD risk:

- age: PD can be diagnosed at any age, but the mean age of PD diagnosis is in the seventh decade of life; only an estimated 3% of cases are initially recognized in individuals younger than age 50 (Shulman et al., 2011). In a epidemiological study carried on the basis of data from Kaiser Permanente Medical Care Program, Northern California, it has been shown how the incidence rates rose rapidly after the age of 60 years, going from 0.50 per 100,000 in the fourth decade to 107.2 per 100,000 in the eighth decade (Van Den Eeden et al., 2003).
- Gender: there is a greater incidence of PD in men than in women; rate ratios of different studies have been compared in two meta-analysis, which reported similar age-adjusted male:female incidence of 1.49 (95% confidence interval (CI) 1.24–1.95, $p = 0.031$) and 1.46 (95% CI 1.24–1.72, $p < 0.001$) (Pavon et al., 2010). Neuroprotective effects of estrogens have been suggested as a possible explanation for this difference in gender incidence, but their role is still controversial (Saunders-Pullman 2003; Cordellini et al., 2011).
- Family history: about 20% of PD subjects reported a positive family history; more details are presented in the chapter "Genetics".
- Occupational exposures: in 1983 it was surprisingly discovered that the toxin MTPT was able to selectively damage dopaminergic cells in the Substantia Nigra and induce typical signs of PD in humans; some pesticides and herbicides, like rotenone and paraquat, have been found to have the same mechanism of action of MTPT in animals (Betarbet et al., 2000). Since then, many epidemiological studies have been done to examine the association between exposure to such substances, as well as hypothesized surrogate measures, such as farming, living in rural areas, and drinking of well water, and the risk of PD. The relation between (self-reported) pesticide exposure and plantation work and PD has only been examined prospectively in one large study among men (Petrovitch et al., 2002). A significantly increased risk of PD was found among men who worked for more than 10 years on a plantation, and a non significant association for men exposed to pesticides.
- Dietary and habitual factors: both cigarette smoking and coffee consumption are associated with reduced PD susceptibility (de Lau and Breteler, 2006).

Ultimately, however, epidemiological association does not necessarily imply causation, but the potential yield of these cohort studies is of high importance in better understanding mechanisms of pathogenesis, (Shulman et al., 2011) and potentially evaluating individual predisposition to PD.

1.1.2 Pathology and pathogenesis

The cardinal neuropathological feature of PD is dopaminergic cell loss within the SNpc. Because dopaminergic cells contain melanin, cell loss within the SNpc is accompanied by depigmentation of the midbrain, that is readily visible in gross material postmortem. Surviving neurons appear rich in intracytoplasmic inclusions termed Lewy Bodies (Spillantini and Goeder, 2000).

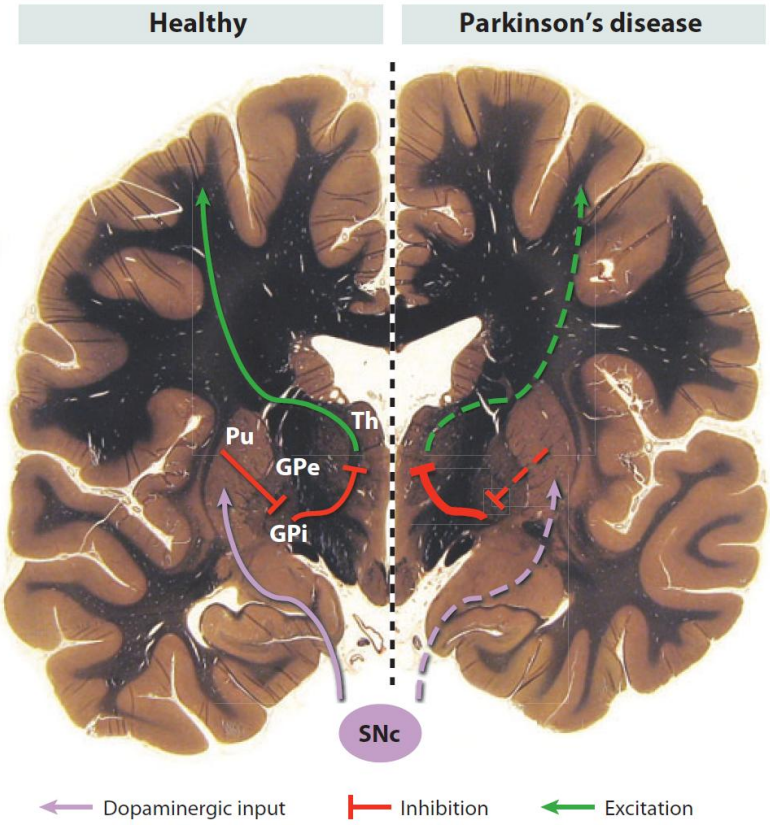

Fig. 1: Anatomy and physiology of PD motor manifestations. A simplified schematic of the neuronal circuits involving the basal ganglia, thalamus, and cortex and their derangement in PD. It normally functions to facilitate movements (*left*), but in PD the output is attenuated (*right*). The midbrain substantia nigra pars compacta (SNc) provides dopaminergic input to the putamen (Pu), which is excitatory to the direct pathway. The putamen inhibits (*red*) the globus pallidus interna (GPi), which subsequently inhibits the thalamus (Th). The thalamus projects excitatory input (*green*) to the motor cortex. In PD, degeneration within the SNc leads to net increased inhibition of the thalamocortical projection. Taken from Shulman et al., 2011.

Dopaminergic neurons in the SNpc project primarily to the striatum, (Fig. 1) therefore, nigral cell loss result in the depletion of striatal dopamine. Decreased nigrostriatal input leads to a net increase of inhibitory output from the globus pallidus interna to the thalamus and, indirectly, to the cortex, thereby repressing the initiation of movements and leading to the characteristic motor manifestations (Shulman et al., 2011).LB are spherical and eosinophilic inclusions, mainly composed by alpha-synuclein (α-syn) and extensively ubiquitinylated proteins. On autopsy, the brains of

individuals with PD are additionally characterized by α-synuclein-positive accumulations within neuronal processes, termed Lewy neurites (Spillantini and Goeder, 2000; Shulman et al., 2011). α-Syn is a small protein of 140 amino acids, whose function is not completely understood so far. Its conformation can range from unfolded state in solution, to α-helical in the presence of lipid-containing vesicles, to β-pleated sheet or amyloid structure in fibrils (McNaught and Olanow, 2006).

Given the positivity for α-syn in LB and Lewy neurites, and the fact that mutations in the α-syn gene cause rare familial forms of PD (see below), it was initially suggested that the accumulation of α-syn might cause the selective degeneration of dopaminergic neurons (Thomas and Beal, 2007; Fasano and Lopiano, 2008). On the other hand, α-syn expressed at low levels appears to be neuroprotective and anti-apoptotic in dopaminergic neurons, indicating a dual role for this protein (Colapinto et al., 2006; Cookson 2006). Several lines of evidence suggest that the upregulation of α-synuclein represents a compensatory mechanism adopted by neurons to protect themselves from chronic oxidative stress (Alberio et al., 2010).Molecular mechanisms leading to degeneration of SNpc neurons are not fully understood. A number of evidences indicate some factors important for the final degeneration, but temporal and mechanistic relationships among them are not well characterized. Major factors have been identified as mitochondrial impairment, ubiquitin-proteasome dysfunction, altered calcium homeostasis and oxidative stress (Banerjee et al., 2009; Surmeier et al., 2010; Alberio and Fasano, 2011).

Nigral dopaminergic neurons are particularly susceptible to oxidative stress because of their exposure to a high oxidative load: first of all, the metabolism of dopamine gives rise to various molecules that can act as endogenous toxins and start the formation of oxygen reactive species (ROS). Normally, these species are eliminated by intracellular antioxidant systems, which might be impaired by aging or by specific alterations owing to the disease pathogenesis (Alberio and Fasano, 2011).

For instance, dopamine (DA), that is normally stored into acidic vesicles, can autooxidize to dopamine quinone and hydrogen peroxide when it is released into the neutral pH cytoplasm. The release is usually avoided, but it could occur when the system of vesicles is damaged; in this context, α-syn has a role in vesicular trafficking, and when α-syn is overexpressed and accumulate into the cells, it starts to aggregate into protofibrils (the toxic species) and fibrils (as observed in LB) (Bisaglia et al., 2010). Protofibrils are able to form pores through membranes of vesicles, permitting DA to exit and form cytotoxic hydroxyl radicals in a reaction catalyzed by iron, the levels of which are higher in SNpc than in other brain regions (Fasano et al., 2006). Moreover, dopamine quinone reacts with alpha-synuclein to form covalent adducts that slow the con-version of toxic protofibrils to fibrils, shifting the equilibrium of α- synuclein's forms into the most toxic one (Fasano et al., 2008).

Iron also seems to play a key role in the increased susceptibility of these pigmented, neuromelanin (NM)-containing neurons, and the dopamine-derived NM pigment appears to be a critical regulator of iron homeostasis (Fasano et al., 2006).

The increased susceptibility of dopaminergic SNpc neurons has also been associated to their morphology: they have long, thin, poorly myelinated and branched projections, thus accounting for a peculiar need for mitochondrial activity with a consequent higher ROS production (Thomas and Beal, 2007). Furthermore, dopaminergic SNpc neurons maintain their basic activity through L-type calcium channels instead of sodium channels, a situation that needs an increased ATP production to control calcium homeostasis and, at the same time, exposes cells to elevated mitochondrial oxidative stress (Surmeier et al., 2010).

Mitochondria are a major source of free radicals in the cell, causing the appearance or the increase of oxidative stress conditions. They also sequester calcium when intracellular calcium levels rise during the excitotoxic process. The threshold for excitotoxicity might decrease if mitochondrial ATP production is impaired. Mitochondria also have a pivotal role in apoptotic cell death: release of the pro-apoptotic factor cytochrome c, usually associated with the inner membrane of the mitochondrion, into the cytoplasm triggers a cascade of events, culminating in cell death (Henchcliffe and Beal, 2008). Strong evidence exists to support a role for aberrant mitochondrial form and function in the pathogenesis of PD (Schapira 2011): for instance, activity of the mitochondrial respiratory complex I (NADH-quinone oxidoreductase) is reduced in the substantia nigra of PD patients (Schapira et al., 1990). Another indication of mitochondrial implication in PD pathogenesis is given by genetic evidences of PD-causing mutations in genes of mitochondrial proteins (see below).

As a whole, in a disease where the etiology is still largely unknown, many of the genetic and environmental factors variously linked to it contribute to a redox imbalance that seems to have the strongest effect on the more sensitive dopaminergic SN cells (Alberio et al., 2012a).

1.1.3 Genetics

According to recent epidemiological studies, 10–30% of PD subjects reported a positive family history, and first-degree relatives of subjects with PD were estimated to have a twofold- to sevenfold-increased relative risk of PD. In many cases, penetrance is not complete, thus accounting for an intrinsic difficulty in their identification (Shulman et al., 2011).

Autosomal recessive forms of parkinsonism are linked to mutations in *parkin* (PARK2, the most common), *PINK1* (PTEN-induced putative kinase 1; PARK6), *DJ-1* (PARK7), *ATP13A2* (PARK9), *PLA2G6* (PARK14) and *FBXO7* (PARK15) genes, and are characterized by age at onset usually before 40 years. Worth of note, most genes responsible of three early-onset, autosomal recessive forms of PD (parkin,

PINK1, DJ- 1 and maybe ATP13A2) all belong to the pathway aimed at the elimination of damaged mitochondria. Carriers of these mutations display the upsurge of PD motor symptoms before 50 years of age and the available post-mortem studies often show an atypical PD pathology in that Lewy bodies (LB) may be absent (Shulman et al., 2011).

To what concerns autosomal dominant forms, mutations in six genes have been identified: *SNCA* (coding for α-syn; PARK1 for point mutations, PARK4 for duplication or triplication of the gene), *UCHL1* (ubiquitine C-terminal ligase L1; PARK5), *LRRK2* (leucine-rich repeat kinase 2; PARK8), *GIGYF2* (PARK11), *OMI/HtrA2* (PARK13) and the recently discovered *GBA*. (Gasser 2009; Shulmann et al., 2011; Alberio et al., 2012a). LRRK2 mutations are the most common cause of dominant familial PD, accounting for 1% of sporadic PD cases (Shulman et al., 2011).

Table 2. Parkinson's disease-related proteins. Gene and protein names are indicated for genetic PD forms. For gene products, official Uniprot protein names are listed. Proteins are cited in the text using their aliases. Adapted from Alberio et al., 2012a.

PARK locus	**Gene name**	**Gene product**	**Alias**
PARK1 / PARK4	SNCA	Alpha-synuclein	α-synuclein
PARK2	PARK2	E3 ubiquitin-protein ligase parkin	PARKIN
PARK5	UCHL1	Ubiquitin carboxyl-terminal hydrolase isozyme L1 (UCH-L1)	UCH-L1
PARK6	PINK1	Serine / threonine-protein kinase PINK1	PINK1
PARK7	PARK7	Protein DJ-1	DJ-1
PARK8	LRRK2	Leucine-rich repeat serine / threonine-protein kinase 2	LRRK2
PARK9	ATP13A2	Probable cation-transporting ATPase 13A2	ATP13A2
PARK11	GIGYF2	PERQ amino acid-rich with GYF domain-containing protein 2	GIGYF2
PARK13	HTRA2	Serine protease HTRA2 (HtrA2)	HtrA2
PARK14	PLA2G6	85 kDa calcium-independent phospholipase A2 (IPLA2)	IPLA2
PARK15	FBXO7	F-box only protein 7	FBXO7
PARK17	VPS35	Vacuolar protein sorting-associated protein 35 (hVPS35)	hVPS35
PARK18	EIF4G1	Eukaryotic translation initiation factor 4 gamma 1 (EIF-4G1)	EIF-4G1
Gaucher's locus	GBA	Glucosylceramidase	GBA

Although the different mutations and loci identified so far appear to be directly responsible in only a relatively small number of families each, there is accumulating evidence that the molecular pathways

identified may be common to more than one genetic form of PD and may also play a role in the common sporadic disease (Gasser 2009).

Worth of note, patients with onset before age 45 (Early Onset PD Patients, EOPD) have more frequently a positive family history, and consequently an increased likelihood of a genetic etiology compared with patients with late-onset PD (LOPD), though also late-onset PD may have a substantial familial component (Payami et al., 2002).

1.1.4 Therapy

Motor symptoms respond well to dopamine replacement therapy, which has been the pillar of PD treatment since its introduction (late 1960). Although currently available PD therapies both delay disability and prolong life expectancy, none has been proven to significantly alter the ongoing neurodegenerative process (Rascol et al., 2011).

The dopamine precursor L-dihydroxyphenylalanine (L-DOPA) represents the most effective treatment. The addition of a peripheral dopa decarboxylase inhibitor enhances the therapeutic benefit of L-DOPA and prevents peripheral effects. However, chronic oral treatment with L-DOPA is associated with the development of motor complications: fluctuations in motor performance, reflecting rises and falls of L-DOPA plasma levels ("on"/"off" states), L-DOPA induced involuntary movements and painful dystonia. The exact pathophysiology of these L-DOPA related motor complications still remains incompletely understood (Rascol et al., 2011). Improvements in pharmacokinetic have been reached with continuous duodenal L-DOPA infusions (Kurlan et al., 1986), but system-related complications such as occlusions or dislocation of catheters, local inflammation around the gastrostomy site, and mechanical pump problems, together with high costs, still limit the broad-scale use of this approach (Rascol et al., 2011).

Another important category of antiparkinsonian drugs is represented by dopamine agonists, which can be used as monotherapy or in combination with L-DOPA. They exert their action by directly activating DA receptors , bypassing the presynaptic synthesis of DA. The activation of D2-like receptors (especially D3) is important for antiparkinsonian effects of dopamine agonists, although concurrent D1-like and D2-like stimulation is required to produce optimal physiological and behavioral effects (Jankovic and Aguilar, 2008). Some commonly used dopamine agonists in the clinical practice are Ropinirole, Pramipexole and Rotigotine.

Other strategies to prolong DA response make use of inhibitors of enzymes that metabolize dopamine, such as catechol-O-methyltransferase (COMT) and monoamine oxidase (MAO). When used in combination therapy, they extend the duration of action of L-DOPA. COMT inhibitors are used with caution because of hepatic side effects (Benabou and Waters, 2003).

Unfortunately, most nonmotor symptoms, that are due to degeneration of more diffuse areas than SN, show little or no response to dopamine replacement and contribute substantially to overall disability, especially late in disease. In advanced disease, direct modulation of basal ganglia activity via deep brain stimulators implanted in the subthalamic nucleus can also be effective (Shulman et al., 2011; Zibetti et al., 2011).

Although currently available PD therapies both delay disability and prolong life expectancy, none has been proven to significantly alter the ongoing neurodegenerative process (Shulman et al., 2011; Alberio and Fasano 2011).

1.1.5 Diagnosis

PD can be diagnosed at any age, but the mean age of PD diagnosis is in the seventh decade of life; however, due to PD's insidious nature, the onset of symptoms may precede clinical recognition by many years (Shulman et al., 2011). Given the aging population, the prevalence of PD is anticipated to increase dramatically, which would lead to increased urgency for the need to identify improved therapies that delay progression and mitigate disability.

The diagnosis is currently based on clinical manifestations of the disease, but 60% of dopaminergic neurons, which is paralleled by the loss of 80% of dopamine in the striatum, are lost when motor symptoms appear, rendering difficult protective or restorative therapies in a such advanced stage of neurodegeneration (Shulman et al. 2011).

Diagnostic features of PD are asymmetrical onset, rigidity, bradykinesia, unilateral tremor at rest and acute L-DOPA response. Additional non motor symptoms, such as impaired olfaction, disordered sleep and constipation appear several years before motor symptoms, but are unspecific and difficult to detect (Shulman et al., 2011). The picture is made more complicated by a large heterogeneity in terms of predominance of one of the motor symptoms over the others and in terms of disease progression. Misdiagnosis rate ranging from 10% (diagnosis performed by movement disorders experts) to 50% (as it is the case with primary healthcare) (Tolosa et al. 2006). The occurrence of tremor may be of iatrogenic or psychogenic origin, and patients affected by essential tremor are sometimes erroneously diagnosed as PD patients. Likewise, the occurrence of parkinsonian signs is common also in other neurodegenerative disorders, named atypical degenerative parkinsonisms (ATP) for the similarity of initial symptoms (Shulman et al., 2011).

These syndromes are less frequent than PD, and have different pathologies. The most frequent atypical parkinsonian disorders are progressive supranuclear palsy (PSP), corticobasal degeneration (CBD), multiple system atrophy (MSA) and dementia with Lewy bodies (LBD) .MSA is a rapidly progressive disorder consisting in prominent failure of the autonomic nervous system, including

urinary incontinence and orthostatic intolerance, accompanied by parkinsonism and/or cerebellar dysfunction and associated with glial α-syn inclusion pathology (Jecmenica-Lukic et al., 2012). PSP is a neurodegenerative tauopathy which can manifest clinically in a variety of syndromes, in particular one of them begin with same symptoms of PD and is responsive to L-DOPA (Boeve 2012).

Diagnosis is helped by molecular imaging with positron (PET) or single photon (SPECT) emission tomography. These techniques provide information on presynaptic dopaminergic function through emission of 6-[18F]fluoro-L-dopa (FD) or 6-[18F]fluoro-*m*-tyrosine (FMT), used as radiotracer of the vesicular monoamine transporter type 2 (VMAT2) and the plasmalemmal dopamine transporter (DAT). In PD, substantial reductions in tracer uptake is observed: while this pattern is typical of PD, it may be also seen in MSA and in parkinsonism associated with spinocerebellar atrophy, and is accordingly not sufficient to robustly differentiate PD from other akinetic-rigid syndromes. (Stoessl 2012).

Objective, accessible, and easily measurable biologic parameters, correlating either with the presence or the severity of PD, are a major prerequisite for a more refined diagnosis and the development of novel therapeutic strategies. Currently, there is no reliable biomarker for PD, neither markers exist to objectively measure the severity and the rate of progression of PD-related cellular dysfunction and neurodegeneration in the substantia nigra.

The availability of peripheral PD biomarkers would have a dramatic feedback (Fig. 2). They would allow the differentiation of susceptible individuals from normal ones before motor symptoms appear (early diagnosis), and would help the identification of true idiopathic PD from atypical degenerative parkinsonisms (differential diagnosis). Moreover, the differentiation of patients in terms of their response to a pharmacological treatment would be possible (therapy assessment) (Michell et al., 2004). It would be desirable to have available a panel of biomarkers that not only allow the diagnosis of PD at an early, pre-motor stage, but possibly correlate with the progression of the neurodegeneration progress. This would allow researchers to develop neuroprotective or neurorestorative agents and to follow directly their efficacy. Although restorative therapies are still far from actuality, clinical trials on new PD treatments cannot be foreseen in the absence of affordable biomarkers (Fasano et al., 2008).

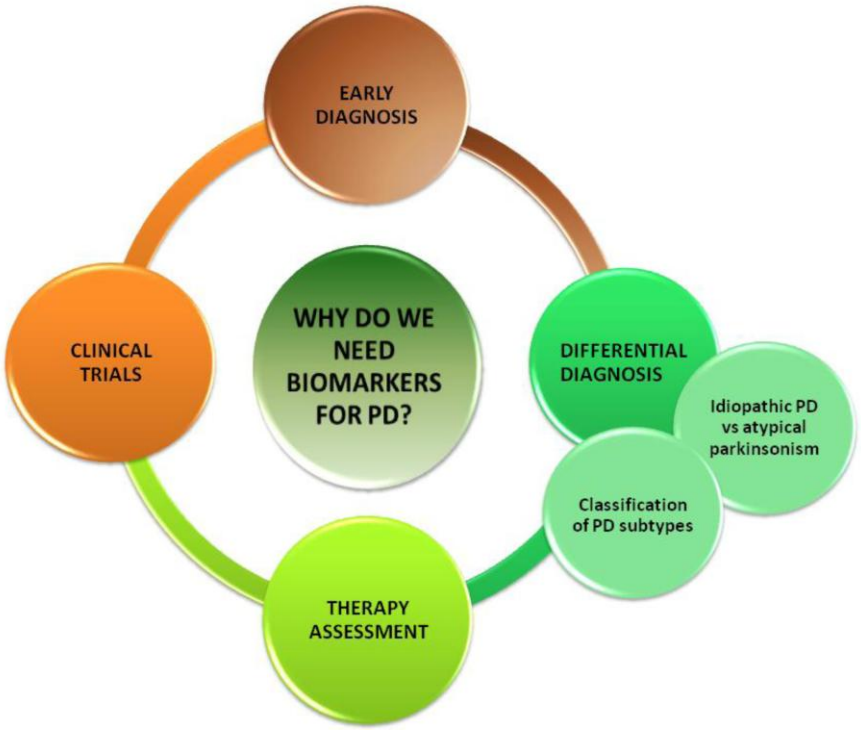

Fig. 2: Peripheral biomarkers are required to accomplish different tasks: early diagnosis, possibly at a pre-motor stage; differential diagnosis of parkinsonian syndromes and of PD subtypes that may require different therapeutic plans; assessment of a personalized therapeutic plan; objective measurement of the actual extent of neurodegeneration so that neuroprotective and/or neurorestorative interventions could be monitored (taken from Fasano et al., 2008).

1.2 A POTENTIAL SOURCE FOR BIOMARKERS OF PD: PERIPHERAL T LYMPHOCYTES

Besides of its action on the nervous system, DA has been identified in other organs and tissues, including the vascular beds, the hearth, the gastrointestinal tract, and the kidney. Moreover, a number of studies showed DA components in the immune system, and suggested that DA plays a key role on neural-immune interactions and immune cells in particular (Pacheco et al., 2009; Buttarelli et al., 2011; Sarkar et al., 2010).

1.2.1 The dopaminergic system in peripheral blood lymphocytes

The original discovery of endogenous DA in PBL was made by Bergquist et al. (Bergquist et al., 1994). The authors applied capillary electrophoresis, and subsequently electrospray ionization mass spectroscopy (Bergquist and Silberring, 1998), to quantify DA and its metabolites in peripheral blood lymphocytes (PBL). Moreover, they observed reduced catecholamine levels after pharmacological inhibition of tyrosine hydroxylase (TH), the rate-limiting enzyme in the synthesis of catecholamines, by α-methyl-p-tyrosine, suggesting direct synthesis of catecholamines by PBL, while intracellular DA levels were increased by exposure to extracellular DA, suggesting also the presence of an active cellular uptake mechanism. In a different study, it was shown that T-lymphocytes contained L-DOPA and norepinephrine, whereas B-lymphocytes contained only L-DOPA. (Musso et al., 1996).

Catecholamine (including DA) synthesis by human PBL was confirmed in 2004 (Qiu et al., 2004). Subsequently, Cosentino and coworkers showed that a subset of human T-lymphocytes, $CD4^+CD25^+$ regulatory T lymphocytes (Treg), but not other subtypes (*e.g.*, effector T-lymphocytes, Teff), constitutively express TH; moreover, they contain substantial amounts of DA, epinephrine and norepinephrine, which may be released upon treatment with reserpine (Cosentino et al., 2007).

Despite such converging evidence for the presence in PBL of catecholamines (of DA in particular), characterization of DA receptors has been more difficult. After many years of rather contradictory results, the presence of DA receptors in PBL was confirmed (McKenna et al., 2002).

Confocal laser microscopy demonstrated the presence and localization of vesicular monoamine transporter 2 (VMAT-2): its immunoreactivity was appreciable mainly in cytoplasmic puntiform areas, that were likely to correspond to vesicles, and to a lower extent was associated to plasma membrane, whereas DAT and VMAT-1 immunoreactivities were located almost exclusively in PBL plasma membrane and cytoplasm, respectively (Amenta et al., 2001).

1.2.2 Physiology and pharmacology of DA system in immune cells

By stimulating DA receptors expressed on PBL membrane, DA from diverse sources (plasma, sympathetic nervous system, autocrine or paracrine secretion by immune cells, CNS) may contribute to regulate the initiation and development of immune responses (Pacheco et al., 2009).

The stimulation of D1-like receptors, and the consequent increase of intracellular cAMP, determines the inhibition of cytotoxic $CD8^+$ cells, impairs function and differentiation of Treg cells, and induces polarization of naive $CD4^+$ cells toward T-helper 17 (Th17) phenotype (Besser et al., 2005). Because Th17 and Treg are involved in autoimmunity as auto-aggressive and beneficial cells respectively, it is likely that D1-like receptors expressed on T-cells are involved in the interface between autoimmunity and health. Interestingly, the decreased expression of D5 receptors in PBL has been found in patients suffering from multiple sclerosis (Giorelli et al., 2005).

D2-like receptors, which stimulation results in decreased intracellular cAMP, are also involved in the modulation of T-cells physiology: stimulation of D3 receptors controls T-cell adhesion and migration and induces differentiation of naive $CD8^+$ cells into cytotoxic T-lymphocytes (Besser et al., 2005); on the other hand, it also contributes to polarization of naive $CD4^+$ cells toward T-helper 1 phenotype (Ilani et al., 2004). Eventually, D2 and D4 receptors regulate the activation and differentiation of naive $CD4^+$ cells, for example, by promoting the polarization toward Treg cells (D2) or by triggering T-cell quiescence (D4) (Pacheco et al., 2009; Sarkar et al., 2010).

1.2.3 Changes of PBL dopaminergic system in PD

Following the characterization of the DA system in human PBL, the question raised of whether PBL may represent a useful cellular model with which to investigate the derangement of DA transmission in patients suffering from neurological or psychiatric disorders. Because of the prominent role of DA derangement in parkinsonian syndromes, most studies were centered on PD. Nagai reported the statistically significant decrease of the D3 receptor mRNA expression in PBL from PD patients (Nagai et al., 1993), while Barbanti showed that PBL from PD patients have a higher density of both D1-like and D2-like binding sites than those of neurological or healthy control subjects (Barbanti et al., 1999). Reduction of intracellular DA concentration and TH immunoreactivity in PBL from PD patients with respect to healthy subjects has been observed as well as reduction of DAT immunoreactivity in PBL from *de novo* PD patients (Caronti et al., 1999).

Regarding protein level alterations in PBL, a preliminary investigation on PBL of advanced PD patients has demonstrated that a proteomic profiling based on 2-DE highlights differences at the peripheral level between patients and control subjects. This panel of proteins included cofilin 1, a basic actin variant, ATP synthase beta subunit, tropomyosin and gamma-fibrinogen (Mila et al., 2009).

Taken together, the results from a number of studies support the hypothesis that PBL may represent a useful tool for investigating the changes of DA system in CNS pathologies, as well as to monitor the consequences of pharmacological manipulations of DA transmission (Alberio and Fasano, 2011). This is particularly relevant in the case of patients carrying a familiar form of the disease, in which gene expression of patterns implicated in pathological mechanisms damaging selectively dopaminergic neurons could be appreciated also in peripheral dopaminergic cells. T lymphocytes are the population of immune cells that better could reflect some of the alterations that impair the function of SNpc dopaminergic neurons at a peripheral level, because they express some dopaminergic features (receptors, transporters, vesicles) and because DA plays an active role in their functions, as activation and differentiation of various T subtypes into other ones (Pacheco et al., 2009).

1.3 THE PROTEOMIC APPROACH

Proteomics is the study of both the structure and function of proteins by a variety of methods. Originally proposed as the protein complement of the genome, the proteome assumed in more recent times a more functional significance (Alberio and Fasano, 2011). No limitations are set in terms of cellular functions or specific signal transduction pathways, thus enabling the investigation of proteins that are not a priori expected to be linked to any condition. Intrinsically, proteomics is an unbiased approach, aimed at generating a list of candidate proteins deserving further targeted studies. Such a global approach allows to manage with the great complexity of the system being investigated, thus overcoming limits of conventional biochemistry or molecular biology tools (Villoslada et al., 2009).

One of the major issues in clinical proteomics studies is the investigation of alterations in protein abundance and post-translational modifications eventually related to pathological conditions: the development of quantitative proteomics, aimed at the measurement of quantitative changes in the protein profile of the biological system under investigation, has stimulated great interest in applying proteomics to study mechanisms of diseases and biomarker discovery (Caudle et al., 2010; Alberio and Fasano, 2011).

Technologies used in proteomic research include two-dimensional gel electrophoresis (2-DE), mass spectrometry and bioinformatics; a single proteomic technology is not able of resolving all the highly analytical difficulty for global identification, quantitation and characterization of a complex proteome, but the combination of separation technologies with mass spectrometry results particularly successful in characterizing whole proteome of a chosen system (Alberio and Fasano 2011; Rotilio et al., 2012).

1.3.1 Gel-based methods

1.3.1.1 2D-PAGE

Two-dimensional electrophoresis (2-DE), developed in the 1970s, is the first approach and probably still the most frequently used technique to separate complex protein mixtures prior to downstream protein characterization by mass spectrometry (Gorg et al., 2004). Complex protein mixtures are separated on the basis of the isoelectric points along a pH gradient using isoelectric focusing (first dimension) and further of the apparent molecular mass using SDS-PAGE (second dimension) on a polyacrylamide gel, under the application of an electric field. After electrophoresis separation and gel

staining for protein visualization, image analysis is performed using one of the several software packages currently available, specifically designed to match protein spots of different gels, compare protein patterns and detect protein changes, both qualitative (presence/absence) and quantitative (spot intensities).

2-DE delivers gels that are at the same time an image of protein distribution and levels, and a container of separated proteins available for further characterization (Görg et al., 2004). One of the main strengths of 2-DE is the ability to visualize protein processing and modification-associated isoforms due to post-translational modifications. Specific fluorescent staining facilitates the specific detection and identification of relevant PTMs such as glycosylation and phosphorylation of proteins separated in 2-DE gels (Jacob and Turck, 2008).

Nevertheless, there are intrinsic weaknesses in 2-DE. Due to the reduced dynamic range of the detection technique, less represented proteins are lost, thus limiting the global characteristic of the proteomic approach. Moreover, proteins of extreme hydrophobicity and those of extreme basic or acidic pI are not considered in the majority of published studies (Wilkins 2009). To circumvent these limitations a number of network enrichment procedures were proposed to complete the list of proteins that could have changed in level, but were not observed for intrinsic technical limitations.

Interestingly, the dynamic range does not differ so much in gel-based and gel-free proteomic approaches (Miller et al., 2006; Schulze and Usadel, 2010). Although there is a strong technological push towards gel-free techniques, 2-DE continues to be highly preferred for its capacity to resolve thousands of spots simultaneously and represents the only technique that can be routinely applied for parallel quantitative expression profiling of large sets of complex protein mixtures such as whole-cell lysates (Görg et al., 2004; Alberio and Fasano, 2011).

1.3.1.2 DIGE

Differential in-gel electrophoresis (DIGE) permits the simultaneous separation of up to three samples on a single gel. In DIGE, samples - usually two samples and one internal standard - are covalently labeled with three separate fluorescent dyes, each with a unique excitation/emission wavelength, then combined and run together on the same 2D gel (Unlu et al., 1997). Labeling with DIGE fluorophors is extremely sensitive, capable to detect as little as 150 pg of a single protein with a linear response in protein concentration over five orders of magnitude (Sapra 2009). In addition, this method reduces the number of gels needed for an experiment, however the relative high cost of the equipment, software and chemicals also limit a wide application of the technique.

1.3.1.3 Gel staining

The most commonly employed methods to visualize proteins after 2-DE are Coomassie and silver staining, both compatible with downstream mass spectrometric analyses (Shevchenko et al., 1996) and whose limits of detection are at picomole and femtomole order, respectively (Miller et al., 2006). Silver staining is approximately 100 times more sensitive than Coomassie, but it is lengthy and quite laborious, prone to lab-to-lab variability and less reproducible due to the subjective end-point of the staining procedure. Moreover it has a narrow linear dynamic range and limits subsequent protein analysis by mass spectrometry due to protein cross-linkage (Görg et al., 2004). Colloidal Coomassie dispersions (Neuhoff et al., 1988; Candiano et al., 2004) are more sensitive than the classical Coomassie stain, but are still less sensitive than the majority of chemical stains employed in 2-DE for proteomics (Görg et al., 2004). The development of fluorescent protein dyes with sensitivity comparable to silver stain, wide linear dynamic range and compatible with mass spectrometry analysis largely improved the comparison of protein amounts in 2-DE gels (Miller et al., 2006). Several fluorescent dyes are commercially available, such as Nile red, SYPRO Red, SYPRO Orange and SYPRO Tangerine, but the ruthenium-based dye SYPRO Ruby seems the most suitable for proteomic applications (Berggren et al., 2000; Rabilloud et al., 2001). Sensitivity is similar to that obtainable with silver staining (Berggren et al., 2000; Rabilloud et al., 2001), being the detection limit in the range of the femtomole and the linear dynamic range of quantitation of about three orders of magnitude, thus overcoming both silver and Coomassie stains in performance. Synthesis and application of the metal chelate ruthenium(II) tris(bathophenanthroline disulfonate) (RuBPs), an economic and patent-free compound, has been described and compared with its commercial analogue SYPRO, demonstrating its similar detection limit and dynamic range (Rabilloud et al., 2001).

1.3.1.4 Protein identification by mass spectrometry

Upon separation by 2-DE and staining, gel images can be analyzed and spots of interest are cut and destained to prevent staining interference with mass spectrometry analysis. Then, the proteins are digested within the gel in order to obtain small peptides (up to 20 residues long). Several digestion enzymes can be used to this purpose, but trypsin is the most common, as it very specifically cleaves proteins at the C-terminal side of lysine and arginine and generates peptides in the preferred mass range for subsequent mass spectrometry analysis (about 500 to 4000) (Steen and Mann, 2004; Gromova and Celis, 2006). Processed proteins are identified using one of the mass spectrometry techniques described below, usually MALDI-TOF peptide mass fingerprinting (PMF) or LC-MS/MS.

1.3.2 Gel-free methods

1.3.2.1 MALDI-TOF

Matrix-assisted laser desorption/ionization-time of flight (MALDI-TOF) is a fast and user-friendly mass spectometric technique, has good mass accuracy, high resolution and sensitivity. It is widely used in proteomics to identify proteins from simple mixtures, as the ones derived either by 2DE or DIGE gel spots (Rotilio et al., 2012). In the MALDI ion source samples are co-crystallized with an organic matrix on a metal target. A pulsed laser is used to excite the matrix, which causes rapid thermal heating of the molecules and eventually desorption of ions into the gas phase. After ionization the samples reach the TOF mass analyzer, where ions are separated on the basis of their mass-to-charge (m/z) ratios. Ion motion in the mass analyzer can be manipulated by electric or magnetic fields to direct ions to a detector, which registers the ion current at each individual m/z value (Balluff et al., 2011). Based on this TOF information, a characteristic spectrum is recorded and constitutes a list of peptide mass values, that is compared with those obtained by virtual digestion of all protein sequences in a reference database (e.g, Uniprot; see Wieser et al., 2012).

The main limitations of the MALDI-based PMF approach are: i) it is not reliable for organisms whose genomes have not been completely sequenced and annotated; ii) it cannot identify proteins post-translationally modified, since the peptides generated from these proteins may not match with the unmodified protein in the database, iii) it does not work well if several different proteins are present in the same spot.

1.3.2.2 LC-MS/MS

In LC-MS/MS peptides generated from the digestion of complex mixtures of proteins or single spots derived by 2DE gels are separated on the basis of hydrophobicity by microscale liquid chromatography and introduced into the mass spectrometer, in most of the cases directly via online electrospray ionization (ESI).

During ESI ionization the liquid samples flow through a thin needle at the end of the capillary chromatography column and form small drops. Desolvated ions are generated by desorption of analyte ions from the droplet surface due to high electrical fields. Peptides are then transferred into the mass spectrometer and detected over a wide m/z range; then, single peptide species are isolated within the mass spectrometer, usually via a quadrupole mass filter and subjected to collision-induced dissociation, resulting in a ladder of peptide fragments, which are detected in a second mass spectrum. Peptides' sequences are blasted in sequence databases (for example PeptideSearch, Sequest, Mascot) but only whose having sufficient information to match uniquely to a pre-registered peptide sequence (on the basis of the observed and expected fragment ions) contribute to identify the original protein (Steen and Mann, 2004). The ESI source can be coupled to several mass

analyzers, such as quadrupole, ion trap, orbitrap or Fourier transform ion cyclotron resonance system, whose accuracy and sensitivity is extremely different (Yates et al., 2009).

1.3.2.3 Stable isotope labeling

Stable isotope labeling by amino acids in cell culture (SILAC) incorporates isotopic labels into proteins via metabolic labeling in the cell culture itself, instead of using covalently linked tags. Cell samples to be compared are grown separately in media supplied with either a heavy or light form of an essential amino acid, which cannot be synthesized by the cell itself. This makes proteins from the light and heavy cells distinguishable and differentially quantifiable by MS (Ong et al., 2002).

A new quantitative method, isobaric tags for relative and absolute quantitation (iTRAQ), has been developed and can be used to profile up to eight different samples (Ross et al., 2004). In contrast to the majority of other labeling procedures, iTRAQ relies on quantification at the MS/MS level rather than at the MS level. To this purpose, peptides are derivatized with an amine-reactive tagging reagent that is available in eight isotope-coded variants, all with an identical molar mass (isobaric). In this way, the derivatized peptides are indistinguishable in MS, but exhibit intense low-mass MS/MS signature ions that support quantitation. In a comparison of methods for stable isotope labelling and DIGE, iTRAQ was reported to be more sensitive for quantitation, but more susceptible to errors in precursor ion isolation. (Wuvet al., 2006).

1.3.3 Omics discovery of PD biomarkers

According to FDA, biomarkers are “any characteristic that can be objectively measured and evaluated as an indicator of normal biological processes, pathogenic processes or pharmacological responses to therapeutic interventions” (Biomarkers Definitions Working Group, 2001). The definition includes, though it is not limited to, the measurement of biochemical components in body fluids and tissues.

Compared to other areas of clinical interest, biomarker research in PD is still in its early stages of both discovery and validation, despite of their need for clinical development of new disease-modifying therapies and for an optimal patient stratification (Alberio and Fasano, 2011). It has to be taken into account the great heterogeneity of PD patients, that requires to enroll a large number of patients and of suitable controls, including patients affected by non-PD neurodegenerative disorders (Robinson 2010). Moreover, the selection of the appropriate biofluid to search for biomarkers appears a fundamental issue (Fasano et al., 2008).

Several groups attempted to diagnose PD on the basis of the measurement at the peripheral level of a single protein or gene transcript, however these proposed tests lacked sufficient sensitivity and specificity, or were not confirmed by others (Alberio and Fasano, 2011; Gerlach et al., 2012).

Recently, a panel of four gene transcripts, selected on the basis of their altered transcription at the nigral level, was measured in total blood cells of a large group of sporadic PD patients (n = 105) with respect to a smaller group of control subjects (n = 34) (Grunblatt et al., 2010). Although performance parameters of this model were good, it is unlikely that genes are differentially expressed both at the peripheral and at the central level. Likewise, measurement of α-synuclein, tau and total protein concentrations in CSF of patients with PD (n = 51), AD (n = 62), DLB (n = 55), MSA (n = 29) and non-neurodegenerative neurological disorders (n = 76) allowed Mollenhauer and coworkers to define a very accurate predictive model: value of area under the ROC (receiver operating characteristic) curve (ROC AUC) is 0.909 for the training set, but in a subsequent validation phase displayed a ROC AUC = 0.706 for the classification of PD patients (n = 257) and neurological control subjects (n = 47) (Mollenhauer et al., 2011). Despite the impressive number of patients and the strong rationale behind the search for PD biomarkers in CSF, it appears that the association of a small number of targets does not grant a satisfactory performance when a cross-validation is performed. Eventually, one must consider the discomfort for the patient to undergo a CSF sampling.

Unbiased discovery studies that use proteomic or metabolomic techniques have the great advantage to identify a larger panel of targets to be included in the predictive model, and to explore a greater universe of candidates without limiting to those that have been related to pathogenesis, as it is the case with the metabolomic profiling of plasma proposed by Bogdanov correctly classified PD patients (n = 66) and control subjects (n = 25) in a cross-validation procedure by permutation test (Bogdanov et al., 2008).

As a whole, a general procedure can be put forward for the outcome of a biomarker discovery project: (i) a suitable model should be proposed on the basis of a strong rationale, as a biomarker discovery strategy; (ii) subject enrolment conditions should be set on the basis of the given rationale; (iii) proteins that are significantly correlated with the conditions set at point (ii) need to be unambiguously identified; (iv) a new set of biomarker candidates coming up from this approach should be independently confirmed; (vi) eventually, the cohort of subjects should be re-evaluated by means of conventional (biochemical) methods to deepen findings that emerged by the unbiased (proteomic) approach (Alberio and Fasano, 2011) (Fig. 3).

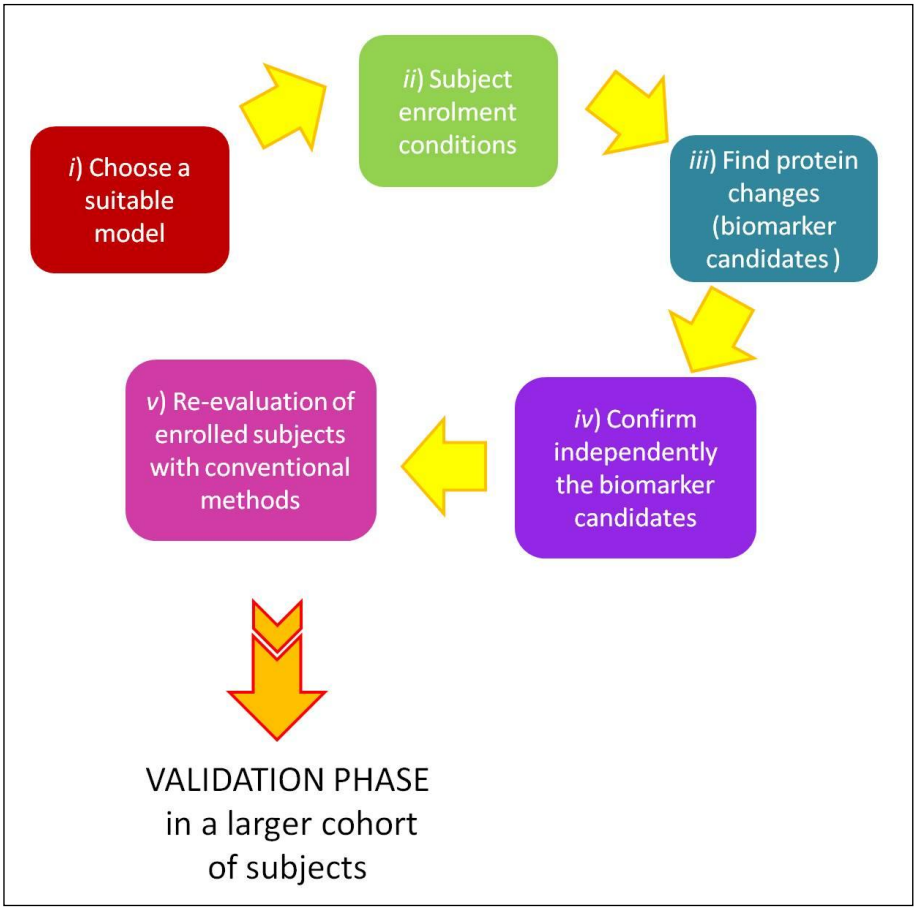

Fig. 3: Ideal flowchart of an hypothesis-generating proteomic investigation, starting from the design of a suitable model for a biomarker discovery strategy, leading to the identification of the involved panel of protein, to end with the confirmation of the new hypothesis by a focused validation. Adapted from Alberio and Fasano, 2011.

2. AIM OF THE PROJECT

Diagnosis of PD is currently based on clinical manifestations of the disease. The great interest in biomarker discovery for PD is due to their need for early diagnosis and clinical development of new disease-modifying therapies.

(T)-Lymphocytes express some features of the dopaminergic system, so in PD patients they could carry some protein alterations peculiar of dopaminergic cells. In particular, patients affected by familial forms of PD (about 20% of all PD cases) may express, also at the peripheral level, alterations that mirror the pathogenic process at the central level.

We decided to investigate this possibility through un unbiased approach, detecting differences in T cells proteome from PD patients and control subjects; we enriched PD patients' group with Early Onset PD patients, who have a greater probability to be affected by a genetic form of the disease, in order to highlight possible effects due to the genetic background. Protein expression's differences between PD patients and control subjects' groups will be evaluated using two-dimensional electrophoresis (2-DE).

Once significant differences will be found, a function taking into account contributes of changing proteins will be calculated in order to rightly predict PD patients and controls.

Our aim is also to identify proteins correlating with other parameters of disease: duration, gravity of symptoms, age at onset. This will confirm that T-lymphocyte proteome changes are a valid tool to correctly classify PD patients and to follow progression of the disease from a peripheral system.

This is the discovery phase of a broader study of biomarker identification for PD. Results shown in this thesis will be validated in a subsequent project in which proteome changes of PD patients' T cells will be confirmed in a larger cohort of subjects through a different technique.

Furthermore, as we consider T cells as dopaminergic circulating cells, we suppose that long term dopaminergic therapy daily assumed by PD patients could induce changes in T cells proteome, so also this possibility will be evaluated in this research.

3. MATERIALS AND METHODS

3.1 Subjects

Patients and control subjects were enrolled by the Parkinson's Disease Center at the Department of Neuroscience, University of Torino, and by the Neurology Division at the Department of Translational Medicine, University of Eastern Piedmont. Every subject was associated to an alphanumeric code to ensure that his/her identity was not disclosed to investigators.

For biomarker discovery, 32 subjects were recruited. Among them, 15 subjects were PD patients, varied in terms of age, age at onset, pharmacological treatment and familiarity. This population was intentionally enriched in early-onset patients (eight of 15) to highlight possible effects due to the genetic background. In particular, we classified as Early Onset PD patients (EOPD) those patients that had onset of the disease before age 45. Similarly, we recruited 17 control subjects. This cohort included also three patients affected by atypical degenerative parkinsonisms. Table 3 reports demographic and clinical data for enrolled subjects. A cohort of 17 patients (partially overlapping with those of the previous recruitment) were enrolled by the same Centers to evaluate the effect of dopaminergic therapies and their data are listed in Table 4.

The summary of demographic and clinical data for all enrolled subjects are reported in Table 5.

Gender and age distributions were similar in different groups. Absolute inclusion criteria for PD patients were: idiopathic PD, absence of atypical signs and a good response to L-DOPA. Supportive criteria were: asymmetry of symptoms or signs at onset, clinical course of more than five years without atypical signs, L-DOPA induced motor fluctuations or dyskinesias. Exclusion criteria for patients and control subjects were: use of neuroleptic drugs, focal cerebral lesions and a history of encephalitis (Jancovic 2008; Litvan et al., 2003; Litvan et al., 1996; Gilman et al., 2008). Subjects suffering from inflammatory or infectious diseases and subjects that took drugs capable of interfering with T-lymphocytes at the time of enrollment were excluded from the study. All patients signed an informed consent before being recruited for the present study, according to the guidelines of the Institutional Review Boards of the Centers where patients were recruited.

Table 3: Demographic and clinical data of subjects enrolled for the part of biomarker discovery. The code contains specification of each subject: CTM stands for Male Control Subject, CTF for Female Control Subject, LOM and LOF for Male and Female Late Onset PD patient, respectively, EOM and EOF for Male and Female Early Onset PD patient, respectively, and APF and APM for Male and Female Atypical Parkinsonism patient, respectively.

Code	Gender	Age (years)	Age at onset (years)	Daily L-DOPA dose (mg/day)	Dopamine agonists	Familiarity	H&Y score
CTF_NO021	F	63	*n.a.*	0	0	No	0
CTF_TO035	F	68	*n.a.*	0	0	No	0
CTF_TO027	F	63	*n.a.*	0	0	No	0
CTF_TO033	F	63	*n.a.*	0	0	Yes	0
APF_TO047	F	73	59	0	0	No	0
APM_NO015	M	70	64	600	0	No	0
CTM_TO059	M	44	*n.a.*	0	0	No	0
CTF_TO063	F	59	*n.a.*	0	0	No	0
CTF_TO065	F	55	*n.a.*	0	0	No	0
CTF_TO043	F	65	*n.a.*	0	0	No	0
CTM_NO022	M	51	*n.a.*	0	0	No	0
APF_TO042	F	79	75	600	0	No	0
CTM_NO027	M	64	*n.a.*	0	0	No	0
CTM_TO058	M	43	*n.a.*	0	0	No	0
CTM_TO051	M	60	*n.a.*	0	0	No	0
CTF_TO060	F	47	*n.a.*	0	0	No	0
CTM_TO054	M	51	*n.a.*	0	0	No	0
EOM_NO017	M	50	47	400	1	No	1
EOF_TO048	F	43	32	900	0	Yes	2
EOM_NO018	M	43	36	300	1	No	4
EOM_TO049	M	55	43	500	0	No	3
EOM_TO008	M	47	39	500	1	No	2.5
EOM_TO022	M	39	37	0	0	No	1
EOF_TO050	F	57	45	450	0	Yes	2
EOM_NO028	M	48	42	150	1	No	2.5
LOM_TO040	M	68	67	0	0	Yes	1
LOF_TO021	F	64	63	0	1	Yes	2
LOF_TO016	F	58	52	400	1	No	1.5
LOM_TO006	M	65	52	1200	1	No	3
LOM_TO064	M	67	63	400	1	Yes	1
LOF_NO023	F	56	52	0	0	Yes	1
LOM_TO066	M	58	54	400	1	No	2

n.a.: not applicable.

Table 4: Demographic and clinical data of patients enrolled for the evaluation of effects of dopaminergic therapy.

Patient Code	Gender	Age (years)	Age at onset (years)	Disease duration (years)	Daily L-DOPA dose (mg/day)	Dopamine agonist (mg/die)	H&Y Score
1	F	43	32	11	900	0	2
2	M	55	43	12	500	0	3
3	M	39	37	2	0	0	1
4	F	57	45	12	450	0	2
5	F	46	36	10	600	0	2
6	M	68	67	1	0	0	1
7	F	56	52	4	0	0	1
8	M	43	36	7	300	Rotigotine (16)	4
9	M	47	39	8	500	Ropinirole (8)	2.5
10	M	48	42	6	150	Ropinirole (20)	2.5
11	F	64	63	1	0	Pramipexole (2.1)	2
12	F	58	52	6	400	Rotigotine (4)	1.5
13	M	65	52	13	1200	Ropinirole (16)	3
14	M	67	63	4	400	Pramipexole (1.05)	1
15	M	58	54	4	400	Pramipexole (2.1)	2
16	M	62	46	16	450	Pramipexole (2.1)	2.5
17	M	50	47	3	400	Rotigitine (8)	1

Table 5: Summary of demographic and clinical data for all enrolled subjects.

	Biomarkers Discovery		**Effect of DA therapy**
	PD patients (*n* = 15)	Controls (*n* = 17)	PD Patients (*n* = 17)
Age ± SD (years)	54.5 ± 9.2	59.9 ± 10.2	54.5 ± 9.1
Male %	67	41	65
PD duration ± SD (years)	6 ± 4		7 ± 5
Medications			
Unmedicated	3	-	3
L-DOPA	3	2	4
DA agonists	1	0	1
L-DOPA + DA agonists	8	0	9

3.2 T-lymphocyte isolation

All subjects underwent a venous blood sampling (20 ml) from the antecubital vein, between 9 and 10 a.m., after an overnight fast. Whole blood was collected into vacuum tubes containing EDTA, diluted with 50 ml of phosphate-buffered saline (PBS) and stratified in two 50 ml tubes on top of 15 ml of Lympholyte®-H (Cedarlane) each. After centrifugation (800×g, 20 min, 20°C) peripheral blood mononuclear cells (PBMC) were removed and pelleted through centrifugation (400×g, 15 min, 20°C). Pellets were washed twice with 10 ml of magnetic-activated cell sorting (MACS) buffer (Miltenyi Biotec). The isolation of T lymphocytes was achieved by MACS with the Pan T-cell isolation kit (Miltenyi Biotec) using the manufacturer's protocol.

3.3 Two-dimensional electrophoresis and image analysis

T-lymphocytes were resuspended in 120 µl UTC (7 M urea, 2 M thiourea and 4% 3-[(3-cholamidopropyl)dimethylammonio]-1-propanesulfonate (CHAPS)) with a protease inhibitors cocktail (Sigma-Aldrich). Cells were left in this solution for 30 min to allow a complete cell lysis, sonicated (3×5 sec) and centrifuged (12000×g, 20 min, 10°C) to precipitate the cellular debris. Protein concentration in the extracts was determined Bradford assay (Serva). Total proteins (200 µg) were separated through two-dimensional electrophoresis (2-DE) using 18 cm IPG DryStrips with a nonlinear 3–10 pH gradient (GE Healthcare) followed by 14% SDS-PAGE. The resulting maps were stained with Ru(II) tris(bathophenanthroline disulfonate) (Serva). Images were acquired (12 bit grayscale) with the GelDoc-It Imaging System (UVP) and analyzed with ImageMaster 2D Platinum (GE Healthcare); spots showing significant variation among subject groups (Wilcoxon test, $p<0.05$) were excised from gels and the corresponding proteins identified by LC-MS/MS fragmentation.

3.4 Statistical analysis

Spot volumes were normalized by the total volume of a subset of spots common to all gels. Spots that were missing in more than 25% of gels were not taken into account. Missing spot values in less than 25% of gels were replaced by the mean value of the spot volume of the group or, if the mean was lower than the 98th percentile, by the minimum value observed in the group (Albrecht et al., 2010).

Relative volumes were analyzed by the non-parametric Wilcoxon test to find significant differences in patients with PD with respect to control subjects, in early-onset patients with respect to late-onset patients and in PD patients treated or not with dopamine agonists (McDonald 2009). Spots showing

significant differences ($p < 0.05$) in patients administered with dopamine agonists with respect to patients not treated with dopamine were excluded by the subsequent analysis for biomarker discovery.

The Pearson linear correlation coefficient r was evaluated according to Eq. 1, where x is the independent variable (i.e., Hoehn and Yahr score, age, years from onset, daily L-DOPA dose), y is the relative spot volume, $\bar{x}$ is the mean x value, $\bar{y}$ is the mean y value, xy is the x·y product, $\overline{xy}$ is the product of $\bar{x}$ and $\bar{y}$ mean values (Surinova et al., 2011).

(1) $$r = \frac{\frac{\sum xy}{n} - \overline{xy}}{\sqrt{\frac{\sum x^2}{n} - \bar{x}^{-2}} \sqrt{\frac{\sum y^2}{n} - \bar{y}^{-2}}}$$

Spots showing linear correlation with age and daily L-DOPA dose were excluded by the subsequent analysis for biomarker discovery.

Predictive models for the classification of PD patients with respect to control subjects and of early-onset patients with respect to late-onset were built by linear discriminant analysis (LDA) of the spots identified as described above (McDonald 2009). In this case, missing values were set to half of the minimum value observed in the gel. A likelihood score was assigned to each subject by linear combination of relative spot volumes according to Eq. 2.

(2) $$\text{PD } Score = \sum_i c_i Vol_i$$

Simplified models were obtained by progressively removing groups of spots in terms of their discriminating weight (*W*), calculated according to Eq. 3,

(3) $$W = \left| c_i \left(\overline{Vol_{i,CO}} - \overline{Vol_{i,PD}} \right) \right|$$

where c_i is the LDA coefficient for spot *i* and $\left| \left(\overline{Vol_{i,CO}} - \overline{Vol_{i,PD}} \right) \right|$ is the absolute separation of the mean values of spot *i* in control subjects (CO) and PD. Each predictive model has been tested with the leave-one-out method (McDonald 2009). The performance of predictive models has been quantified by measuring the area under the ROC curve.

Aggregative nesting of spots included in the predictive model was based on pairwise Pearson correlation (Eq. 1), where x and y are relative spot volumes.

The minimum number of subjects to be included in validation studies was calculated according to Eq. 4,

(4) $$n = \frac{(N_{CO} - 1) \cdot \sigma_{CO}^2 + (N_{PD} - 1) \cdot \sigma_{PD}^2}{(N_{CO} + N_{PD} - 2) \cdot \left(\frac{\mu_{CO} - \mu_{PD}}{2.2} \right)^2}$$

where σ_{CO} and σ_{PD} are standard deviations of relative spot volumes in CO and PD groups, N_{CO} and N_{PD} are numbers of subjects in the groups, and μ_{CO} and μ_{PD} are mean values of relative spot volumes in the groups (McDonald 2009).

The minimum number of subjects needed to reach statistical significance for the part "Dopaminergic therapies modulate T cell proteome of PD patients" was calculated in analogy to Eq. 4, according to the Eq. 5:

(5) $$n = \frac{(N_{Dago-} - 1) \cdot \sigma_{Dago-}^2 + (N_{Dago+} - 1) \cdot \sigma_{Dago+}^2}{(N_{Dago-} + N_{Dago+} - 2) \cdot \left(\frac{\mu_{Dago-} - \mu_{Dago+}}{2.2} \right)^2}$$

where σ_{Dago-} and σ_{Dago+} are standard deviations of relative spot volumes in groups of patients not assuming (Dago-) or assuming (Dago+) dopamine agonists; N_{Dago-} and N_{Dago+} are numbers of patients in each group; and μ_{Dago-} and μ_{Dago+} are mean values of relative spot volumes in each group.

All procedures for data analysis and graphics were written in R, an open-source environment for statistical computing (R Development Core Team, 2009).

3.5 In-gel digestion, mass spectrometry and protein identification

Spots were manually excised and destained (50% ethanol), dehydrated with acetonitrile (2 × 20 min 100 µl) and then dried at 37°C by vacuum centrifugation. The gel pieces were then swollen in 10 µl digestion buffer containing 50 mM NH4HCO3 and 12.5 ng/µl modified porcine trypsin (sequencing grade, Promega). After 10 min, 30 µl of 50 mM NH_4HCO_3 were added to the gel pieces and digestion allowed to proceed at 37°C overnight. The supernatants were collected and peptides were extracted in an ultrasonic bath for 10 min (twice 100 µl 50% acetonitrile, 50% H_2O, 1% formic acid; twice 50 µl acetonitrile). All the supernatants were collected in the same tube, dried by vacuum centrifugation and dissolved in 5 µl 2% acetonitrile, 0.1% formic acid in water.

Peptides from each sample were then separated by reversed phase nano-HPLC-Chip technology (Agilent Technologies) online-coupled with a 3D ion trap mass spectrometer (model Esquire 6000, Bruker Daltonics) installed at the Department of Biotechnology, University of Verona. The chip was composed of a Zorbax 300SB-C18 (43mm×75µm, with a 5µm particle size) analytical column and a Zorbax 300SB-C18 (40 nL, 5µm) enrichment column. The complete system was fully controlled by

ChemStation (Agilent Technologies) and EsquireControl (Bruker Daltonics) softwares. The scan range used was from 300 to 1800 m/z. For tandem MS experiments, the system was operated with automatic switching between MS and MS/MS modes. The three most abundant peptides of each m/z were selected to be further isolated and fragmented. The MS/MS scanning was performed in the normal resolution mode at a scan rate of 13000 m/z per second. A total of five scans were averaged to obtain an MS/MS spectrum. Protein identification was manually performed by searching the National Center for Biotechnology Information non-redundant database using the Mascot 2.3 MS/MS Ion Search program (http://www.matrixscience.com). The following parameters were set: specific trypsin digestion, up to one missed cleavage; complete carbamidomethylation of cysteines, partial oxidation of methionines, partial protein N-terminal acetylation, peptide mass tolerance ± 0.9 Da, fragment mass tolerance ± 0.9 Da, 1+ to 3+ peptide charge, species restriction to human. All identified proteins had a Mascot score corresponding to a statistically significant ($p < 0.05$) confident identification according to Fisher's test. At least 2 different peptides had to be assigned. Peptide and protein identifications corresponding to keratins or trypsin were not taken into account.

Double assignments were refined by matching spots with reference 2-DE maps available in the swiss-2Dpage database (http://world-2dpage.expasy.org/swiss-2dpage/). In particular, we referred to the LYMPHOCYTE_HUMAN map for disambiguation. In the case the ambiguous assignment was not resolved by matching, we checked the correct assignment by western blotting.

3.6 Quantitative Western blotting analysis

For one-dimensional Western blotting, cell lysates (20 µg) were denatured in Laemmli sample buffer for 5 min at 98°C and electrophoresed on 10% SDS-PAGE gel. 2-DE was performed as described above. Gels were transferred to polyvinylidene difluoride (PVDF) membranes at 1mA/cm2, 1.5 h (TE77pwr, Hoefer). Membranes were saturated in 5% non-fat milk in TBS-T (0.1 M Tris-HCl pH 7.4, 1.5 M NaCl and 0.5% Tween-20) and incubated in the same buffer at 4°C overnight with the following primary antibodies:

- goat anti-fibrinogen polyclonal antibody (Abnova), 1:10000 dilution, or
- mouse anti-transaldolase polyclonal antibody (Abcam), 1:500 dilution, or
- mouse antiperoxiredoxin 6 monoclonal antibody (Abnova), 1:5000 dilution, or
- mouse antiprolidase polyclonal antibody (Abnova), 1:1000 dilution, or
- mouse anti-beta actin monoclonal antibody (GeneTex), 1:3000 dilution, or
- mouse anti-alpha tubulin monoclonal antibody (Sigma), 1:10000 dilution, or
- goat anti-serpin B9 polyclonal antibody (Abcam), 1:2000 dilution, or
- mouse anti- beta tubulin monoclonal antibody (Sigma Aldrich), 1:4000 dilution.

Membranes were then washed with TBS-T and incubated with secondary peroxidase-conjugated antibody in 5% milk-TBS-T (anti-goat-IgG antibody, Millipore, 1:8000, or anti-mouse-IgG antibody, Upstate, 1:3000) for chemiluminescence detection (Millipore). Photographic films were scanned with a Epson Perfection V750 Pro transmission scanner (Epson) and images (16 bit grayscale) were analyzed using ImageJ software (http://rsb.info.nih.gov/ij/). Images showing dynamic range saturation were discarded. Signal intensities were corrected for protein loading by normalization to beta actin intensity.

3.7 Cell culture

The human liver carcinoma Hep G2 cell line was maintained at 37°C in a 5% CO_2 humidified atmosphere in RPMI 1640, supplemented with 10% fetal bovine serum (FBS), 100 U/ml penicillin, 100 µg/ml streptomycin, and 2 mM L-glutamine. Stock flasks were transferred for culture twice weekly or as required to maintain optimal cell growth.

The Jurkat T-cell leukemia cell line was maintained at 37°C in a 5% CO_2 humidified atmosphere in RPMI 1640, supplemented with 10% fetal bovine serum (FBS), 100 U/ml penicillin, 100 µg/ml streptomycin, and 2 mM L-glutamine. Stock flasks were transferred for culture twice weekly or as required to maintain optimal cell growth. When flasks were filled, cells were collected by centrifugation, lysed with 120 µl RIPA buffer (25 mM Tris-HCl pH 7.4, 0.15 M NaCl, 0.1% SDS, 1% Triton X-100, 1% sodium deoxycholate) and centrifuged (13000 g, 30 min, 10 °C). Proteins were collected in the supernatant and resolved by SDS-PAGE.All cell culture media and reagents were from Euroclone S.p.A.

3.8 RNA extraction, retrotranscription and PCR

RNA was extracted from T lymphocytes and PBMC of the same control subject and from HepG2 cells using NucleoSpin RNA II (Macherey-Nagel) following manufacturer's instructions and treated with recombinant DNase (Promega) in order to remove genomic DNA. One microgram of RNA was reverse transcribed into first-strand cDNA in a 20 µl final volume using the Maxima™ First Strand cDNA Synthesis Kit (Fermentas). PCR was performed by Thermocycler One Personal (Euroclone).

The expression of beta fibrinogen (FGB) and glyceraldehyde-3-phosphate dehydrogenase (GAPDH) as housekeeping gene was evaluated using primers reported in Table 6. Optimal PCR conditions were identified for each primer pair. Reactions were incubated at 95°C for 3 min, then 35 cycles of 95°C for 30 sec, 57°C for 30 sec, 72°C for 45 sec, then a final extension step at 72 for 5 min.

The expected size of the fragments was visualized in a 2% agarose gel stained with ethidium bromide.

3.9 Primer design

Primer design was performed by using Primer3 software (http://primer3.sourceforge.net/) and manually adjusted if needed. Primer pairs were designed to avoid the amplification of undesired sequences that share high identity degree and the amplification of common sequences among the splicing variants of the same transcript. Moreover, primers were designed to have comparable melting temperature and reaction efficiency. Primer specificity was tested by BLAST (http://blast.ncbi.nlm.nih.gov/Blast.cgi) and experimentally by the positive control amplification.

Table 6: sequences of specific primers: F = forward primer; R = reverse primer.

Gene	Primer Sequence	Amplicon size (bp)
FGB F	TGGCAAAAGAGGCAGAAGCAAG	145
FGB R	CCAGGATTGAACGAAGCACACG	
GAPDH F	GAGTCAACGGATTTGGTCGT	238
GAPDH R	TTGATTTTGGAGGGATCTCG	

3.10 Separation of membrane proteins

Freshly isolated T lymphocytes and PBMC from the same subjects were treated for separation of cell surface protein. The separation was achieved through biotinylation of whole cells with the Pierce Cell Surface Protein Isolation Kit (Thermo Fisher Scientific).

After the separation, cell surface proteins and internal proteins were loaded on SDS-PAGE and transferred onto a PVDF membrane for Western blotting.

4. RESULTS

4.1 Two-dimensional electrophoresis profiling of T-cell proteins

Human T-cell protein expression profiles of PD patients and control subjects were obtained through 2-DE; a representative map from subject CTF_NO021 is showed in Fig. 4. A total of about 250 spots were detected in 75% of gels and included in the analysis.

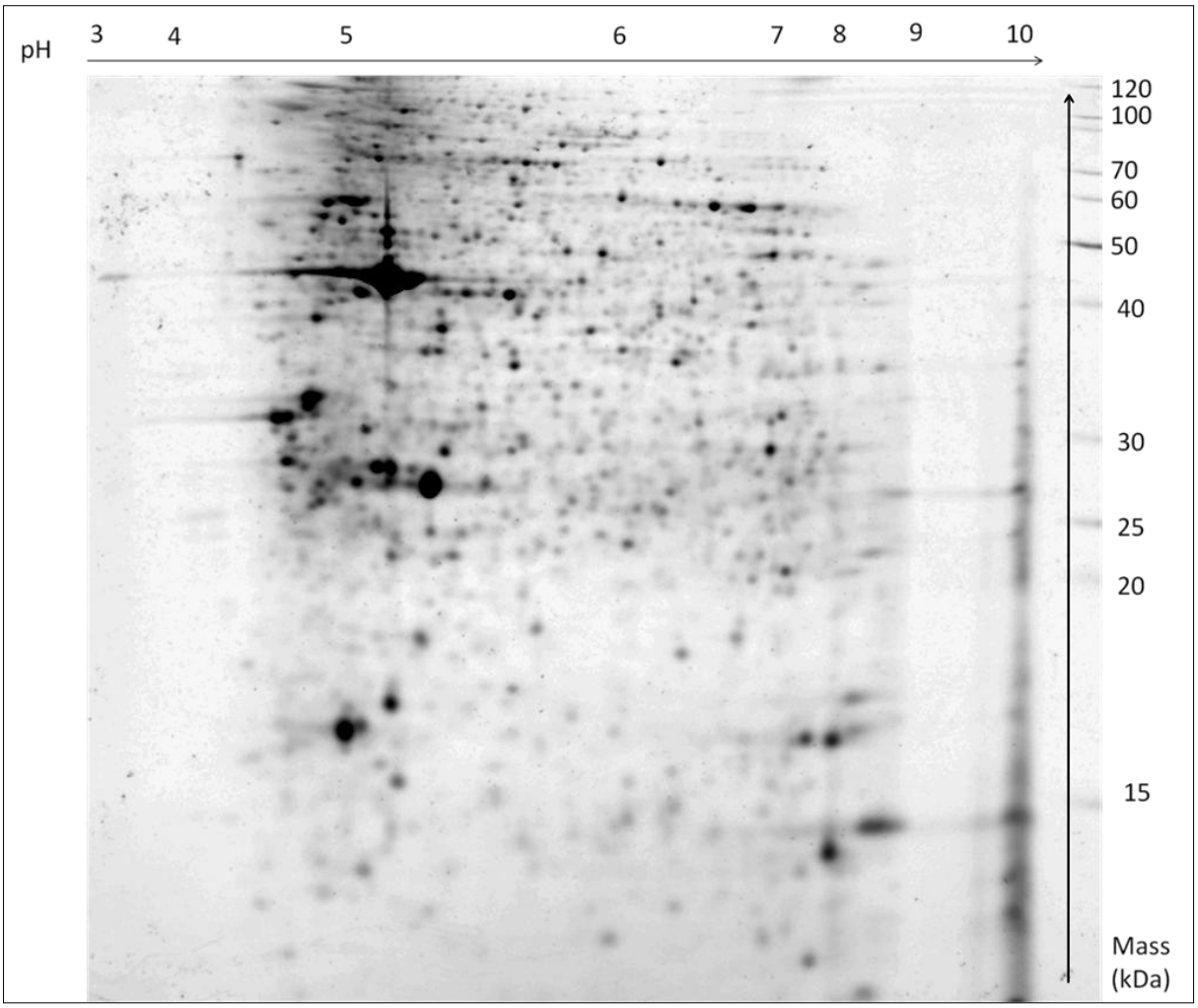

Fig. 4: illustrative map of T-cell protein expression profile obtained by 2-DE.

The 32 maps were screened to identify at first proteins or protein modifications whose changes were linked to confounding factors such as therapy and age. Spots showing linear Pearson correlation with age (evaluated in control subjects only) or daily L-DOPA dose, or showing significant differences between patients treated or not with dopamine agonists (Wilcoxon test, $p<0.05$) were excluded from the further analysis. By comparing 2-DE maps from 15 PD patients to 17 control subjects, we selected 20 protein spots showing significantly different levels in the two groups (Wilcoxon test, $p<0.05$). The distribution of fold of change values (in Log_2 scale) of patients *vs.* control subjects and of Wilcoxon test p values are shown in Fig. 5a and 5b. Selected spots are annotated on the 2-DE map in Fig. 6.

Proteins corresponding to selected spots were identified by LC-MS/MS; identities of these 20 proteins and fold of induction in the two groups are reported in Table 7. Additional information about details on protein identification by mass spectrometry are listed in Table 15, at the end of this chapter.

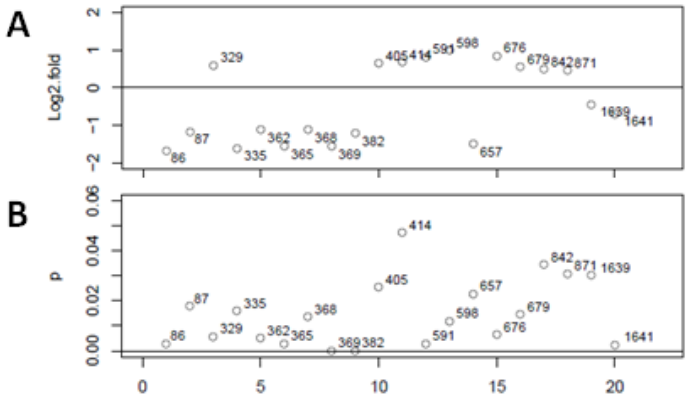

Fig. 5: For each of the 20 spots showing significantly different levels in PD patients and control subjects, the fold of change in Log_2 scale (A) and the Wilcoxon test p value (B) are reported.

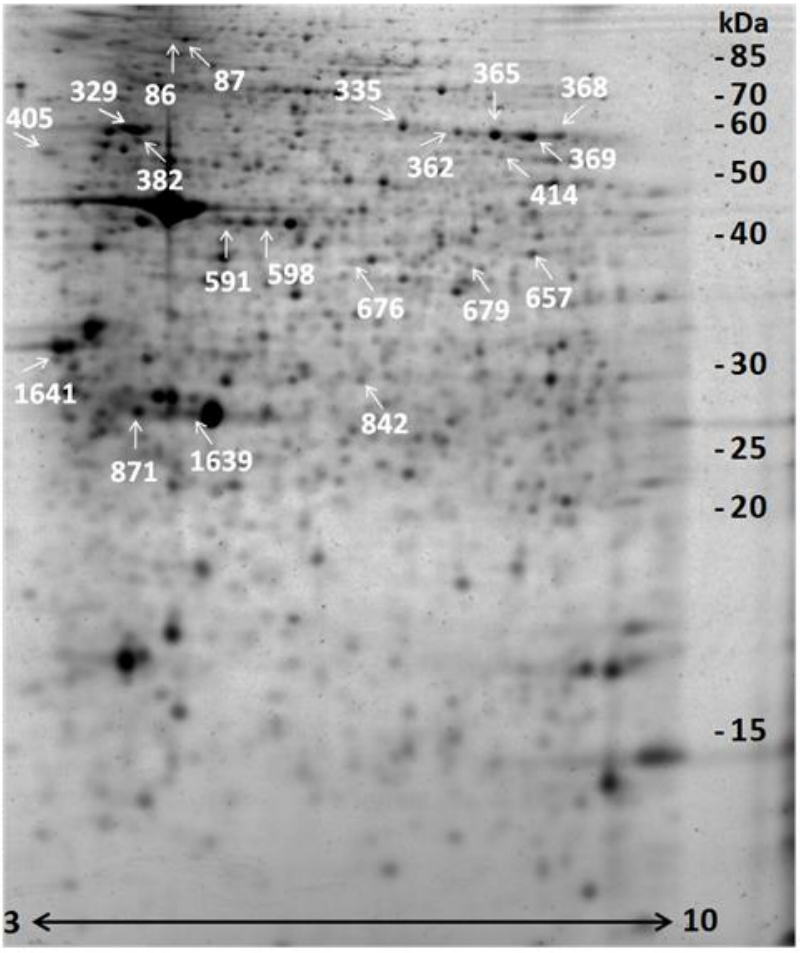

Fig. 6: position in the 2-DE map of the 20 proteins showing different levels in PD's and control's group.

Table 7: Identification of protein spots that are significantly different in PD patients.

Spot No.	**Protein**	**Uniprot Id**	**Correlation**	**p (Wilcoxon test)**
86	Vinculin	P18206	↓ PD	0.003
87	Vinculin	P18206	↓ PD	0.018
329	Vimentin	P08670	↑ PD	0.006
335	Talin-1	Q9Y490	↓ PD	0.016
362	Beta-fibrinogen	P02675	↓ PD	0.005
365	Beta-fibrinogen	P02675	↓ PD	0.003
368	Beta-fibrinogen	P02675	↓ PD	0.014
369	Beta-fibrinogen	P02675	↓ PD	<0.001
382	Filamin-A	P21333	↓ PD	<0.001
405	Lymphocyte-specific Protein 1	P33241	↑ PD	0.025
414	Septin-6	Q14141	↑ PD	0.047
591	Vimentin	P08670	↑ PD	0.003
598	Moesin	P26038	↑ PD	0.012
657	Gelsolin	P06396	↓ PD	0.023
676	Transaldolase	P37837	↑ PD	0.007
679	Transaldolase	P37837	↑ PD	0.014
842	Twinfilin-2	Q6IBS0	↑ PD	0.034
871	Rho GDP dissociation inhibitor isoform 2	P52566	↑ PD	0.031
1639	Beta actin fragment	P60709	↓ PD	0.030
1641	14-3-3 epsilon	P62258	↓ PD	0.002

4.2 Correlation of selected spot volumes with Hoehn and Yahr score and disease duration

The occurrence of linear correlation of selected spot volumes (spots changing in PD patients and control subjects) with the Hoehn and Yahr score (H&Y score) and the duration of the disease, was evaluated in order to test if some of the proposed biomarkers changed with time or disease severity. Correlation with the Hoehn and Yahr score was observed for 8 spots, listed with their corresponding identities in Table 8. These spot volumes were linearly combined to afford a function that significantly tracks the Hoehn and Yahr score. Multiple regression on PD patients allowed us to determine a set of coefficients for the eight spots listed above (Table 8). In this way, the spot volume combination linearly correlates with the Hoehn and Yahr score ($r = 0.674$, $p = 0.006$) (Fig. 7A). The significance of the correlation is improved by adding control subjects at $x = 0$ ($r = 0.603$, $p < 0.0005$) (Fig. 7B).

Table 8: Coefficients for linear combinations of spots to build a function that tracks disease severity (H&Y score) and duration (Years from onset).

Spot No.	**Protein**	**Coefficients**	
		H&Y Score	*Years from onset*
86	Vinculin	21.5	
362	Beta-fibrinogen	112	
365	Beta-fibrinogen	-52.4	
368	Beta-fibrinogen	36.7	
369	Beta-fibrinogen	-7.09	53.5
405	Lymphocyte-specific Protein 1	60.5	
591	Vimentin		76.6
598	Moesin	-38.2	158
1641	14-3-3 epsilon	-162	-606

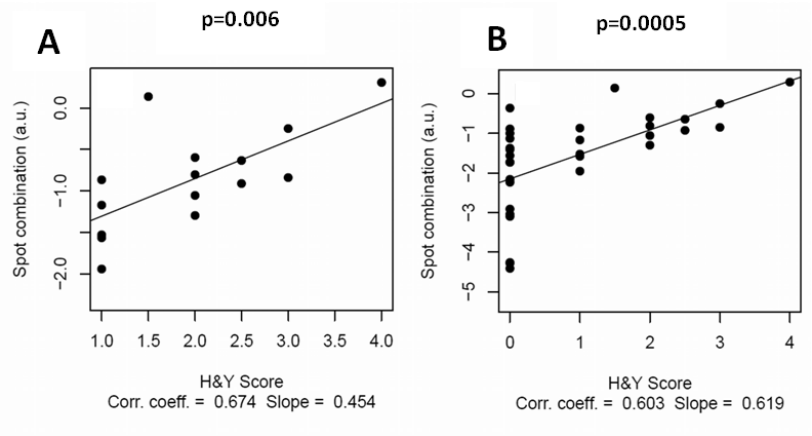

Fig. 7: Predictors of PD progression. A linear combination of eight spots correlates linearly with the Hoehn and Yahr score. Linear correlation is significant both excluding (A) and including (B) control subjects.

Correlation with the duration of the disease, measured in years from onset, was observed for 4 spots (Table 8). These spot volumes were linearly combined to afford a function that significantly tracks disease duration. Multiple regression on PD patients allowed us to determine a set of coefficients for the four spots listed above (Table 8). In this way, the spot volume combination linearly correlates with the disease duration (r = 0.516, p = 0.049) (Fig. 8A). The correlation is improved by adding control subjects at x = 0 (r = 0.548, p = 0.001) (Fig. 8B). Worth of note, spots 369, 598 and 1641 correlate with both parameters (score H&Y and disease duration).

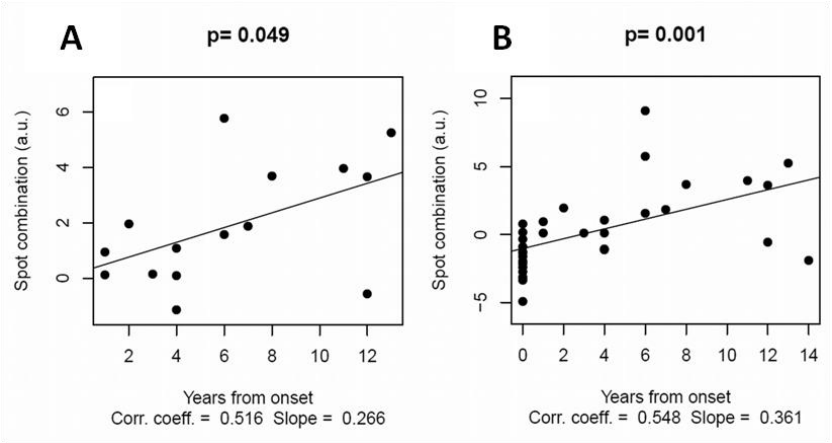

Fig. 8: Predictors of PD progression. A linear combination of eight spots correlates linearly with the disease duration. Linear correlation is significant both excluding (A) and including (B) control subjects.

Pearson correlation analysis of single spots with the disease stage (Score H&Y) and disease duration (Years from onset) are shown in Figs. 9 e 10, respectively.

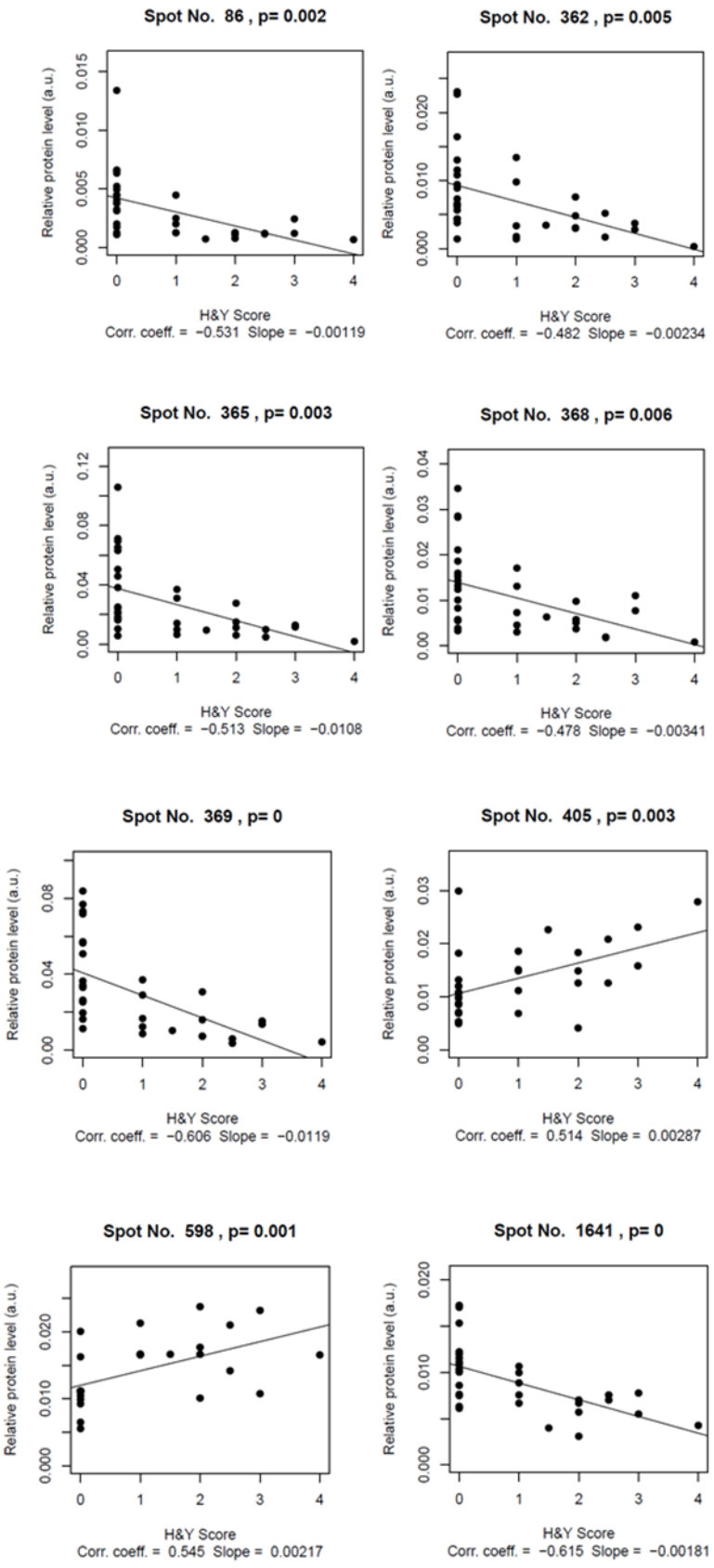

Fig. 9: Pearson correlation analysis of spots 86 (vinculin), 362 (vinculin), 365 (β-fibrinogen), 368 (β-fibrinogen), 369 (β-fibrinogen), 405 (lymphocyte-specific protein 1), 598 (moesin) and 1641 (14-3-3 epsilon) with the disease stage, expressed as Hoehn and Yahr score. Correlation coefficients are calculated according to Eq. 1.

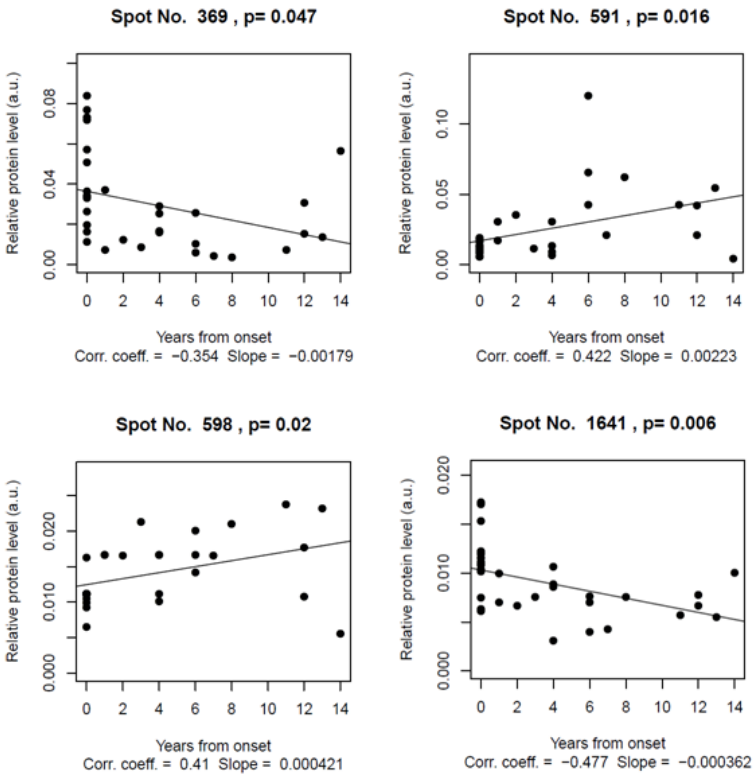

Fig. 10. Pearson correlation analysis of spots 369 (β-fibrinogen), 591 (vimentin), 598 (moesin) and 1641 (14-3-3 epsilon) with the disease duration, expressed as years from onset. Correlation coefficients are calculated according to Eq. 1.

4.3 Linear discriminant analysis of selected spot levels

We analyzed all spots (n = 20) showing significantly different levels in PD patients by LDA so to obtain a likelihood score (PD Score) expressed as a linear combination of relative spot volumes (linear coefficient and weights of each spot are reported in Table 10). Spot combinations were significantly different in PD patients with respect to control subjects (Wilcoxon test, $p < 10^{-8}$, Fig 11A), with a cutoff value of 0.67. To effectively test the performance of the model, each subject was iteratively excluded by the training set and predicted on the basis of the other subjects. According to the "leave-one-out" procedure (Mc Donald 2009) we obtained 87% sensitivity and 81% specificity. Predictions so obtained were used to build a ROC curve with an area under curve of 0.906 (Fig. 11B).

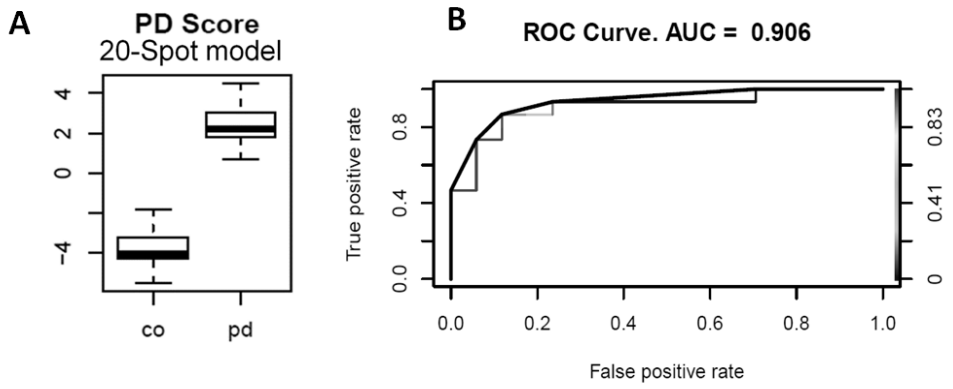

Fig. 11: Scoring functions built on set of 20 spots yield the PD likelihood. Classifiers obtained by the leave-one-out cross-validation have been used to build ROC curve.

A simplification of the model was achieved by ranking the 20 spots in terms of their ability to discriminate PD patients from control subjects. Thus, the six spots showing the worst contribution (weight < 0.3, Table 10) were discarded and the LDA was performed on the remaining 14 spots. PD Scores were significantly different in PD patients with respect to control subjects (Wilcoxon test, $p < 10^{-8}$, fig 12A), with a cutoff value of -0.31. In this case, the "leave-one-out" cross-validation procedure of the model allowed us to obtain 100% sensitivity and 94% specificity. Predictions obtained so far were used to build a ROC curve with an area under curve of 0.996 (Fig. 12B).

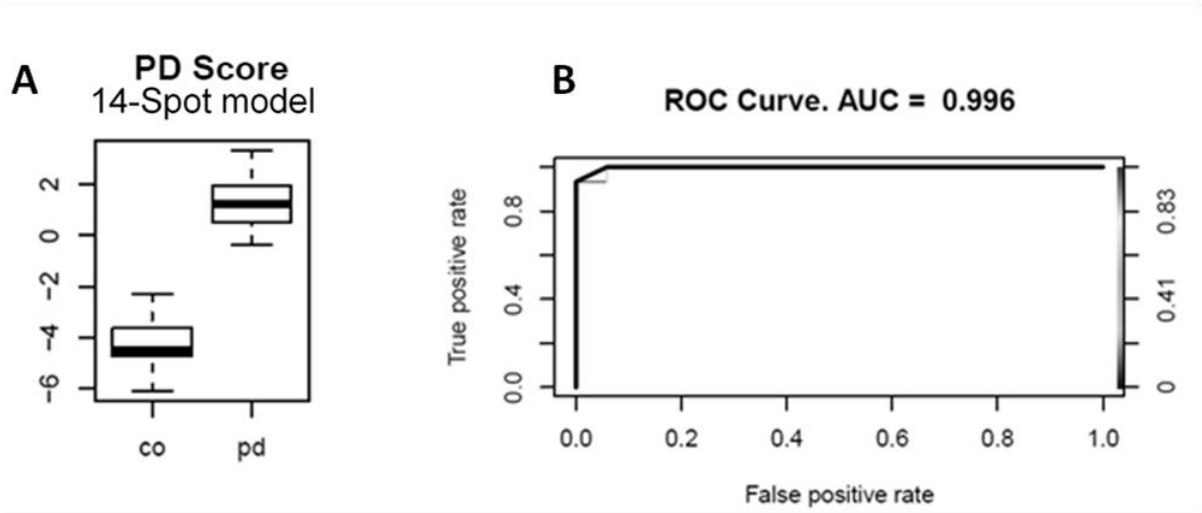

Fig. 12: Scoring functions built on set of 14 spots yield the PD likelihood. Classifiers obtained by the leave-one-out cross-validation have been used to build ROC curve.

We further simplified the model by removing spots with weight < 1, thus obtaining a 9-spot model (Table 10). Again, LDA yielded PD Score significantly different in PD patients with respect to control

subjects (Wilcoxon test, $p < 10^{-8}$, Fig 13A), with a cutoff value of -2.90. The "leave-one-out" cross-validation procedure of the model allowed us to obtain 100% sensitivity and 88% specificity, and the ROC curve built with these predictions had an area under curve of 0.992 (Fig. 13B).

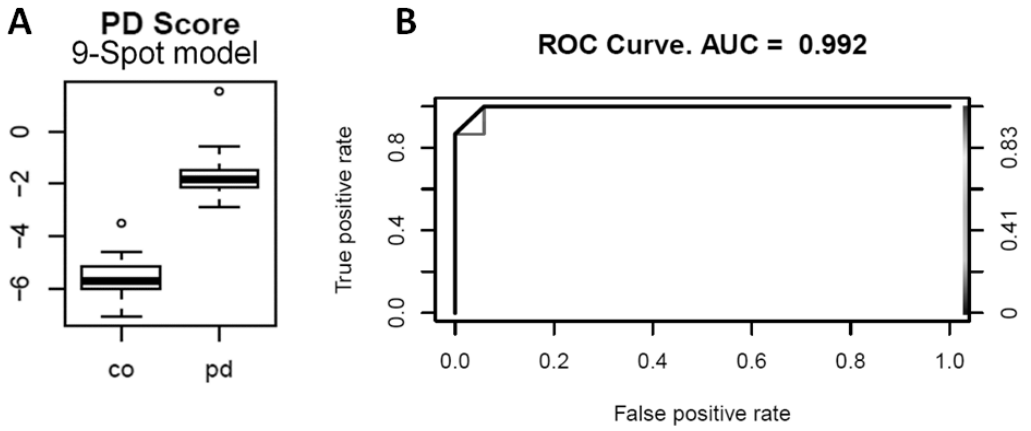

Fig. 13: Scoring functions built on set of 9 spots yield the PD likelihood. Classifiers obtained by the leave-one-out cross-validation have been used to build ROC curve.

For comparison, results of the three proposed predictive models are summarized in Table 9.

Table 9: Summary of performance parameters for the three predictive models. Cutoff values are expressed in terms of the likelihood PD score obtained as a linear combination of selected spot relative volumes; ROC = receiver operating characteristic; AUC = area under curve; p values refer to Wilcoxon test on PD scores. Sensitivity, specificity and ROC AUC were obtained by leave-one-out cross-validation.

	20-spot model	**14-spot model**	**9-spot model**
Cutoff	0.67	-0.31	-2.90
Sensitivity (%)	87	100	100
Specificity (%)	81	94	88
ROC AUC	0.906	0.996	0.992
p value	$< 10^{-8}$	$< 10^{-8}$	$< 10^{-8}$

Table 10: Linear discriminant analysis coefficients and weights

Spot No.	**Protein**	**20-spot model**		**14-spot model**		**9-spot model**	
		Coefficient	*Weight*	*Coefficient*	*Weight*	*Coefficient*	*Weight*
86	Vinculin	-600.7	1.742	-497.3	1.442	-320.2	0.9286
87	Vinculin	-264.4	1.369	-267.3	1.384	-289.3	1.498
329	Vimentin	10.37	0.2096	-	-	-	-
335	Talin-1	215.5	1.203	233.0	1.300	148.8	0.8304
362	Beta-fibrinogen	636.0	3.296	525.1	2.722	401.0	2.078
365	Beta-fibrinogen	83.49	2.182	68.00	1.777	91.44	2.389
368	Beta-fibrinogen	248.5	1.939	267.9	2.090	192.6	1.503
369	Beta-fibrinogen	-237.4	6.758	-232.9	6.630	-217.2	6.184
382	Filamin-A	-172.3	1.828	-162.4	1.723	-108.2	1.148
405	Lymphocyte-specific Protein 1	116.0	0.6441	109.0	0.6048	-	-
414	Septin-6	95.30	0.1718	-	-	-	-
591	Vimentin	-32.40	0.4060	-30.29	0.3796	-	-
598	Moesin	68.17	0.3576	77.40	0.4060	-	-
657	Gelsolin	-276. 7	1.058	-326. 1	1.247	-281.2	1.075
676	Transaldolase	288.6	0.5737	249.38	0.4958	-	-
679	Transaldolase	-93.18	0.1289	-	-	-	-
842	Twinfilin-2	7.034	0.01180	-	-	-	-
871	Rho GDP dissociation inhibitor isoform 2	9.525	0.1493	-	-	-	-
1639	beta actin fragment	-1.948	0.02010	-	-	-	-
1641	14-3-3 epsilon	-87.95	0.3231	17.97	0.06600	-	-

A comparison of ROC curves of the three models is showed in Fig. 14; the prediction of single subjects through the procedure described above and performance's parameters for the three models are represented in Fig. 15.

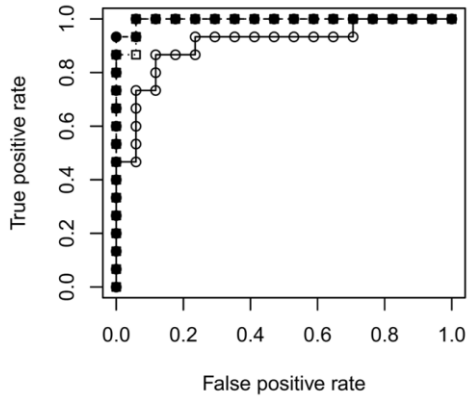

Fig. 14: ROC curves of the three models obtained by the leave-one-out cross-validation. Open circles are for the 20-spot model; filled squares for 14-spot model; open squares for 9-spot models.

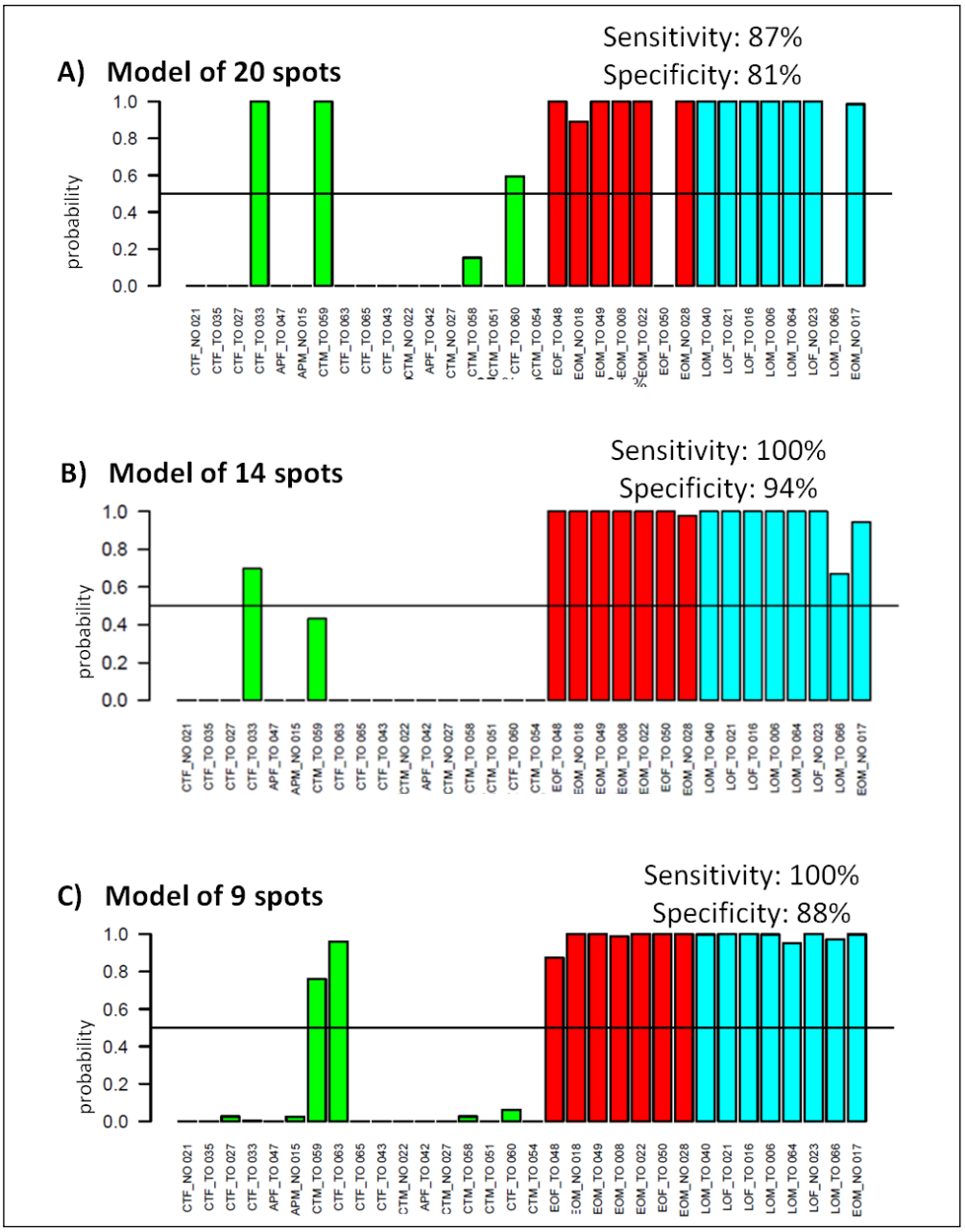

Fig. 15: prediction of single subjects and performance parameters for the 20-spots model (A), the 14-spots model (B) and the 9-spots model(C). The bars represent the predicted probability of a subject to be a control (green), or a PD patient (EOPD are red bars, LOPD are blue bars, respectively), calculated with the scoring function obtained with the other 32 subjects. The true identity of each subject is indicated in its code and refers to codes expounded in Table 3.

To test the power of our analysis we evaluated the intra-group variance and the difference of mean values for each spot included in the three models (Eq. 4). The minimum number of subjects required for a significant verification is in the range from 10 to 30 for most spots (Table 11).

Table 11: Power analysis of the 20 spots showing the minimum number of subjects to be included in validation studies.

Spot No.	Number of subjects	Spot No.	Number of subjects
86	3	414	13
87	6	591	19
329	8	598	12
335	9	657	10
362	5	676	4
365	3	679	32
368	4	842	14
369	2	871	8
382	6	1639	>100
405	8	1641	6

4.4 Linear discriminant analysis of spots showing differences between late-onset and early-onset patients

To test the possibility to discriminate PD subtypes, we compared LO PD patients to EO PD patients (Fig. 16). We selected 7 protein spots (Wilcoxon test, $p < 0.05$) and identified them by LC-MS/MS (Table 12; see Table 15 for mass spectrometry details). We performed a LDA on selected spots in LO patients with respect to EO patients so to obtain a likelihood score (LO vs. EO Score) expressed as a linear combination of relative spot volumes (Table 12).

The position of these spots in the 2-DE map is shown in Fig. 17A.

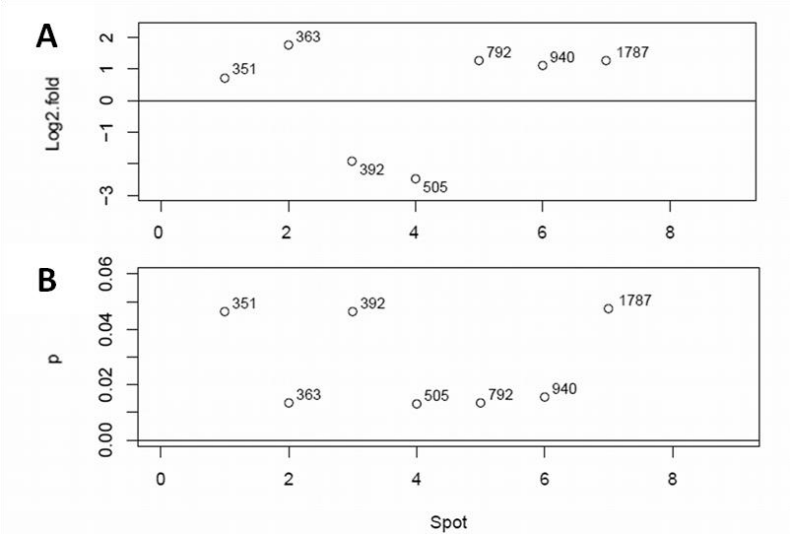

Fig. 16: 7 spots discriminate late-onset (LO) from early-onset (EO) patients. For each of the 7 spots, the fold of change in Log2 scale (A) and the Wilcoxon test p value (B) are reported.

Table 12: LOPD patients vs. EOPD patients: Identification, fold of change and p value of Wilcoxon test. Coefficients and weights refer to the LDA refinement procedure described in the text.

Spot No.	**Protein**	**Uniprot Id**	**Correlation**	**p**	**Coefficient**	**Weight**
351	Beta tubulin	P07437	↑ LOPD	0.047	100.4	2.081
363	Protein disulfide isomerase A3	P30101	↑ LOPD	0.013	33.97	0.5704
392	Vimentin	P08670	↓ LOPD	0.046	41.20	1.279
505	Plastin-2	P13796	↓ LOPD	0.013	178.1	1.132
792	Purine nucleoside phosphorylase	P00491	↑ LOPD	0.013	467.5	2.894
940	Glutathione S-transferase P	P09211	↑ LOPD	0.016	-22.84	0.2074
1787	PDCD6 interacting protein	Q8WUM4	↑ LOPD	0.047	559.0	1.144

Spot combinations were significantly different in LO PD patients with respect to EO PD patients (Wilcoxon test, p = 0.006, Fig 17B), with a cutoff value of 11.0. To effectively test the performance of the model, we performed the "leave-one-out" procedure described above and obtained 71% sensitivity and 100% specificity. Predictions obtained so far were used to build a ROC curve with an area under curve of 0.911 (Fig. 17C).

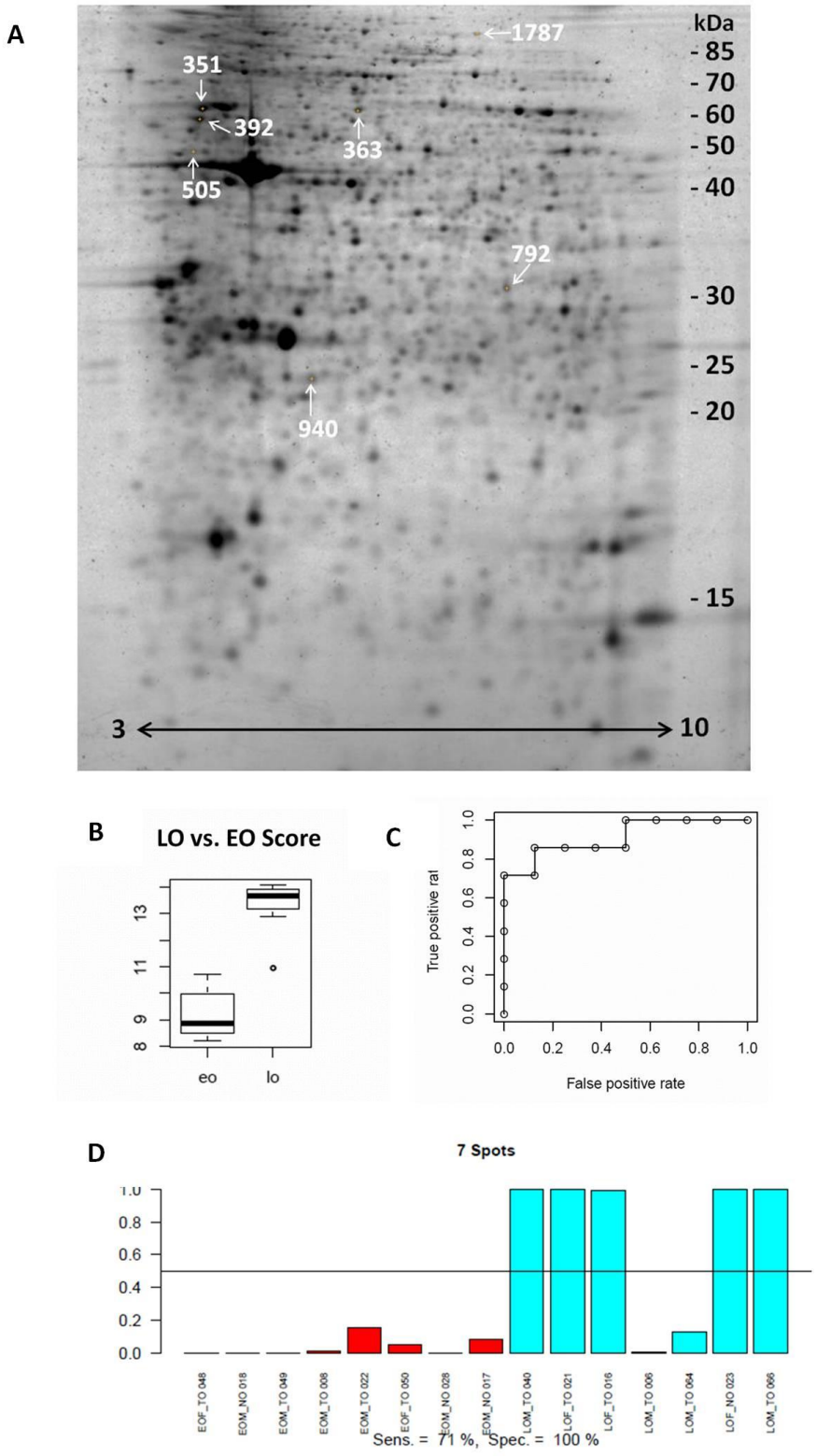

Fig. 17: Panel A: position in the 2-DE map of the 7 proteins showing different levels in EOPD respect to LOPD. Panel B and C: definition of a clinical subtype predictive model by linear discriminant analysis. The scoring function yields LO vs. EO classification scores (B) and the ROC curve obtained by the leave-one-out cross-validation (C).
Panel D: prediction of single patients. The bars represent the predicted probability of a patient to be a EOPD patient (red), or a LOPD patient (blue), calculated with the scoring function obtained with the other 14 subjects. The true identity of each subject is indicated in its code and refers to codes expounded in Table 3.

4.5 Dopaminergic therapies modulate T cell proteome of PD patients

To evaluate the possible effect of dopaminergic therapy on T-lymphocyte proteome, relative volumes of spots from the 2-DE maps were analyzed by the non-parametric Wilcoxon test to find significant differences in patients with PD treated or not with dopamine agonists (Ropinirole, Pramipexole or Rotigotine). Seven spots were found to vary significantly as a function of the treatment with dopamine agonists: they were identified by LC/MS-MS as prolidase, actin-related protein 2, F-actin capping protein subunit beta, tropomyosin alpha-3 chain, proteasome activator complex subunit 1, peroxiredoxin 6 and an isoform of glyceraldehyde-3-phosphate dehydrogenase (GAPDH). Fig 18 summarize the changes in terms of box-and-whiskers plots.

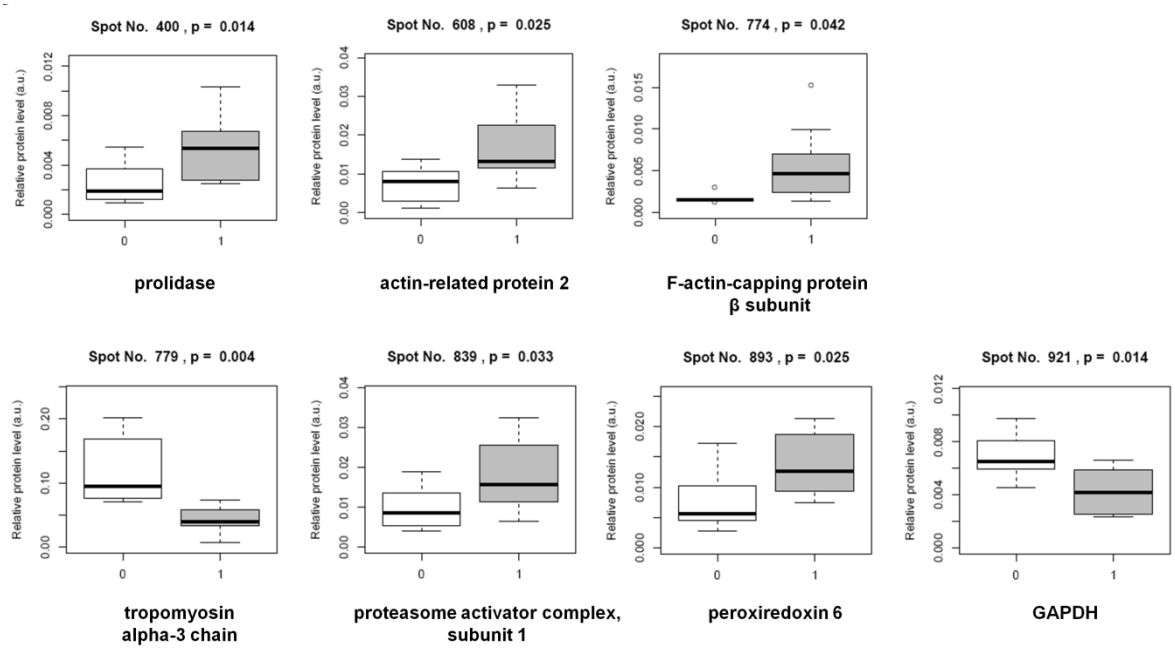

Fig. 18: Box-and-whiskers plots of spots whose relative volume is significantly different in patients under DA agonist therapy (1) with respect to patients assuming no DA agonists (0). p Values refer to the non-parametric Wilcoxon test.

The occurrence of any correlation between spot levels and daily L-DOPA dose was evaluated by Pearson's linear correlation [Eq. (1)]. Among the detected spots, two of them (ATP synthase subunit beta and proteasome subunit beta type-2) displayed a significant linear correlation with the dose of L-DOPA assumed daily by each subject (Fig. 19).

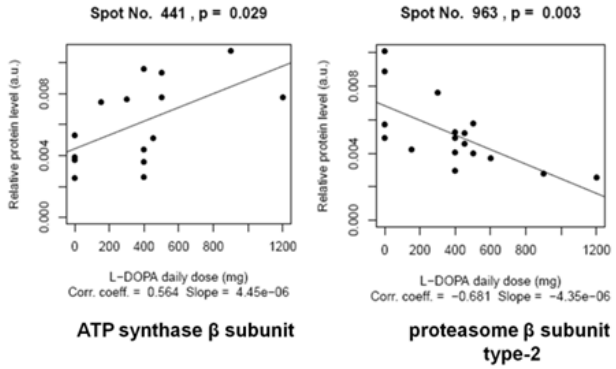

Fig. 19: linear correlation of spot 441 and spot 963 relative volumes to the L-DOPA daily dose (mg). p Values refer to Pearson's correlation analysis. The Pearson correlation coefficient and the slope of the straight line are indicated below the graphs.

Identification by LC/MS-MS of proteins correlating with dopaminergic therapy are reported in Table 13, while their position in a representative 2-DE map is showed in Fig. 20. Mass spectrometry identification details are reported Table 15.

Table 13: Identity of proteins showing correlation with dopamine agonist therapy or with L-DOPA daily dose.

Spot No.	Protein name	Uniprot ID	Correlation	P*
400	Prolidase	P12955	Dago[a] ↑	0.014
441	ATP synthase subunit beta, mitochondrial	P06576	L-DOPA ↑	0.029
608	Actin-related protein 2	P61160	Dago ↑	0.025
774	F-actin-capping protein subunit beta	P47756	Dago ↑	0.042
779	Tropomyosin alpha-3 chain	P06753	Dago ↓	0.004
839	Proteasome activator complex subunit 1	Q06323	Dago ↑	0.033
893	Peroxiredoxin 6	P30041	Dago ↑	0.025
921	Glyceraldehyde-3-phosphate dehydrogenase (GAPDH)	P04406	Dago ↓	0.014
963	Proteasome subunit beta type-2	P49721	L-DOPA ↓	0.003

*for protein correlating with dopamine agonist therapy, p values refer to the Wilcoxon test. For spots showing linear correlation with daily L-DOPA dose, P values refer to Pearson's correlation analysis.

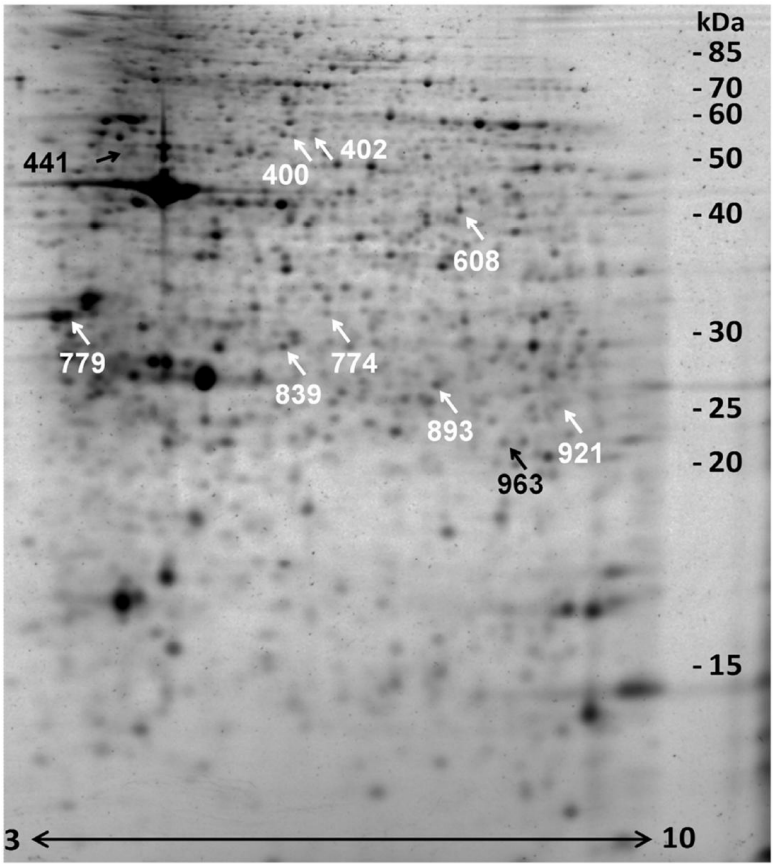

Fig. 20: Position in the 2-DE map of the proteins showing different levels in relation to dopaminergic therapy.
Spots labeled in white are observed to change in patients under dopamine agonist therapy, whereas spots in black are correlated to L-DOPA daily dose.

The minimum number of subjects required to obtain statistical significance of changes, calculated according to Eq. 5, was about four in each group (Table 14).

Table 14: Power analysis of the 7 spots changing according to Dago therapy, showing the minimum number of subjects to be included in validation studies**.**

Spot	Subjects
400	3
608	3
774	3
779	2
839	4
893	3
921	2

4.6 Validation of differences by Western Blot

4.6.1 Disambiguation of multiple identifications

In the LC-MS/MS identification of selected protein spots, a few double assignments occurred. In most cases, we refined them by matching with reference 2-DE maps (see Methods). In the case the ambiguous assignment was not resolved by matching, we checked the correct assignment by western blotting.

Spot 382, for instance, was not confirmed as α-tubulin by Western Blot (Fig. 21) and therefore we assigned it to filamin-A, the second LCMS/MS identification with significant mascot score. Actually, alpha-tubulin is a highly abundant protein that localizes in the close proximity of spot 382, thus a contamination is expected to take place.

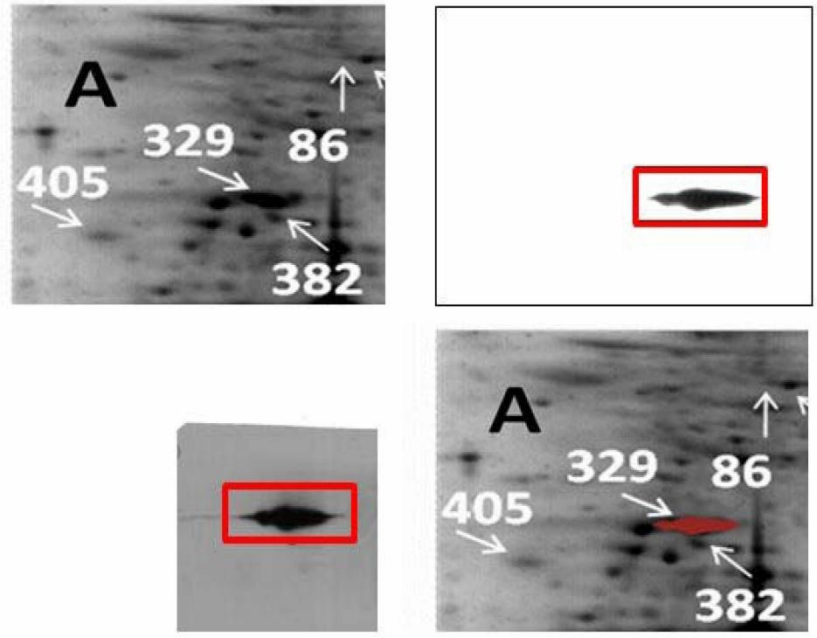

Fig. 21: Verification of spot 382 as alpha-tubulin. Upper left: a detail of the original 2-DE map as shown in Figure 1. Lower left: antialpha-tubulin Western blot, with the region of interest in the red box. Upper right: registered Western blot after background subtraction and rescaling of the area boundaries using molecular weight markers and the anti-beta-fibrinogen Western blot as landmarks, with the corresponding region of interest in the red box. Lower right: overlay of the 2-bit Western blot (in red) with the original 2-DE map region.

In a similar case, we ambiguously assigned spot 598 to serpin B9 and moesin. Western blot validation displayed that serpin B9 has a different localization on the 2-DE map (Fig. 22) and a repeated LC-MS/MS identification allowed us to assign its identity to moesin unambiguously.

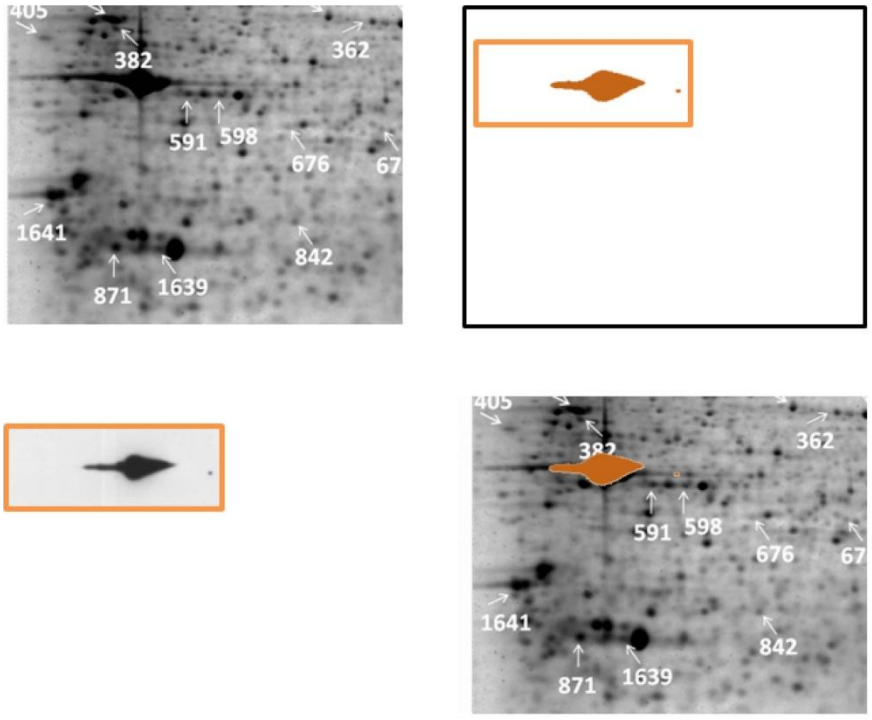

Fig. 22: Verification of spot 598 as serpin B9. Upper left: a detail of the original 2-DE map as shown in Figure 1. Lower left: anti betaactin (left) and anti-serpin B9 (small spot on the right) Western blot, with the region of interest in the orange box. Upper right: registered Western blot after background subtraction and rescaling of the area boundaries using molecular weight markers, the anti-beta-fibrinogen Western blot and the anti-beta-actin Western blot as landmarks, with the corresponding region of interest in the orange box. Lower right: overlay of the 2-bit Western blot (in orange) with the original 2-DE map region.

4.6.2 Total beta-fibrinogen levels are reduced in PD patients

We clustered spot groups by aggregative nesting according to Pearson correlation (Fig. 23). Spots 362, 365, 368 and 369, all corresponding to β-fibrinogen, were clustered in a single outgroup, showing the most stringent similarity among spots considered in each model. To verify their proper identification and confirm the differences observed by 2-DE with another technique, we measured total β-fibrinogen levels by Western blotting in three control subjects and three PD patients, taken from the training set, and correlated them to the sum of relative volumes for spots 362, 365, 368 and 369 ($r = 0.927$; $p = 0.003$). Downregulation of β-fibrinogen involves all 2-DE isoforms, without an appreciable qualitative change of the pattern (Fig. 24).

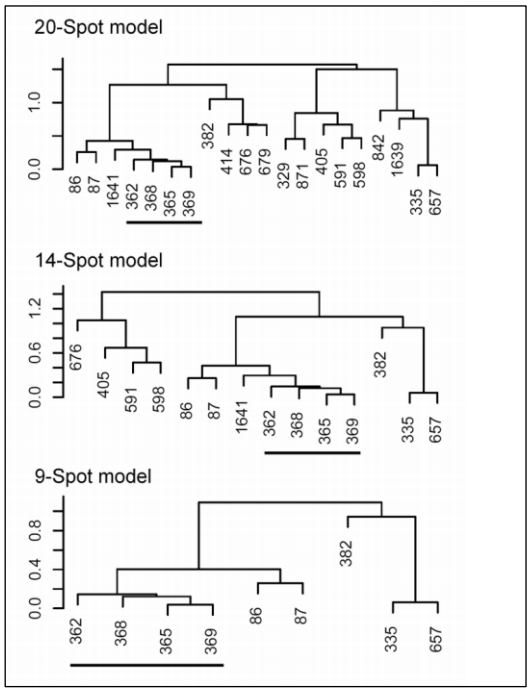

Fig. 23: Aggregated nesting based on linear Pearson correlation (Eq. 1) of relative volumes of spot pairs. Bars indicate clustering of the four β-fibrinogen spots.

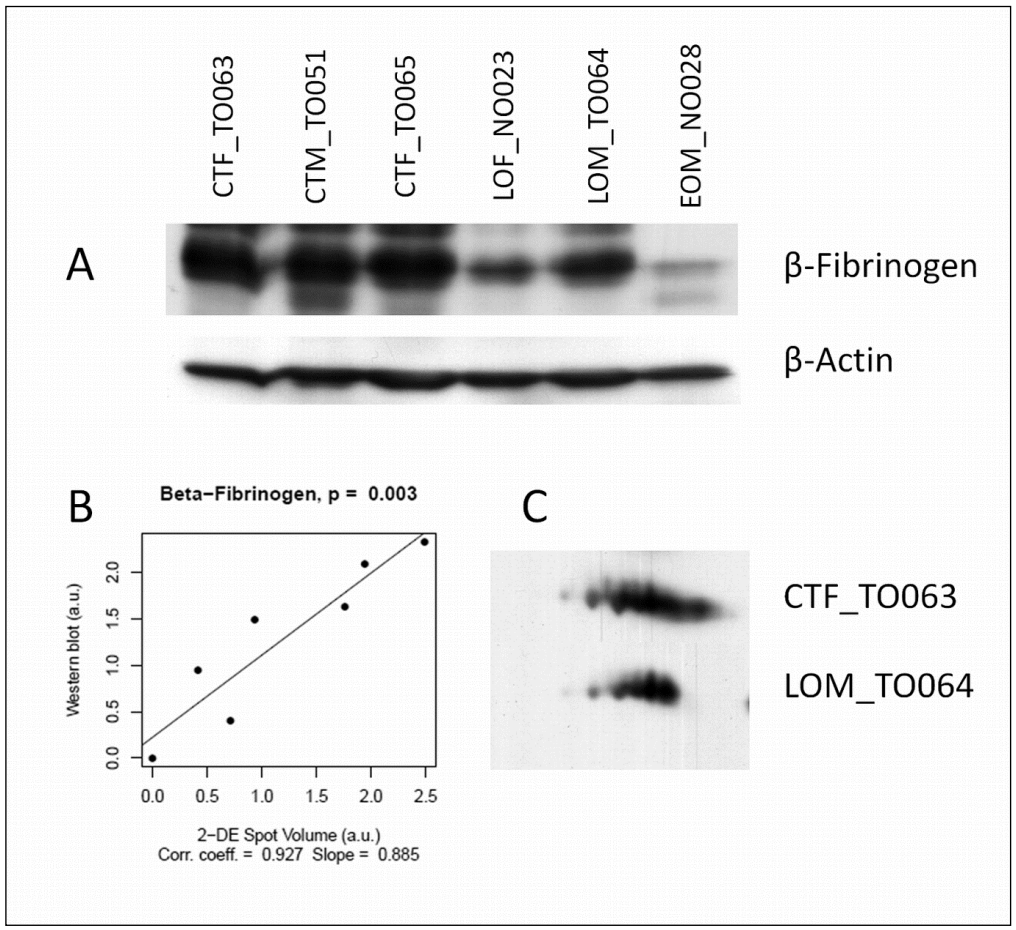

Fig. 24: Western blotting validation of beta fibrinogen. Panel A: Western blotting of total β-fibrinogen from six subjects selected among those enrolled in the biomarker discovery study. Panel B: Linear correlation of total β-fibrinogen levels as measured by 2-DE spot volume and by Western blotting. The correlation coefficient is calculated according to Eq. 1. Panel C: Two representative 2-DE Western blotting experiments.

4.6.3 Total transaldolase levels are increased in PD patients

Spots 676 and 679, both corresponding to transaldolase, showed increased levels in PD patients by 2-DE quantification and close correlation by aggregative nesting (Fig. 20). To confirm this finding we evaluated transaldolase expression by two-dimensional Western blotting. Fig. 25 shows the characteristic 2-DE pattern of transaldolase, with two trains of spots at different apparent molecular weight. In particular, its pattern was altered in three PD patients (two LO PD and one EO PD) with respect to three control subjects (two healthy subjects and one with atypical parkinsonism), patients showing a higher abundance of the higher molecular weight isoforms.

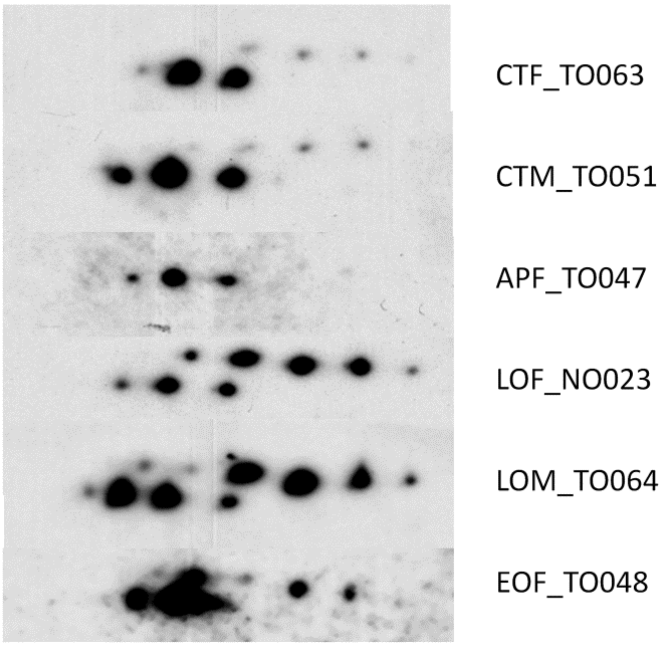

Fig. 25: Two-dimensional Western blotting of transaldolase, showing two distinct pI distributions at different MW. Samples have been selected in the training set among those showing larger discrepancies in the 2-DE quantification to validate the correct assignment of protein spots.

4.6.4 Validation of proteins changing with dopaminergic therapy

The level change of both prolidase and peroxiredoxin 6 was validated by Western blotting, thus confirming results obtained by 2-DE experiments and mass spectrometry identifications. Fig. 26 reports representative two-dimensional Western blots of prolidase (Fig. 26A) and peroxiredoxin 6 (Fig. 26B) in PD patients assuming (Dago+) or not (Dago-) dopamine agonists. Relative protein levels were quantified with respect to β-actin and correlated to relative protein levels measured by RuBPS

staining in 2-DE gels (Fig. 27). Remarkably, the identity of ATP synthase subunit beta, F-actin capping protein subunit beta, tropomyosin alpha-3 chain and proteasome activator complex subunit 1 was assumed to be unambiguous on the basis of accurate matching with the reference 2-DE annotated map of human lymphocytes in the swiss-2dpage database (http://world-2dpage.expasy.org/swiss-2dpage; entry LYMPHOCYTE_HUMAN; see Methods).

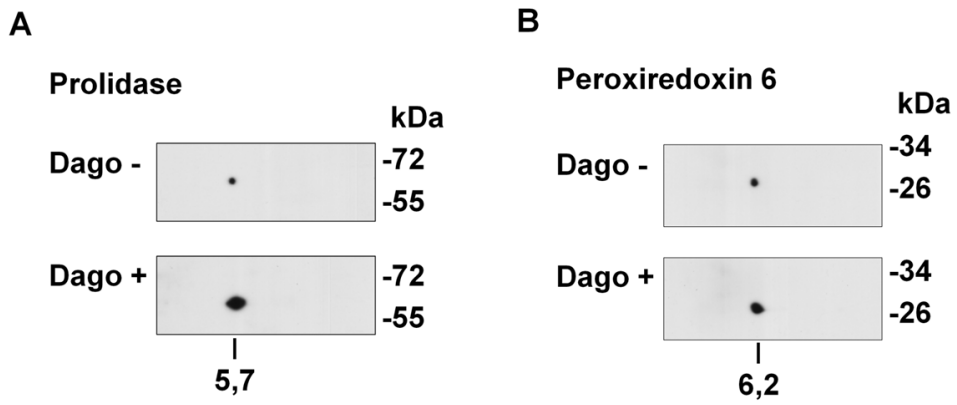

Fig. 26: Western blot validation of prolidase and peroxiredoxin 6 altered levels. Panel A: representative Western blot of prolidase in patients under dopamine agonists treatment (Dago+) with respect to patients that do not assume dopamine agonists (Dago-). Panel B: representative Western blot of peroxiredoxin 6 in patients under dopamine agonists treatment (Dago+) with respect to patients that do not assume dopamine agonists (Dago-).

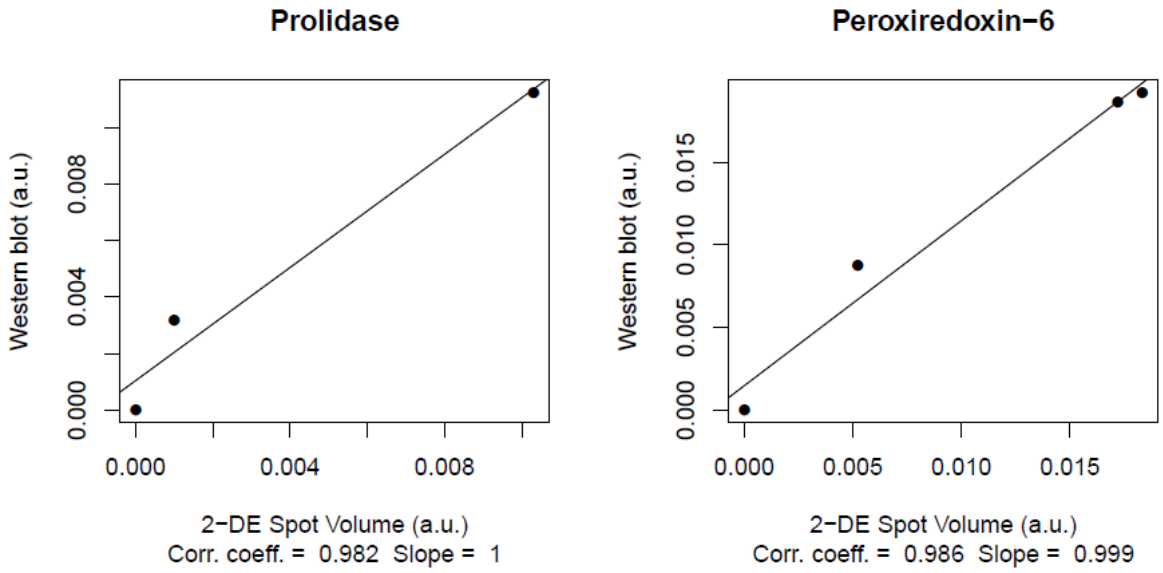

Fig. 27: Quantitative validation of prolidase and peroxiredoxin-6 expression. Protein levels (arbitrary units) measured by Western blotting are quantified with respect to β-actin and correlated to protein levels (arbitrary units) measured by 2-DE and RuBPS staining.

4.7 Further investigations on beta fibrinogen

4.7.1 T lymphocytes and PBMC do not express beta fibrinogen.

Since four spots with high weight were all identified as beta fibrinogen (Table 10) and since, after aggregative nesting, they showed stringent similarity (Fig. 23), we decided to deepen into this change, even because little is known about the link between beta fibrinogen, or fibrinogen in general, and T lymphocytes (or lymphocytes in general) (Ugarova and Yakubenko, 2001; Jennewein et al., 2011).

Through RT-PCR we investigated the possibility that T lymphocytes or total PBMC from human subjects constitutively express beta fibrinogen (FGB). The experiment was simultaneously conducted also on Hep G2 cells, as a positive control. The expression for FGB at the transcriptional level was not detected for both T lymphocytes and PBMC (Fig. 28), despite of positive detection of FGB in HepG2 cells. The expression of GAPDH in all cell types guaranteed the accuracy of the procedure used.

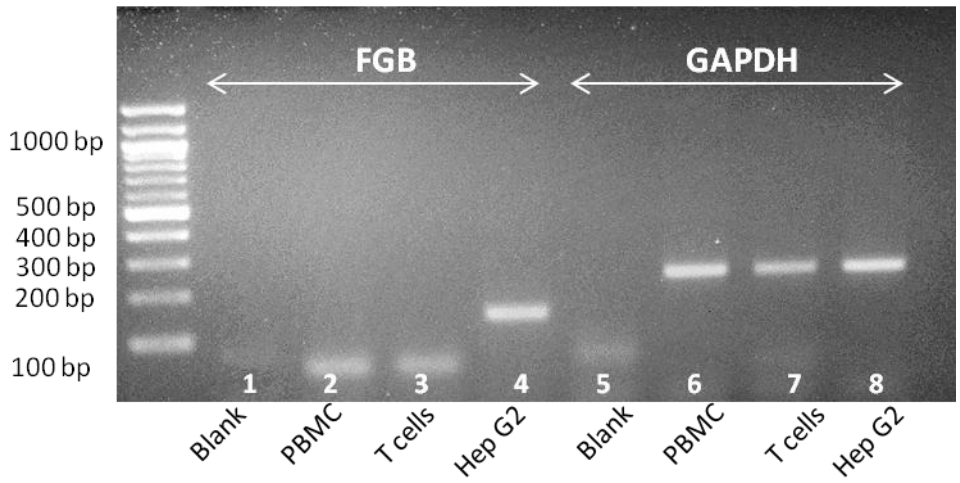

Fig. 28: Expression at the transcriptional level of FGB and GAPDH (housekeeping) in PBMC, T lymphocytes and Hep G2 (positive control). Bands are visualized on a 2% agarose gel stained with ethidium bromide after RNA extraction, reverse transcription and PCR amplification.
Lanes 1 and 5: blank for FGB and GAPDH primers, respectively.
Lanes 2 and 6: PMBC from human subjects for FGB and GAPDH primers, respectively.
Lanes 3 and 7: T Lymphocytes for FGB and GAPDH primers, respectively.
Lanes 4 and 8: Hep G2 cells for FGB and GAPDH primers, respectively.

4.7.2 Fibrinogen is not present on the cell surface of T lymphocytes.

After being isolated from freshly obtained T lymphocytes, cell surface proteins and non surface proteins were qualitatively detected by Western blotting for beta fibrinogen and for beta tubulin as cytoplasmic marker.

Presence of fibrinogen was detected only in the fraction containing all proteins but surface proteins, while it was not detected in cell surface proteins. Beta tubulin was not detected in the cell surface protein fraction, as expected (Fig. 29).

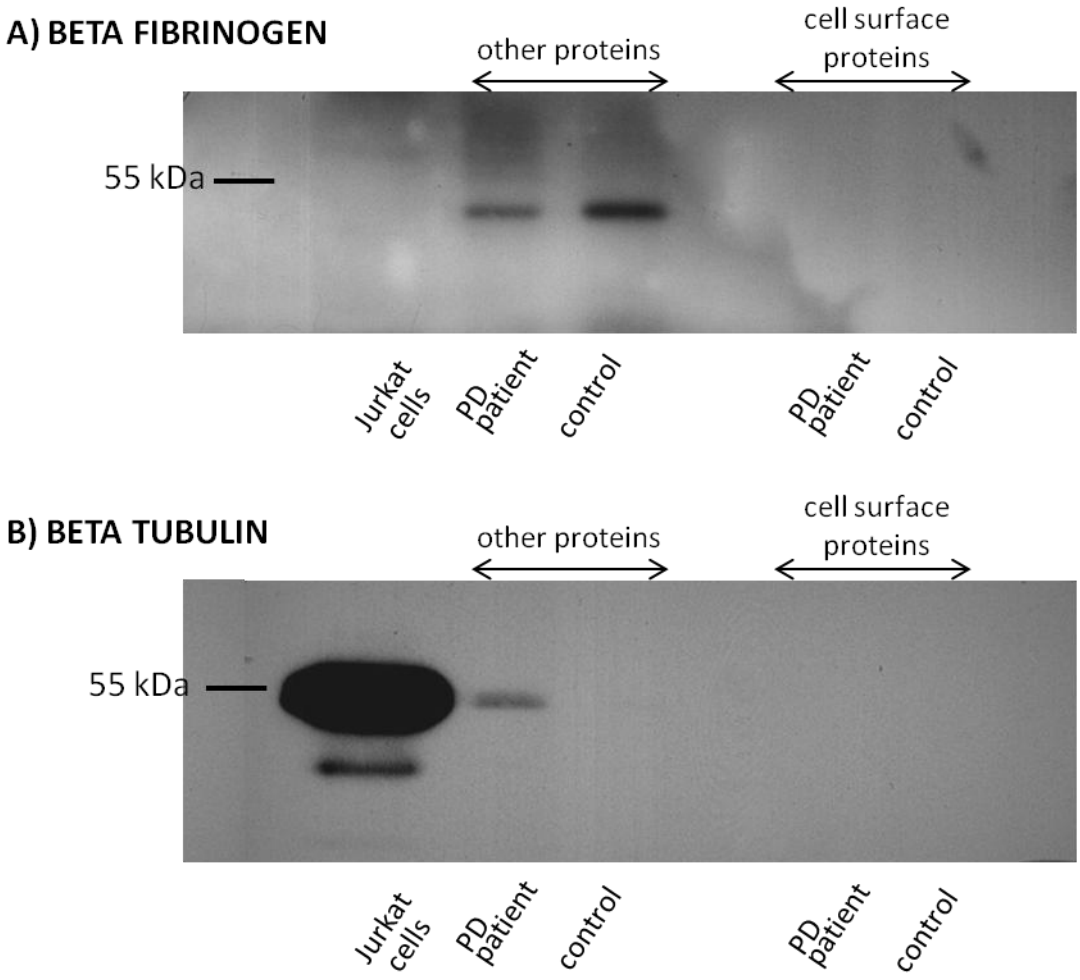

Fig. 29: Western blotting of beta fibrinogen (A) and beta tubulin (B) from cell surface protein fraction and non surface proteins. Samples of T lymphocytes from a PD patient and a control subject were loaded, together with a whole lysate of Jurkat cells as positive (for beta tubulin) and negative (for beta fibrinogen) control.

Table 15: LC-MS-MS identification of proteins.

Spot	Protein name	SwissProt ID	Correlation	Mascot score	Seq Cov (%)	PEPTIDES					Mr. (Da) theor.	pI theor.	Mr. (Da) exp.	pI exp.
						m/z	charge	start-end	sequence	Ion score				
86	Vinculin	P18206	↓PD	230	6	729.41	2+	353–366	AQQVSQGLDVLTAK	29	123668	5.51	110000	5.32
						657.92	2+	465–476	QVATALQNLQTK	37				
						742.98	2+	548–561	VDQLTAQLADLAAR	75				
						587.41	2+	571–581	ALASQLQDSLK	28				
						585.84	2+	670-680	ELTPQVVSAAR	35				
						654.84	2+	709-720	MTGLVDEAIDTK Ox(M)	33				
87	Vinculin	P18206	↓PD	214	17	995.64	2+	88-105	LVQAAQMLQSDPYSVPAR Ox(M)	28	123668	5.51	110000	5.34
						615.33	2+	200-210	ELLPVLISAMK Ox(M)	30				
						615.43	2+	200-210	ELLPVLISAMK Ox(M)	27				
						596.39	2+	237-246	MSAEINEIIR Ox(M)	51				
						755.36	2+	327-339	MLGQMTDQVADLR 2Ox(M)	18				
						755.43	2+	327-339	MLGQMTDQVADLR 2Ox(M)	29				
						729.43	2+	353-366	AQQVSQGLDVLTAK	62				
						553.34	2+	434-444	SLGEISALTSK	38				
						657.92	2+	465-476	QVATALQNLQTK	24				
						742.95	2+	548-561	VDQLTAQLADLAAR	82				
						587.42	2+	571-581	ALASQLQDSLK	35				
						794.49	3+	608-629	LLAVAATAPPDAPNREEVFDER	22				
						585.86	2+	670-680	ELTPQVVSAAR	38				
						585.88	2+	670-680	ELTPQVVSAAR	44				
						654.88	2+	709-720	MTGLVDEAIDTK Ox(M)	33				
						652.42	2+	721-732	SLLDASEEAIKK	32				
						1037.65	2+	739-758	VAMANIQPQMLVAGATSIAR 2Ox(M)	61				
329	Vimentin	P08670	↑PD	816	54	504.38	3+	14-28	MFGGPGTASRPSSSR Ox(M)	16	53520	5.05	60000	5.00
						457.80	2+	29-36	SYVTTSTR	33				
						714.89	2+	51-64	SLYASSPGGVYATR	60				
						794.38	2+	101-113	TNEKVELQELNDR	33				
						558.35	2+	105-113	VELQELNDR	39				
						435.35	2+	114-120	FANYIDK	19				
						435.78	2+	114-120	FANYIDK	20				
						585.43	2+	130-139	ILLAELEQLK	61				
						514.08	3+	130-143	ILLAELEQLKGQGK	26				
						635.81	2+	146-155	LGDLYEEEMR Ox(M)	1				

Spot	Protein name	SwissProt ID	Correlation	Mascot score	Seq Cov (%)	PEPTIDES					Mr. (Da) theor.	pI theor.	Mr. (Da) exp.	pI exp.
						m/z	charge	start-end	sequence	Ion score				
						635.84	2+	146-155	LGDLYEEEMR Ox(M)	17				
						608.85	2+	159-168	RQVDQLTNDK	28				
						852.91	2+	171-184	VEVERDNLAEDIMR Ox(M)	26				
						852.94	2+	171-184	VEVERDNLAEDIMR Ox(M)	30				
						569.05	2+	171-184	VEVERDNLAEDIMR Ox(M)	24				
						660.43	2+	187-196	EKLQEEMLQR Ox(M)	36				
						662.36	2+	197-207	EEAENTLQSFR	35				
						323.19	2+	218-222	LDLER	31				
						767.53	2+	223-235	KVESLQEEIAFLK	82				
						512.28	2+	274-282	QQYESVAAK	21				
						547.33	2+	295-304	FADLSEAANR	43				
						793.13	3+	322-342	QVQSLTCEVDALKGTNESLER Carbamidomethyl (C)	27				
						883.85	2+	365-378	LQDEIQNMKEEMAR 2 Ox (M)	17				
						883.88	2+	365-378	LQDEIQNMKEEMAR 2 Ox(M)	29				
						561.31	2+	382-390	EYQDLLNVK	27				
						656.37	2+	391-401	MALDIEIATYR Ox(M)	52				
						530.83	2+	402-410	KLLEGEESR	28				
						466.80	2+	403-410	LLEGEESR	9				
						466.81	2+	403-410	LLEGEESR	36				
						834.95	2+	425-439	ETNLDSLPLVDTHSK	7				
						557.07	3+	425-439	ETNLDSLPLVDTHSK	14				
						587.47	2+	441-450	TLLIKTVETR	8				
335	Talin-1	Q9Y490	↓PD	139	4	435.83	2+	278-284	KIFQAHK	12	269767	5.77	60000	5.98
						728.48	2+	828-841	ILAQATSDLVNAIK	34				
						728.99	2+	828-841	ILAQATSDLVNAIK	11				
						708.92	2+	2044-2057	LAQAAQSSVATITR	70				
						494.88	2+	2090-2099	ALGDLISATK	49				
						614.37	2+	2105-2115	VGDDPAVWQLK	24				
						602.93	2+	2120-2130	VMVTNVTSLLK	51				
						610.94	2+	2120-2130	VMVTNVTSLLK Ox(M)	56				
						570.88	2+	2145-2154	ALEATTEHIR	24				
						570.93	2+	2145-2154	ALEATTEHIR	23				
						516.31	2+	2351-2361	SIAAATSALVK	31				
						516.35	2+	2351-2361	SIAAATSALVK	22				
						730.42	2+	2430-2443	QVAASTAQLLVACK Carbamidomethyl (C)	45				
351	Beta tubulin	P07437	↑LOPD	100	22	651.38	2+	47-58	ISVYYNEATGGK	29	49671	4.78	68000	4.98

Spot	Protein name	SwissProt ID	Correlation	Mascot score	Seq Cov (%)	PEPTIDES					Mr. (Da) theor.	pI theor.	Mr. (Da) exp.	pI exp.
						m/z	charge	start-end	sequence	Ion score				
						808.55	2+	63-77	AILVDLEPGTMDSVR	19				
						816.49	2+	63-77	AILVDLEPGTMDSVR Ox(M)	18				
						668.38	2+	163-174	IMNTFSVVPSPK Ox(M)	52				
						565.85	2+	242-251	FPGQLNADLR	13				
						565.86	2+	242-251	FPGQLNADLR	15				
						629.92	2+	242-252	FPGQLNADLRK	14				
						644.45	2+	252-262	KLAVNMVPFPR Ox(M)	14				
						580.38	2+	253-262	LAVNMVPFPR Ox (M)	15				
						580.38	2+	253-262	LAVNMVPFPR Ox (M)	52				
						819.02	2+	263-276	LHFFMPGFAPLTSR Ox(M)	44				
						546.37	3+	263-276	LHFFMPGFAPLTSR Ox(M)	25				
						830.55	2+	283-297	ALTVPELTQQVFDAK	43				
						554.04	3+	283-297	ALTVPELTQQVFDAK	15				
						520.36	2+	310-318	YLTVAAVFR	16				
362	Fibrinogen beta chain	P02675	↓PD	176	16	795.78	3+	247-267	KGGETSEMYLIQPDSSVKPYR	14	55928	8.54	56000	6.20
						893.42	2+	314-328	NYCGLPGEYWLGNDK Carbamidomethyl (C)	24				
						846.44	2+	335-348	MGPTELLIEMEDWK	38				
						846.44	2+	335-348	MGPTELLIEMEDWK	15				
						620.32	2+	427-436	EDGGGWWYNR	13				
						620.33	2+	427-436	EDGGGWWYNR	35				
						834.89	3+	446-458	YYWGGQYTWDMAK	46				
						842.88	2+	446-458	YYWGGQYTWDMAK Ox(M)	23				
						516.84	2+	484-491	IRPFFPQQ	18				
363	Protein disulfide-isomerase A3	P30101	↑LOPD	182	14	820.40	2+	1-14	SDVLELTDDNFESR	17	56782	5.98	56000	5.64
						820.40	2+	1-14	SDVLELTDDNFESR	27				
						596.34	2+	39-49	LAPEYEAAATR	26				
						596.35	2+	39-49	LAPEYEAAATR	37				
						498.33	2+	107-116	QAGPASVPLR	34				
						594.85	2+	312-320	FVMQEEFSR Ox(M)	43				
						680.35	2+	328-338	FLQDYFDGNLK	25				
						790.45	2+	459-472	EATNPPVIQEEKPK	17				
365	Fibrinogen beta chain	P02675	↓PD	71	7	651.20		54-72	EEAPSLRPAPPPISGGGYR	39	55928	8.54	56000	6.37
						422.85		200-206	SILENLR	26				
						654.82		301-313	QGFGNVATNTDGK	9				
368	Fibrinogen beta	P02675	↓PD	NA[a]							55928	8.54	56000	7.00

Spot	Protein name	SwissProt ID	Correlation	Mascot score	Seq Cov (%)	PEPTIDES					Mr. (Da) theor.	pI theor.	Mr. (Da) exp.	pI exp.
						m/z	charge	start-end	sequence	Ion score				
	chain													
369	Fibrinogen beta chain	P02675	↓PD	79	4	884.93	2+	164 – 178	DNENVVNEYSSELEK	58	55928	8.54	56000	6.70
						516.79	2+	484 - 491	IRPFFPQQ	22				
382	Filamin-A	P21333	↓PD	81	1	713.92	2+	2230 - 2245	EAGAGGLAIAVEGPSK	55	280608	5.70	58000	5.00
						631.36	2+	2300 - 2311	LTVSSLQESGLK	27				
392	Vimentin	P08670	↓LOPD	151	29	748.43	2+	37-50	TYSLGSALRPSTSR	6	53520	5.05	56000	4.98
						714.87	2+	51-64	SLYASSPGGVYATR	41				
						794.45	2+	101-113	TNEKVELQELNDR	25				
						558.34	2+	105-113	VELQELNDR	28				
						558.36	2+	105-113	VELQELNDR	39				
						435.78	2+	114-120	FANYIDK	22				
						585.38	2+	130-139	ILLAELEQLK	71				
						635.83	2+	146-155	LGDLYEEEMR Ox(M)	40				
						852.92	2+	171-184	VEVERDNLAEDIMR Ox(M)	23				
						568.95	3+	171-184	VEVERDNLAEDIMR Ox(M)	4				
						546.80	2+	176-184	DNLAEDIMR Ox(M)	30				
						662.36	2+	197-207	EEAENTLQSFR	44				
						767.47	2+	223-235	KVESLQEEIAFLK	43				
						547.31	2+	295-304	FADLSEAANR	42				
						547.33	2+	295-304	FADLSEAANR	14				
						561.35	2+	382-390	EYQDLLNVK	16				
						656.36	2+	391-401	MALDIEIATYR Ox(M)	8				
						656.36	2+	391-401	MALDIEIATYR Ox(M)	63				
400	Prolidase	P12985	↑Dago	56	6	727.77	3+	36 – 56	KNPAVQAGSIVVLQGGEETQR	22	54348	5.47	55000	5.70
						561.32	2+	188-196	TDMELEVLR	29				
405	Lymphocyte-specific protein 1	P33241	↑PD	133	21	630.84	2+	2-13	AEASSDPGAEER Acetyl (Protein N-term)	41	37192	4.69	55000	4.70
						955.45	3+	140-166	EGPGPEDTVQDNLGAAGAEEEQEEHQK	36				
						608.92	3+	195-204	LIDRTESLNR	17				
						492.85	2+	215-223	SQPDLPISK	17				
						774.95	2+	247-261	QASIELPSMAVASTK Ox(M)	22				
414	Septin-6	Q14141	↑PD	82	8	643.85	2+	56-66	STLMDTLFNTK Ox(M)	14	49585	6.25	53000	6.45
						643.85	2+	56-66	STLMDTLFNTK Ox(M)	19				
						461.79	2+	164-171	SLDLVTMK Ox(M)	17				
						490.94	2+	177-185	VNIIPIIAK	21				
						569.31	2+	388-397	SLDDEVNAFK	25				

Spot	Protein name	SwissProt ID	Correlation	Mascot score	Seq Cov (%)	PEPTIDES					Mr. (Da) theor.	pI theor.	Mr. (Da) exp.	pI exp.
						m/z	charge	start-end	sequence	Ion score				
441	ATP synthase subunit beta, mitochondrial	P06576	↑L-DOPA	135	10	825.58	2+	95 - 109	LVLEVAQHLGESTVR	34	56525	5.26	50000	5.17
						450.63	2+	125 – 133	VLDSGAPIK	22				
						520.20	2+	134 - 143	IPVGPETLGR	27				
						488.04	2+	202 - 212	IGLFGGAGVGK	14				
						720.11	2+	282 - 294	VALTGLTVAEYFR	38				
505	L-plastin variant	Q59GX5	↓LOPD	88	12	707.45	2+	5-16	GSVSDEEMMELR 2Ox(M)	11	55718	5.21	45000	4.98
						947.05	2+	53-69	EITENLMATGDLDQDGR Ox(M)	22				
						759.48	2+	167-179	MINLSVPDTIDER Ox(M)	37				
						583.61	2+	255-264	EGESLEDLMK Ox(M)	10				
						535.08	2+	265-273	LSPEELLLR	8				
591	Vimentin	P08670	↑PD	59	2	656.38	2+	391 – 401	MALDIEIATYR Ox(M)	59	53520	5.05	42000	5.45
598	Moesin	P26038	↑PD	230	11	658.55	2+	296-306	KPDTIEVQQMK	14	67689	6.09	42000	5.60
						494.14	2+	372-379	ALELEQER	46				
						494.15	2+	372-379	ALELEQER	46				
						444.21	2+	401-408	EALLQASR	20				
						482.16	2+	428-435	ISQLEMAR	41				
						617.03	2+	439-448	ESEAVEWQQK	27				
						595.61	2+	449-458	AQMVQEDLEK	40				
						603.65	2+	449-458	AQMVQEDLEK Ox(M)	37				
						516.12	3+	538-550	KTANDMIHAENMR Ox(M)	12				
						468.13	3+	539-550	TANDMIHAENMR	33				
						710.03	2+	539-550	TANDMIHAENMR Ox(M)	37				
608	Actin-related protein 2	P61160	↑Dago	119	8	675.49	2+	54 - 65	DLMVGDEASELR Ox(M)	41	8	6.30	40000	6.30
						675.51	2+	54 - 65	DLMVGDEASELR Ox(M)	28				
						892.49	2+	66 – 80	SMLEVNYPMENGIVR Ox(M) *Met->Phe (M)*	51				
						400.63	2+	181 - 187	RLDIAGR	29				
						400.67	2+	181 - 187	RLDIAGR	30				
657	Gelsolin	P06396	↓PD	78	5	660.35	2+	534-546	AGALNSNDAFVLK	21	82959	5.72	38000	5.80
						660.43	2+	534-546	AGALNSNDAFVLK	23				
						919.51	2+	547-564	TPSAAYLWVGTGASEAEK	29				
						444.35	2+	565-572	TGAQELLR	29				
676	Transaldolase	P37837	↑PD	54	3	607.43	2+	259 - 269	LLGELLQDNAK	54	37540	6.36	37000	5.78
679	Transaldolase	P37837	↑PD	138	13	638.79	2+	143-154	LSSTWEGIQAGK	17	37540	6.36	37000	6.30
						491.29	2+	231-239	TIVMGASFR	26				
						696.86	2+	246-258	ALAGCDFLTISPK Carbamidomethyl (C)	58				

Spot	Protein name	SwissProt ID	Correlation	Mascot score	Seq Cov (%)	PEPTIDES					Mr. (Da) theor.	pI theor.	Mr. (Da) exp.	pI exp.
						m/z	charge	start-end	sequence	Ion score				
						696.86	2+	246-258	ALAGCDFLTISPK Carbamidomethyl (C)	36				
						607.39	2+	259-269	LLGELLQDNAK	30				
						607.48	2+	259-269	LLGELLQDNAK	36				
774	F-actin-capping protein subunit beta	P47756	↑Dago	76	8	562.40	3+	146 – 159	GCWDSIHVVEVQEK+Carbamidomethyl (C)	57	30609	5.69	30000	5.8
						586.18	2+	226 - 235	STLNEIYFGK	19				
779	Tropomyosin alpha-3 chain	P06753	DAgo ↓	723	64	601.0000	2+	2 - 12	AGITTIEAVKR	29	29015	4.75	30000	4.75
						600.8100	2+	2 - 12 2 -	AGITTIEAVKR	13				
						600.9900	2+	12 13 – 27	AGITTIEAVKR	25				
						885.9800	2+	14 – 27	KIQVLQQQADDAEER	15				
						821.9200	2+	14 - 27	IQVLQQQADDAEER	69				
						821.9300	2+	43 - 54	IQVLQQQADDAEER	46				
						658.8400	2+	43 - 55	EQAEAEVASLNR	28				
						491.6800	3+	56 - 69	EQAEAEVASLNRR	7				
						576.7400	3+	70 - 76	IQLVEEELDRAQER	21				
						372.8200	2+	70 – 82	LATALQK	39				
						722.4200	2+	77 - 89	LATALQKLEEAEK	60				
						738.8400	2+	105 – 113	LEEAEKAADESER	68				
						566.3800	2+	105 - 113	MELQEIQLK	45				
						574.3700	2+	132 - 142	MELQEIQLK	31				
						642.9100	2+	143 - 153	KLVIIEGDLER	62				
						645.8200	2+	143 - 153	TEERAELAESR	26				
						645.8600	2+	154 - 162	TEERAELAESR	25				
						618.8300	2+	163 - 169	CREMDEQIR	38				
						431.3400	2+	163 - 169	LMDQNLK	25				
						431.3400	2+	163 - 169	LMDQNLK	42				
						439.2800	2+	163 - 169	LMDQNLK	36				
						439.3000	2+	191-197	LMDQNLK	41				
						415.8900	2+	198 - 208	ILTDKLK	32				
						654.8000	2+	203 – 208	EAETRAEFAER	17				
						361.6800	2+	203 – 208	AEFAER	19				
						361.7000	2+	203 – 208	AEFAER	20				
						361.7600	2+	216 –225	AEFAER	42				
						595.4300	2+	237 - 248	TIDDLEDKLK	44				
						726.4400	2+		MLDQTLLDLNEM	50				
792	Purine nucleoside	P00491	↑LOPD	78	9	604.86	2+	124 - 133	FEVGDIMLIR Ox(M)	41	32117	6.45	32000	6.35

Spot	Protein name	SwissProt ID	Correlation	Mascot score	Seq Cov (%)	PEPTIDES					Mr. (Da) theor.	pI theor.	Mr. (Da) exp.	pI exp.
						m/z	charge	start-end	sequence	Ion score				
	phosphorylase					900.99	2+	212 - 229	LGADAVGMSTVPEVIVAR Ox(M)	37				
839	Proteasome activator complex subunit 1	Q06323	↑Dago	121	24	582.37	2+	36 - 45	KISELDAFLK	21	28705	5.78	30000	5.64
						706.90	2+	46 - 58	EPALNEANLSNLK	47				
						630.94	2+	59 - 70	APLDIPVPDPVK	14				
						630.94	2+	59 - 70	APLDIPVPDPVK	69				
						759.46	2+	59 - 72	APLDIPVPDPVKEK	28				
						506.69	2+	59 - 72	APLDIPVPDPVKEK	39				
						760.39	2+	142 - 155	IEDGNNFGVAVQEK	26				
						760.42	2+	142 - 155	IEDGNNFGVAVQEK	35				
						661.34	2+	156 - 166	VFELMTSLHTK	14				
						462.29	2+	214 - 220	LMVMEIR	26				
842	Twinfilin-2	Q6IBS0	↑PD	45	9	446.64	2+	164 - 171	TEISVESK	21	39417	6.39	30000	5.82
						712.20	3+	210 - 228	ETIELVHTEPTDVAQLPSR	45				
						509.16	2+	236 - 242	YHFFLYK	22				
871	Rho GDP-dissociation inhibitor 2	P52566	↑PD	149	25	647.24	3+	5-21	APEPHVEEDDDDELDSK	12	22857	5.08	25000	5.00
						854.93	2+	34-47	ELQEMDKDDESLIK Ox(M)	30				
						656.39	2+	51-63	TLLGDGPVVTDPK	53				
						656.42	2+	51-63	TLLGDGPVVTDPK	42				
						428.36	2+	64-71	APNVVVTR	54				
893	Peroxiredoxin 6	P30041	↑Dago	176	22	1049.61	2+	2 - 22	PGGLLLGDVAPNFEANTTVGR	33	25019	6.00	26000	6.2
						543.31	2+	98 - 106	LPFPIIDDR	53				
						504.35	2+	133 - 141	VVFVFGPDK	22				
						568.41	2+	133 - 142	VVFVFGPDKK	31				
						596.38	2+	145 - 155	LSILYPATTGR	37				
921	Glyceraldehyde-3-phosphate dehydrogenase (GAPDH)	P04406	↓Dago	195	19	917.54	2+	146 – 162	IISNASCTTNCLAPLAK	85	36031	8.26	25000	7.4
						612.04	3+	146 - 162	IISNASCTTNCLAPLAK	27				
						706.47	2+	201 - 215	GALQNIIPASTGAAK	15				
						406.33	2+	228 - 234	LTGMAFR	20				
						765.92	2+	235 - 248	VPTANVSVVDLTCR	40				
						765.99	2+	235 - 248	VPTANVSVVDLTCR	42				
						609.33	2+	324 - 334	VVDLMAHMASK	25				
						617.35	2+	324 - 334	VVDLMAHMASK	17				
						411.99	3+	324 - 334	VVDLMAHMASK	11				
						665.91	2+	324 - 335	VVDLMAHMASKE	8				
940	Glutathione S-	P09211	↑LOPD	48	25	568.87	2+	46 - 55	ASCLYGQLPK Carbamidomethyl (C)	8	23225	5.44	23000	5.45

Spot	Protein name	SwissProt ID	Correlation	Mascot score	Seq Cov (%)	PEPTIDES					Mr. (Da) theor.	pI theor.	Mr. (Da) exp.	pI exp.
						m/z	charge	start-end	sequence	Ion score				
	transferase P					942.54	2+	56 - 71	FQDGDLTLYQSNTILR	48				
						376.24	2+	76 - 82	TLGLYGK	26				
						1063.63	2+	122 - 141	ALPGQLKPFETLLSQNQGGK	19				
963	Proteasome subunit beta type-2	P49721	↓L-DOPA	134	17	538.71	2+	20 - 29	VAASNIVQMK.D Oxidation (M)	54	22822	6.51	23000	6.6
						806.56	2+	71 - 85	NGYELSPTAAANFTR	59				
						653.60	2+	171 - 181	FILNLPTFSVR	23				
1639	Beta actin[b]	P60709	↓PD	148	14	488.80	2+	19 - 28	AGFAGDDAPR	9	41736	5.28	26000	5.40
						507.84	2+	184 - 191	DLTDYLMK Ox(M)	24				
						566.81	2+	197 - 206	GYSFTTTAER	29				
						896.02	2+	239 - 254	SYELPDGQVITIGNER	29				
						653.34	2+	315 - 326	KEITALAPSTMK Ox(M)	6				
						589.35	2+	316 - 326	EITALAPSTMK Ox(M)	51				
1641	14-3-3 protein epsilon	P62258	↓PD	113	40	630.38	2+	20-29	YDEMVESMKK	20	29174	4.63	30000	4.74
						724.35	2+	30-42	VAGMDVELTVEER	55				
						732.42	2+	30-42	VAGMDVELTVEER Ox(M)	47				
						454.32	2+	43-50	NLLSVAYK	24				
						459.34	2+	62-69	IISSIEQK	21				
						619.37	2+	107-118	HLIPAANTGESK	15				
						628.88	2+	131-141	YLAEFATGNDR	38				
						692.87	2+	131-142	YLAEFATGNDRK	39				
						597.83	2+	143-153	EAAENSLVAYK	28				
						597.84	2+	143-153	EAAENSLVAYK	34				
						910.55	2+	154-170	AASDIAMTELPPTHPIR	23				
						645.36	2+	245-255	EALQDVEDENQ	24				
1787	Programmed cell death 6-interacting protein	Q8WUM4	↑LOPD	43	5	765.99	2+	216 - 229	LANQAADYFGDAFK	43	95892	6.14	100000	6.13
						766.96	2+	457 - 469	LLDEEEATDNDLR	19				
						660.52	2+	542 - 553	TMQGSEVVNVLK Ox (M)	16				
						465.59	2+	708 - 715	DLQQSIAR	14				

a: identification by 2-DE map matching; b: fragment.

5. DISCUSSION

Development and validation of disease-specific biomarkers for the diagnosis of early PD represents one of the most urgent needs in neurology (Shulman et al. 2011). The goal would be to find a reliable biomarker, or a panel of biomarkers, of PD in a peripheral and readily accessible compartment, in order to identify asymptomatic individuals with early-stage disease who may benefit from a neuroprotective or disease-modifying therapeutic intervention.

In addition to sensitive and specific diagnostic biomarkers, there is also an urgent need for reliable surrogate biomarkers that can be used to accurately track progression of the disease. The developing of sensitive, specific, accurate, and reliable biomarkers in clinical trials of new disease-modifying therapies would permit to quantify their effectiveness with contained costs (Graeber 2009).

In this study, we showed that T lymphocytes proteome changes may be a valid measure both to predict the disease state in human subjects and to track progression and duration, but also to classify PD patients in terms of disease subtypes (*e.g.*, EO *vs* LO patients). Our research is based on the rationale that T-cells show common features with dopaminergic neurons, with the clear advantage that peripheral cells are easily accessible, thus rendering them an ideal and amenable source for peripheral PD biomarker discovery.

We supported the strength of such a rationale with our results: T lymphocytes change their proteome as a consequence of PD, a disease affecting dopaminergic neurons, and, notably, also long term dopaminergic therapy induces proteome changes that are expected in cells responsive to dopamine.

The rationale for searching PD biomarker in peripheral blood lymphocytes (PBL) was previously proven by a "proof of principle" investigation conducted on advanced PD patients, where a proteomic profiling based on 2-DE of PBL was able to highlight differences at the peripheral level between patients and control subjects (Mila et al., 2009).

The intrinsic feature of proteomics as a global and unbiased approach allowed us to explore a great universe of candidates without limiting to those that have been related to pathogenesis. In fact, we compared T lymphocyte proteomes in patients and control subjects by looking at whatever protein was showing a significant difference between the groups without knowing proteins' identities; as a consequence, we did not restrict our attention to proteins necessarily linked to any pathological process. However, their change at the peripheral level might reflect a central pathologic state due to modifications in cells (*i.e.*, DA-ergic neurons) with some similar features with respect to the cells we have chosen as a source of biomarkers (*i.e.*, T lymphocytes). Worth of note, the powerful ability of 2-DE to identify quantitative changes in single protein isoforms or post-translational modifications allowed us to go beyond simple quantification of total protein levels.

Considerations about the predictive model.

After having defined 20 spots showing quantitative differences between PD patients and control subjects (WIlcoxon test, $p<0,05$), their relative volumes were combined by LDA to obtain a predictive function able to classify an unknown subject as PD patient or control subject. The ability of this model in predicting PD was evaluated in terms of sensitivity and specificity, reaching a ROC AUC values of 0.906.

This model was ameliorated when spots with lower weight were eliminated. In this way, we obtained a 14 spots- and a 9 spots-model both able to rightly predict thirty of 32 subjects as PD or control subject and ROC AUC values higher than 0.990. Although a validation on a larger cohort of subjects is needed, these values are suggestive of an excellent performance of both models.

The high sensitivity of these predictive functions are certainly due to the significant inter-group differences of some proteins, but the main strength of our model is attributable to on the inclusion of a panel composed by several proteins rather than observing a single biomarker. Indeed, single biomarkers are difficult to identify, often display low specificity, and, especially when proteins are concerned, can be effectively influenced by drugs or habitual factors.

A panel of biomarkers, instead, take into account several targets, that all together increase the specificity of the model, and it is unlikely that a confounding factor can interfere with more than one among the targets involved. Moreover, it is more robust with respect to the great intra-group variability expected in population-wide studies. As an example, high contribution to our model is given by four spots all corresponding to beta fibrinogen (see Table 7, spots 362, 365, 368 and 369): even if the weights of these spots are very high, their volumes alone are not able to rightly predict PD with acceptable sensitivity and specificity parameters. Moreover, a high level of fibrinogen in plasma is a marker of acute inflammation, so it would be difficult to assess low levels of the same protein as biomarker of PD, even if measured in T cells and not in plasma.

Performance parameters obtained in this investigation need to be compared to similar biomarker discovery and validation studies appeared in the literature so far. As discussed in the introduction of this thesis, several papers on biomarker discovery are present in the literature, although most of them have not been validated on large scale. In some cases, authors attempted to diagnose PD on the basis of the measurement at the peripheral level of a single protein or gene transcript, but these proposed tests lacked sufficient sensitivity and specificity, or were not confirmed by others (see Morgan et al., 2010; Nyhlén et al., 2010; Alberio and Fasano, 2011; Gerlach et al., 2012). A marked improvement is achieved when two or more biomarkers are measured in order to predict a disease probability based on multiple observations. The panel of four gene transcripts measured in total blood cells of sporadic PD patients and control subjects proposed by Grünblatt and coworkers

showed good performance parameters in the discovery phase (Grünblatt et al., 2010; see Introduction), but, in our opinion, will possibly fail in the validation phase: actually, it is reasonable to expect low reproducibility and, in turn, low sensitivity due to the fact that the gene transcripts were selected on the basis of their altered levels in the SNpc. On this ground, it is unlikely that these genes maintain the observed differential expression in a distinct compartment.

A different comment could be made on biomarkers proposed by Mollenhauer and coworkers (Mollenhauer et al., 2011): they measured concentrations of α-synuclein, tau and total protein in CSF of patients with PD, Alzheimer Disease, Dementia with Lewy bodies, MSA, and non-neurodegenerative neurological disorders (overall patients *n* = 273), defining a very accurate predictive model (ROC AUC = 0.909 for the training set), but in a subsequent validation phase (*n* = 304) the classification of PD patients displayed a reduced ROC AUC of 0.706. Although in this case the rationale for the choice was strong and the number of patients was impressive, we think that the cross-validation performance turned out to be unsatisfactory because the number of targets was small. Moreover, it has to be considered that a study contemplating CSF specimens is more difficult to carry on, due to the discomfort associated with CSF sampling.

One of the most promising studies, still to be validated, is the one proposed by Bogdanov and coworkers, that used an unbiased approach: they proposed a metabolomic profiling that correctly classified PD patients (*n* = 66) and control subjects (*n* = 25) in a cross-validation procedure by permutation test (Bogdanov et al., 2008).

Due to the global approach we used, and the number of targets forming our models, we expect that performance parameters will not worsen significantly in a further clinical validation phase, in particular for the models of 14 and 9 spots because they have higher ROC AUC values. In addition, the model composed by 9 spots is the most suitable for an antibody-based validation test (*e.g.*, ELISA) because of the relatively low number of targets to be measured.

We intentionally avoided to focus on the identity of selected proteins. Indeed, every single protein is far from being a significant element for PD early diagnosis (Alberio and Fasano, 2011; Surinova et al., 2011). However, some considerations about identity of changing protein can be made: some details about their functions and localization are shown in Table 16.

Table 16: List of proteins included in the predictive models, with their relative functions, subcellular localization and tissue specificity. Proteins corresponding to more than one spot are not repeated. Data are taken from Uniprot database.

Protein	Uniprot Id	Function(s)	Subcellular location	Tissue specificity
Vinculin	P18206	Actin filament (F-actin)-binding protein involved in cell-matrix adhesion and cell-cell adhesion. May also play important roles in cell morphology and locomotion. It is the cytoplasmic face of adhesion plaques. Recruitment to cell-cell junctions occurs in a myosin II-dependent manner.	Cytoplasm › cytoskeleton. Peripheral membrane protein; Cytoplasmic side.	Ubiquitous
Vimentin	P08670	Vimentins are class-III intermediate filaments found in various non-epithelial cells, especially mesenchymal cells. Vimentin is attached to the nucleus, endoplasmic reticulum, and mitochondria, either laterally or terminally.	Cytoplasm	Highly expressed in fibroblasts, some expression in T- and B-lymphocytes.
Talin-1	Q9Y490	Probably involved in connections of major cytoskeletal structures to the plasma membrane. High molecular weight cytoskeletal protein concentrated at regions of cell-substratum contact and, in lymphocytes, at cell-cell contacts.	Peripheral membrane protein; cytoplasmic side. Cytoplasm › cytoskeleton (by similarity).	Ubiquitous
Beta-fibrinogen	P02675	Fibrinogen has a double function: yielding monomers that polymerize into fibrin and acting as a cofactor in platelet aggregation.	Secreted.	Plasma, liver
Filamin-A	P21333	Promotes orthogonal branching of actin filaments and links actin filaments to membrane glycoproteins. Anchors various transmembrane proteins to the actin cytoskeleton and serves as a scaffold for a wide range of cytoplasmic signaling proteins. Involved in ciliogenesis.	Cytoplasm › cell cortex. Cytoplasm › cytoskeleton.	Ubiquitous
Lymphocyte-specific Protein 1	P33241	May play a role in mediating neutrophil activation and chemotaxis (by similarity). Binds actin.	Cell membrane; peripheral membrane protein; cytoplasmic side.	Activated T-lymphocytes.
Septin-6	Q14141	Filament-forming cytoskeletal GTPase. Required for normal organization of the actin cytoskeleton. Involved in cytokinesis.	Cytoplasm › cytoskeleton. Chromosome › centromere.	Widely expressed.

Protein	Uniprot Id	Function(s)	Subcellular location	Tissue specificity
Moesin	P26038	Probably involved in connections of major cytoskeletal structures to the plasma membrane.	Peripheral membrane protein; Cytoplasmic side (by similarity)	In all tissues and cultured cells studied.
Gelsolin	P06396	Calcium-regulated, actin-modulating protein that binds to the plus (or barbed) ends of actin monomers or filaments, preventing monomer exchange (end-blocking or capping). It can promote the assembly of monomers into filaments (nucleation) as well as sever filaments already formed. Plays a role in ciliogenesis. Binds to actin and to fibronectin.	Isoform 2: Cytoplasm › cytoskeleton. Isoform 1: Secreted.	Phagocytic cells, platelets, fibroblasts, nonmuscle cells, smooth and skeletal muscle cells.
Transaldolase	P37837	Transaldolase is important for the balance of metabolites in the pentose-phosphate pathway.	Cytoplasm (probable)	-
Twinfilin-2	Q6IBS0	Actin-binding protein involved in motile and morphological processes. Inhibits actin polymerization, likely by sequestering G-actin. By capping the barbed ends of filaments, it also regulates motility. Seems to play an important role in clathrin-mediated endocytosis and distribution of endocytic organelles.	Cytoplasm › cytoskeleton. Cytoplasm › perinuclear region.	Ubiquitously expressed (at protein level).
Rho GDP dissociation inhibitor isoform 2	P52566	Regulates the GDP/GTP exchange reaction of the Rho proteins by inhibiting the dissociation of GDP from them, and the subsequent binding of GTP to them.	Cytoplasm	-
Beta actin fragment	P60709	Actins are highly conserved proteins that are involved in various types of cell motility and are ubiquitously expressed in all eukaryotic cells.	Cytoplasm › cytoskeleton.	-
14-3-3 epsilon	P62258	Adapter protein implicated in the regulation of a large spectrum of both general and specialized signaling pathways. Binds to a large number of partners, usually by recognition of a phosphoserine or phosphothreonine motif. Binding generally results in the modulation of the activity of the binding partner.	Cytoplasm	-

Most of changing proteins are part of the cytoskeleton or are involved in cytoskeletal functions; this is a common finding in proteomic studies (Petrak et al., 2008), due to the considerable size of this structure in cells and relative abundance of most cytoskeleton proteins. In our case it was even more

predictable, as it is reasonable that if T cells sense any alteration (for example due to PD), they respond in adaptation of their prominent functions, that are, among others, ability of extravasation and increase of motility. Some proteins, not related to cytoskeleton, reflect key activities of T cells; for instance, the lymphocyte-specific Protein 1, that participates in signaling with other immune cell types. Other proteins take part to biochemical pathways common to many tissues (transaldolase, 14-3-3 epsilon, Rho GDP dissociation inhibitor isoform 2). On the other hand the presence of beta fibrinogen, expressed only by hepatocytes and present in plasma at high concentration is definitely unexpected (see below).

It would be interesting to investigate the reasons why T cells change levels of these selected proteins as a mirror of the central disease, even if it goes beyond the purpose of our study. However, T cells might not reflect the same alterations present in affected neurons. What we wanted to point out was a protein fingerprinting of the disease state, more than a functional correlation between proteins altered at the central level and those that mirror neurodegeneration at the peripheral level.

Considerations about progression trackers

We demonstrated that a total of 9 spots of the 2-DE gel display linear correlation with parameters such as disease duration (expressed as years from onset) and disease progression (expressed as Hoehn and Yahr score). In particular, four spots correlate with duration, and 8 spots correlate with progression of symptoms; 3 of them correlate with both duration and progression.

Progression of symptoms do not correlate linearly with duration of the disease. In fact, PD is a multifactorial disease and various forms of PD have been reported, being patients classified in different subtypes depending also on the rate of worsening of symptoms or predominance of some symptoms on the others (Shulman et al., 2011). For example, between genetic forms we can distinguish forms characterized by rapid progressive course and frequent development of dementia (*SNCA* mutations forms) or slightly more clinically benign, tremor-predominant forms (*LRRK2* mutation forms).

Moreover, duration of disease is a parameter difficult to measure: the onset of the disease precedes the appearance of symptoms by many years and, when motor symptoms appear, these are recognized by patients in a subjective way. This is especially true for motor signs other than tremor, that might not be associated to PD for a long time. In our opinion, this is the reason why we found only four spots correlating with this parameter; more spots could correlate with duration if it was a more objectively measurable parameter.

Then, we propose two distinct linear functions able to track separately duration and progression. Both of them show discrete correlation coefficients ($r = 0.516$ and 0.674, respectively) with statistical significance ($p = 0.049$ and 0.006), and were improved by adding control subjects at $x = 0$.

To the best of our knowledge, few reports pointed out to molecular biomarkers predictive of PD progression (Mila et al., 2009), whereas some attempts have been made to find correlation between functional imaging biomarkers and disease staging (Marek et al., 2011; Gerlach et al., 2012). Evidence of underlying PD progression before the appearance of motor signs together with an advisable neuroprotective treatment would stop disease progression at the prodromic stage. Given the common features between T-cells and dopaminergic neurons, T-lymphocyte proteome biomarkers may reasonably report on the effectiveness of future (or under development) drugs which would interfere with specific cell death mechanisms that target nigral neurons.

Considerations about classification of PD subtypes

As discussed above, PD is a multifactorial disease, with substantial heterogeneity in its presentation, so that some neurologists argue in favor of abandoning PD as a single clinico-pathologic entity, instead enumerating many subtypes on the basis of varying clinical features, familiality, and autopsy findings (Shulman et al., 2011). Taking again as an example genetic forms, the majority of idiopathic and genetic PD patients display, on autopsy, LB in surviving DA neurons, so that their presence is an hallmark of PD. Nevertheless, absence of Lewy bodies in patients with parkin mutations has been noticed, with clinical signs mostly similar to idiopathic PD (Shulman et al., 2011; Chung et al., 2001).

Considering clinical manifestation, subtypes of patients may be recognized on the basis of the age at the onset, predominant clinical features and the progression rate. Tremor predominant forms are often observed in younger people, while bradikynesia-predominant forms and a type known as “postural imbalance and gait disorder” (PIGD), characterized by akinesia, rigidity, and gait and balance impairment, are often observed in older people (Obeso et al., 2010).

In our study we include “typical” patients, with absence of atypical signs and a good response to L-DOPA. Because of the restricted number of patients included in this study, it would be unproductive subdividing them into various subtypes, so we prefer to verify if spot volume differences correlate with a single, major factor of patients' heterogeneity, the age at onset. In fact, aging is the most important risk factor for developing PD, being only 3% of cases initially recognized in individuals younger than age 50. Moreover, patients with young onset have more frequently a positive family history, this suggesting that genetic forms cause a parkinsonism that manifests earlier, by impairing balance mechanisms that usually delay the onset of symptoms.

We subdivided the PD group into two subgroups, EOPD patients and LOPD patients; the number of components of the two groups was comparable because we specifically enriched the patients group in EOPD patients to highlight possible effects due to the genetic background, as they have increased probability to carry a familiar form of PD respect to PD patients.

We found 7 spots whose volumes statistically changed in the EO and LO PD groups. We performed a linear discriminant analysis on selected spots so to obtain a likelihood score (a linear combination of relative spot volumes) able to correctly classify EO PD patients (ROC AUC = 0.911; Fig. 17), with the same "leave-one-out" procedure described and discussed above for the three predictive models. The fact that we were able to distinguish two subtypes of PD patients by analyzing the T cells proteome in a relatively small number of patients allows us to confirm that T-lymphocyte proteome changes are a valid tool to correctly classify PD patients.

In the validation phase of this project, the enrolment of a larger number of patients will allow us to evaluate the possibility to classify PD patients in terms of clinical subtypes, aiming at a personalized therapy.

Moreover, as the younger onset is often a signal of a possible genetic cause of the disease, our discrimination of EO/LO patients could also be seen as an potential tool to discriminate familial and sporadic forms of the disease. The effectiveness of this achievement might be of great relevance for the identification of patients carrying new genetic forms, characterized by low penetrance, where linkage disequilibrium studies are not appropriate. Remarkably, this is the first report of peripheral biochemical markers able to discriminate PD patients in terms of disease subtype.

Statistical methodology

From 2-DE images of gels acquired and detected with the appropriate software we obtained the relative volume of each spot in every single map. As expected, the distribution of spot volumes deviated from normality and intra-group variance values were dissimilar, therefore a parametric test was not a suitable choice (Fig. 30). We chose the non-parametric Wilcoxon test, as it compares median instead of mean values, to detect differences correlated to various parameters (disease, therapy, disease's subtypes, age, etc).

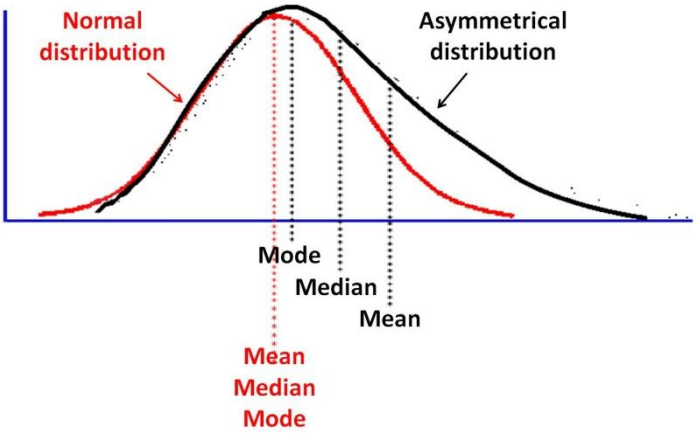

Fig. 30: In any symmetric (normal) distribution, mean, median and mode coincide, while in asymmetrical distribution they do not. The mean is influenced by the limit values, while the median best reflect the values assumed by majority of individuals and is only partly influenced by limit values.

On the other hand, LDA assumes that variances of distinct groups are similar. For this reason, inclusion of all 20 spots in the classification model did not grant the best result. In an original way, we manually calculated the weight of each spot in the model (Eq. 3), so to exclude those with a limited contribution. In this way, performance parameters of the models were markedly improved (Table 9).

Moreover, a model composed by 20 spots is difficult to use in subsequent validation analysis: in fact, a simplified analytical test will be proposed for the measurement of levels of selected proteins on large scale. It would be preferable to use an antibody-based assay like ELISA rather than 2-D electrophoresis, that is the ideal technique for the discovery phase but it is not suited for a screening phase, due to the time required for each analysis and the need of highly-specialized personnel.

The model composed by 14 spots is very promising, nevertheless we further excluded spots with lower contribution in order to find a third model with a reduced number of spots with still comparable performance parameters. The model composed by 9 spots possess both the attributes: it has good specificity and sensitivity and is composed by a low number of targets, so to be suitable for the development of an easy and ready-to-use test applicable on population-wide scale.

Several biomarker discovery investigations do not take into account the effect of medication on proteome or gene expression profiles. This aspect is particularly relevant when dealing with T-cells, expressing dopamine receptors, in patients treated with dopamine agonist drugs. In fact, we found several spots whose volume was correlated to dopaminergic therapy (see below). Apart from enrolling a small number (n = 3/15) of *de novo* patients, we separately considered the effect of dopamine agonist treatment and of L-DOPA daily dose on the T-cell proteome, thus excluding from the LDA analysis those spots that showed significant correlation. Similarly, we excluded from the

discovery procedure of the predictive models those spots that showed significant correlation with the age of control subjects only. Since age is the main risk factor of PD, proteome changes due to age were considered as biases and were eliminated from the dataset in which differences depending on disease or therapy were searched in.

A limitation that may be envisaged in the present investigation is the limited number of cases and control subjects included in the study. Nevertheless, we have enrolled a sufficient number of subjects (about 15 per each group) based on established guidelines for biomarker discovery studies. Being aware that, in the ideal biomarker pipeline, discovery, verification and validation should be decoupled steps of a phased approach (Surinova et al., 2011), we have attempted to evaluate intra-group variance and the difference of mean values for each spot included in the models and to perform a power analysis of our study. On this basis, we assured that the minimum number of subjects required to verify the observed variation is in the 10-20 range, thus permitting an appropriate verification on the same data set by the leave-one-out validation procedure. Worthy of note, we measured protein levels in the verification step in the same cellular population where the discovery procedure was conducted, thus avoiding issues frequently emerging when using plasma and CSF samples (*i.e.*, high dilution of the candidates in the body fluid and mixture with components coming from different body compartments). In this context, enrolment of larger cohorts in the verification phase of the biomarker pipeline would not add much value to the significance of our results (Surinova et al., 2011).

Validation of changes by Western Blot

In order to validate the results obtained by the proteomic approach with an independent technique, we conducted Western Blot quantifications on the same samples used for the 2-DE maps in order to verify those changes that seemed more significant.

We used this technique to univocally clarify double identifications. For two spots, in fact, matching with reference 2-DE maps was not sufficient to understand which protein was involved in the observed change, or because of problems of co-migration, or because of contamination of other proteins migrating in the near space of the 2D gel. In both cases, we run the samples in the same conditions used for obtaining the maps but, instead of staining the resulting gels with the fluorescent dye, proteins were transferred to 18x18 cm^2 PVDF membranes that were subsequently incubated with the antibody against one of the suspected proteins (Fig. 21). Then we overlapped images from Western Blot with 2-DE maps, taking as landmarks beta actin and validated identifications, like fibrinogen and peroxiredoxin 6. In both cases, the matching gave negative results, so we assigned the

identification by a process of elimination. One of them, the spot 598, was confirmed to be Moesin by a repeated LC-MS/MS analysis.

Regarding spots that belong to the predictive models, we verified beta fibrinogen and transaldolase changes. The first protein was chosen because 4 spots were identified as beta fibrinogen and appeared to be correlated by aggregative nesting (Pearson linear correlation, see Fig 23). Moreover, the contribution of beta fibrinogen appeared to be prominent in all three models in terms of its weights as calculated by Eq. 3 (Table 10). Noticeably, they also correlated linearly with the progression of the disease, thus highlighting the importance of this protein in the present study. Because all four spots of beta fibrinogen were downregulated in PD patients, we validated them in a one-dimensional Western Blot. Remarkably, total beta fibrinogen levels displayed a perfect agreement with the proteomic quantification (Fig 24B). We also checked the 2-DE pattern of beta fibrinogen in a PD patient and in a control subject, to exclude a significant qualitative modification of relative volumes of some isoforms with respect to others (Fig 24C). We observed several spots recognized by the anti-fibrinogen antibody, probably more than four, but their volume changes are in the same direction.

These findings show interesting complementarities with the preliminary evidence that two different isoforms of gamma fibrinogen either correlate with the disease state or with the disease duration in PBL (Mila et al., 2009). Although little is known on the role of fibrinogen in lymphocytes, it is notably that we found changing the same protein (also if a different fragment) in two independent, global approaching experiments conducted in similar cellular systems. Apparently, whatever the role of fibrinogen in lymphocytes, far from being elucidated, its abundance in T lymphocytes is unbalanced in PD patients and the reason of this observation needs to be further investigated (see below).

Two spots both identified as transaldolase show increased levels in the 20-spot model. Transaldolase, a key enzyme in the pentose phosphate pathway (PPP), has been associated with regulation of apoptotic cell death both in cancer and in neurodegeneration (Samland and Sprenger, 2009). The protein has a characteristic pattern in 2-DE, with two trains of spots at slightly different apparent molecular weight (Lachaise et al., 2001). Pattern modifications have been linked to regulation of the PPP by protein kinase transduction pathways. When comparing two LO PD and one EO PD patients with two healthy subjects and one with atypical parkinsonism it becomes clear that PD patients have a remarkably higher abundance of the heavy isoform (Fig. 25).

Two proteins changing with dopaminergic therapy were also validated through Western Blot: prolidase and peroxiredoxin 6 (Fig. 26). Also in this case, we obtained overlapping of the results from proteomics and antibody-based technique results (Fig. 27), thus confirming both the accuracy of protein assignments and the correctness of the method to detect proteins' changes.

Dopaminergic therapies modulate T cell proteome of PD patients

We demonstrated that specific stimulation of dopamine receptors has important effects on T-cell proteome in patients under long term treatment with dopamine agonists (Alberio et al., 2012b), thus confirming the concept that T lymphocytes are dopamine-susceptible cells, and they are reasonably modified by dopaminergic stimulation. Indeed, D3 stimulation of T-lymphocytes raises levels of prolidase, actin-related protein 2, F-actin capping protein subunit beta, proteasome activator complex subunit 1 and peroxiredoxin 6, and lowers levels of tropomyosin alpha-3 chain and of an isoform of GAPDH. Despite the limited number of spots displaying significant changes, dopamine agonists effectively alter the proteome of T-lymphocytes. Changes in cytoskeletal or cytoskeleton-related proteins (actin-related protein 2, F-actin capping protein subunit beta, and tropomyosin alpha-3 chain) are consistent with a remodeling of T-lymphocyte cellular architecture induced by dopamine receptor stimulation (see Alberio and Fasano, 2011).

Prolidase (also known as peptidase D) is a member of the prolyl oligopeptidase family able to hydrolyze dipeptides or tripeptides with C-terminal proline or hydroxyproline residues (Lupi and al., 2008). Actually, prolidase expression is higher in T-lymphocytes of PD patients undergoing dopamine agonists treatment. Worth of note, a member of the proline-specific peptidase family regulates apoptosis in quiescent lymphocytes (Chiravuri and Huber, 2000).

Upregulation of peroxiredoxin 6, observed in 2-DE maps and confirmed by Western blotting, is a relevant hint of antioxidant defense challenged by dopamine agonist treatment at pharmacological level in PD patients (Manevich and Fisher, 2005). It was observed that peroxiredoxin 6 and proteosome activator complex subunit 1 are downregulated in human lymphocytes treated with H_2O_2 (Dahlan et al., 2012). The fact that we observe the opposite effect might be due to the specific action of dopamine agonists on dopaminergic receptors, therefore excluding an aspecific effect due to generic oxidative stress.

Protein changes discussed above have not been correlated with the daily dose of dopamine agonists because patients assume different drugs (ropinirole, pramipexole and rotigotine) with different pharmacokinetic profiles; therefore, we stratified PD patients in terms of a general stimulation of dopamine receptors in order to avoid false correlations due to differences in subjects' metabolism and combination of drugs in their therapy. It should be noticed, however, that all dopamine agonists display specific stimulation of D3 dopamine receptors (Beaulieu and Gainetdinov, 2011), thus suggesting that a similar receptor-mediated effect would be expected.

Conversely, we found that L-DOPA induces limited modifications in the proteome of T lymphocytes. Indeed, only two display significant linear correlation with the L-DOPA daily dose, that were identified as proteasome subunit beta type-2 and ATP synthase subunit beta. This finding is in line

with the observation that lymphocytes of PD patients under L-DOPA treatment do not display increased oxidative chromosomal damage (Oli et al., 2010) and that exposure to L-DOPA does not modify dopamine transporter expression at central level as well as in PBLs of PD patients (Fanciulli et al., 2011). On the other hand, the identification of a significant decrease of proteasome β subunit type-2, a component of the proteasome aimed at the degradation of oxidatively-modified proteins, appears to counteract the observation of increased proteasome α subunit in *striata* of dyskinetic L-DOPA treated rats (Valastro et al., 2007). Although several models of proteasome impairment have been developed to understand altered protein homeostasis in PD (see Alberio and Fasano, 2011; Alberio et al., 2012a), this study first disclose a functional relationship between different proteasome subunit levels and L-DOPA therapy. On the other hand, the observed increase in ATP synthase β subunit may reflect a general adaptation of energetic metabolism to an altered turnover of reactive oxygen species (Petrak et al., 2008).

This section of our study may be limited by the relatively small sample size of drug naïve patients (3 patients), as well as by the lack of a cross-sectional perspective. An ideal approach, which we are planning to pursue in future studies, would imply a direct comparison of T-cell proteome from each patient before and after a given period of treatment. Nevertheless, it is likely that most changes we observed would emerge only in the long term, thus rendering the longitudinal approach difficult to pursue.

Beyond the interesting results we obtained regarding correlation between long term dopaminergic therapy and changes in the T cell proteome, two considerations have to be done: first, we initially searched for changing spots in order to exclude them in the analysis for biomarker discovery, as differences correlated to therapy could act as confounding factors, being borne by the patients' group only. Secondly, our results are in keeping with recent studies focusing on the role of dopamine in regulating T-cell activity (Pacheco et al., 2009; Sarkar et al., 2010), suggesting that immunomodulatory therapies using dopamine agonists and antagonists might have a potent rationale, being T lymphocytes modified by dopaminergic therapy.

Focus on Beta Fibrinogen

One of the most impressive changes identified in our study is that regarding the total beta fibrinogen level. As stressed before, four spots that considerably contribute to the predictive model correspond to beta fibrinogen (Table 7; see Fig. 24 for Western blot validation), showed stringent clustering by aggregative nesting (Fig. 23) and correlated with progression and duration of disease. Moreover, two different isoforms of gamma fibrinogen were found to correlate with disease state or with disease

duration in PBLs (Mila et al., 2009). Both evidences of fibrinogen imbalance in lymphocytes of PD patients prompted us to further investigate this protein in our cellular system.

Fibrinogen (also named coagulation factor I) plays an essential role in the hemostatic system by bridging activated platelets and being the key substrate for thrombin in establishing a consolidating fibrin network. Fibrinogen is synthesized in the liver and the plasma concentration is 1 to 5 g/L (Sørensen et al., 2012). Fibrinogen is a complex multifunctional glycoprotein composed of two identical molecular halves, each consisting of three non-identical subunit polypeptides designated as alpha (Aα), beta (Bβ), and gamma (γ) chains, held together by multiple disulfide bridges. The amino terminal ends of Aα and Bβ chains represent fibrinopeptides A and B (FPA and FPB), and are cleaved when thrombin transforms fibrinogen into fibrin during the coagulation process (Fig. 31A). Fibrinogen has a trinodular structure; one central dimeric E domain in which each dimer contains the three amino-terminal regions of polypeptides, and two distal D domains. These three nodules are linked by two coiled-coil regions and contain multiple binding sites (Fig. 31B) (Sørensen et al., 2012; Ugarova and Yakubenko, 2001).

.

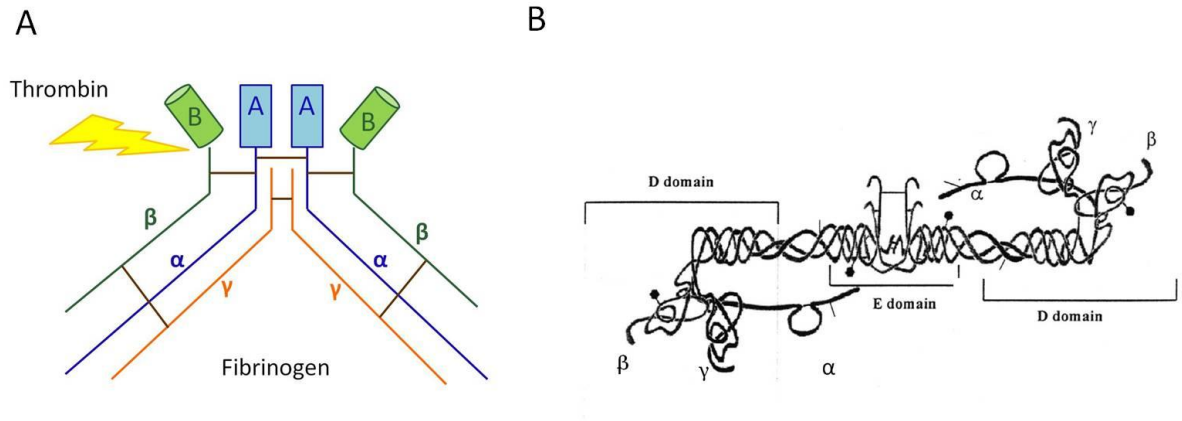

Fig 31: A) schematic representation of polypeptide chains composing fibrinogen molecules and highlight of cleavage sites of thrombin: from the amino terminal ends of Aα and Bβ chains, Fibrinopeptide A and Fibrinopeptide B (represented by a rectangle and a cylinder, respectively) are cleaved, while chains α, β and γ rearrange to form the fibrin coat. B) representation of trinodular structure of fibrinogen: domain E, containing amino-terminal connecting regions of the three chains, is located among the two distal D domains, composed by the three polypeptide chains α, β, and γ (adapted from Ugarova and Yakubenko, 2001).

Beyond its prominent role in the coagulation process, numerous studies provided evidence that fibrinogen also plays a multifaceted role in the immune and inflammatory response (Colvin et al., 1973; Wu et al,. 1994, Tang and Eaton, 1993; reviewed in Ugarova and Yakubenko, 2001). The ability

of fibrinogen to participate in the inflammatory response depends on its specific interaction with leukocyte cell surface adhesion receptors (*e.g.*, integrins). In particular, two leukocyte integrins, $\alpha_M\beta_2$ (also known as Mac-1 or CD11b/CD18) and $\alpha_X\beta_2$ (CD11c/CD18, p150,95) are the main fibrinogen receptors expressed on neutrophils, monocytes, macrophages and several subsets of lymphocytes, as well as on the surface of endothelium cells (Ugarova and Yakubenko, 2001).

The ability of fibrinogen to bind to these receptors indicates the existence of a potential fibrinogen-dependent pathway for leukocyte-endothelium interaction *in vivo.* In this regard, recent studies demonstrated that simultaneous fibrinogen binding to leukocytes and endothelial cells did enhance adhesion of monocytes to endothelium by acting as a molecular bridge between the two cell types (Languino et al., 1995). Most studies regarding the fibrinogen-leukocytes interaction focused on Mac-1 binding sites for fibrinogen, a very complex question as integrins usually recognize more than one molecule (Mosesson 2005; Lishko et al., 2004), while only few concentrate on action of such stimulation (Flick et al., 2004). It is known, however, that integrins' adhesive function is directly coupled with intracellular signaling and reorganization of actin cytoskeleton, that is in line with the concept that fibrinogen provokes leukocyte attraction and enhances activation and extravasation (Ugarova and Yakubenko, 2001).

Elevated levels of plasma fibrinogen are usually reduced in patients with clotting system's problems, while high levels are associated with inflammation and with thrombotic complications (Tousoulis et al., 2011). Altered fibrinogen levels have never been detected in plasma of PD patients, neither were associated with other neurodegenerative disorders. On the other hand, clinical chemistry analysis in 50 PD patients and 50 control subjects affected by non-neurodegenerative neurological disorders (e.g., stroke) displayed elevated fibrinogen levels in the control group (Alberio et al., submitted). It should be noticed, however, that fibrinogen levels might be raised in subjects with hemorrhagic events or brain infarction.

Regardless of a change in plasma beta fibrinogen levels, this protein appears to be surprisingly abundant in T lymphocytes (Fig. 32). Considering that beta fibrinogen is expected to be abundant in plasma and in liver only (Table 16), its presence in T cells was found to be qualitatively elevated when the four selected spots of beta fibrinogen are compared with the most abundant protein (i.e., cytoskeletal beta actin).

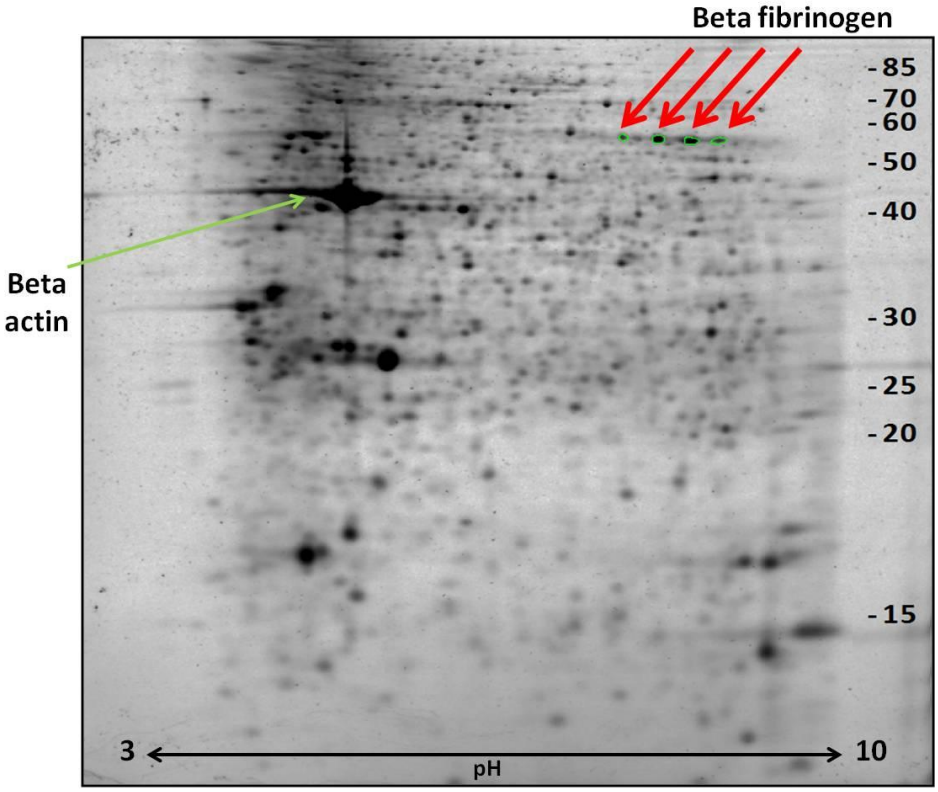

Fig. 32: A 2-DE map of T lymphocytes from a control subject, where beta fibrinogen and beta actin are evidenced for a qualitative volumetric comparison.

The first question we posed is if T lymphocytes, or more generally PBMC from human blood, do synthesize beta fibrinogen by their own or take it from the medium. We conducted a RT-PCR quantification of the beta fibrinogen transcript in T cells, PBMC and Hep G2 cells, as a positive control. We found that neither T cells neither PBMC constitutively express beta fibrinogen at a detectable level (Fig. 28). If beta fibrinogen is not expressed by T cells or PBMC themselves, we should hypothesize that it is necessarily internalized from the blood. However, little is known about internalization processes of fibrinogen by lymphocytes. An interesting research conducted on neutrophils proposes that, in the presence of physiological concentrations of fibrinogen, internalization of both intact and degraded forms of fibrinogen occurred largely via a non-specific pinocytosis process (Kirsch et al., 2002). In order to understand the nature of the fibrinogen internalization process by T lymphocytes, we tried first to localize the beta fibrinogen either at the cell surface or in the cytoplasm. To this purpose, we specifically labeled proteins at the T cell surface so to separate these proteins from the whole protein content. As a result, fibrinogen was not detected by Western blot in the fraction containing cell surface proteins (Fig. 29). Conversely, it is present in the whole protein content deprived of surface proteins. This result is in line with the relatively high amount of protein we found in the 2-DE maps (Fig. 32).

As fibrinogen circulates in blood in its hexameric conformation (Sørensen et al., 2012), it is reasonable to assume that it is internalized in its intact form. The fact that we observed a significant change only for beta fibrinogen may reflect a crowding in the 2-DE map that hampers the appropriate quantification of the other chains. Alternatively, this finding might depend by other unexpected phenomena, such as differential degradation. In support of the first hypothesis, the PD related quantitative change of gamma fibrinogen in PBL previously observed (Mila et al., 2009) seems to delineate an alteration in internalized fibrinogen that involves all polypeptide chains.

In conclusion, this investigation on the role of beta fibrinogen in peripheral T cells, and especially on the reason why its amount is reduced in T cells of PD patients, needs further work. On the basis of present results, we speculate that it is internalized in relatively large amounts, but the internalization could be impaired by various causes. If such internalization occurs via endocytosis (this would explain the large amount we observed in our cells) or pinocytosis (as it apparently happens in neutrophils, see Kirsch et al., 2002), the differences we observed in cytoskeleton proteins (Table 16) could participate to the same context: indeed, modifications of the cytoskeleton system could also reflect in decrease of content of intracellular amount of proteins internalized from plasma, such as fibrinogen. Nevertheless, we prefer to speculate on a mechanism that contemplate specific recognition of fibrinogen, because of the powerful significance of the PD-related quantitative change of this plasma protein in T cells.

6. FUTURE PERSPECTIVES

In this thesis the discovery phase of a broader study of biomarker identification for PD is presented.

As stated by Surinova and coworkers, a discovery study should deal with a small sample of homogeneous subjects to be screened by an unbiased technique to generate a quite large number of candidates; these candidates need to be verified, for instance using a jackknifing (leave-one-out) procedure. After candidates have been individuated, they need to be (pre-)clinically validated using a different, high-throughput methodology across large cohorts of patients and control subjects (Surinova et al., 2011).

In this study, a relatively small number of PD patients and control subjects has been analyzed and differences in a peripheral compartment, that is biochemically related to the central nervous system area involved in PD, have been found. The ideal flowchart of a proteomic investigation for a biomarker discovery strategy, described in Fig. 3 (see Introduction) has been followed, and three lists of potential biomarker candidates have been proposed.

Now a challenging phase of the project faces these results: leading the current finding to the clinical practice, with the final aim of proposing a biomarker panel for the *in vitro* diagnosis of Parkinson's disease. To do that, a validation procedure has to be planned and put into practice, creating a network between neurology divisions (whose task is enrolling and stratifying PD patients and control subjects), analysis laboratories (that would provide the correct procedure for sampling and measuring selected targets) and, obviously, the unit that will arrange and statistically analyze data obtained by collaborators.

A schematic representation of differential purposes of these two distinct phases of a biomarker study is provided in Fig. 33.

The validation phase needs to be conducted on a far more abundant number of subjects. In our case, some considerations about subjects enrollment have to be done: first, we have to enlarge control subjects' group and render it less homogeneous: subjects with other diseases, e.g., inflammatory diseases, subjects taking drugs, subjects of different ethnicity and subjects with family history of PD have to be included, as we need to test our models also in conditions not so controlled as the ones we used for the discovery phase. Since our models are composed by several proteins, we expect that, also if some of them are influenced by other (pathological) conditions, the contribution given by the other (not influenced) targets will permit to calculate the right predictive score. Secondly, by increasing the PD patients number, it will be possible to include and stratify different PD subtypes, as well as patients with varied state of progression and years of disease, so to confirm our preliminary results about capability of monitoring progression and differentiate PD subtypes of some protein candidates. In order to validate disease progression, patients could be followed up in a longitudinal study; moreover, samples taken for the validation could be used to deeply investigate modifications induced by long-term dopaminergic therapy, so to plan a prospectively designed recruitment (e.g., a

direct comparison of T-cell proteome from each patient before and after a given period of treatment).

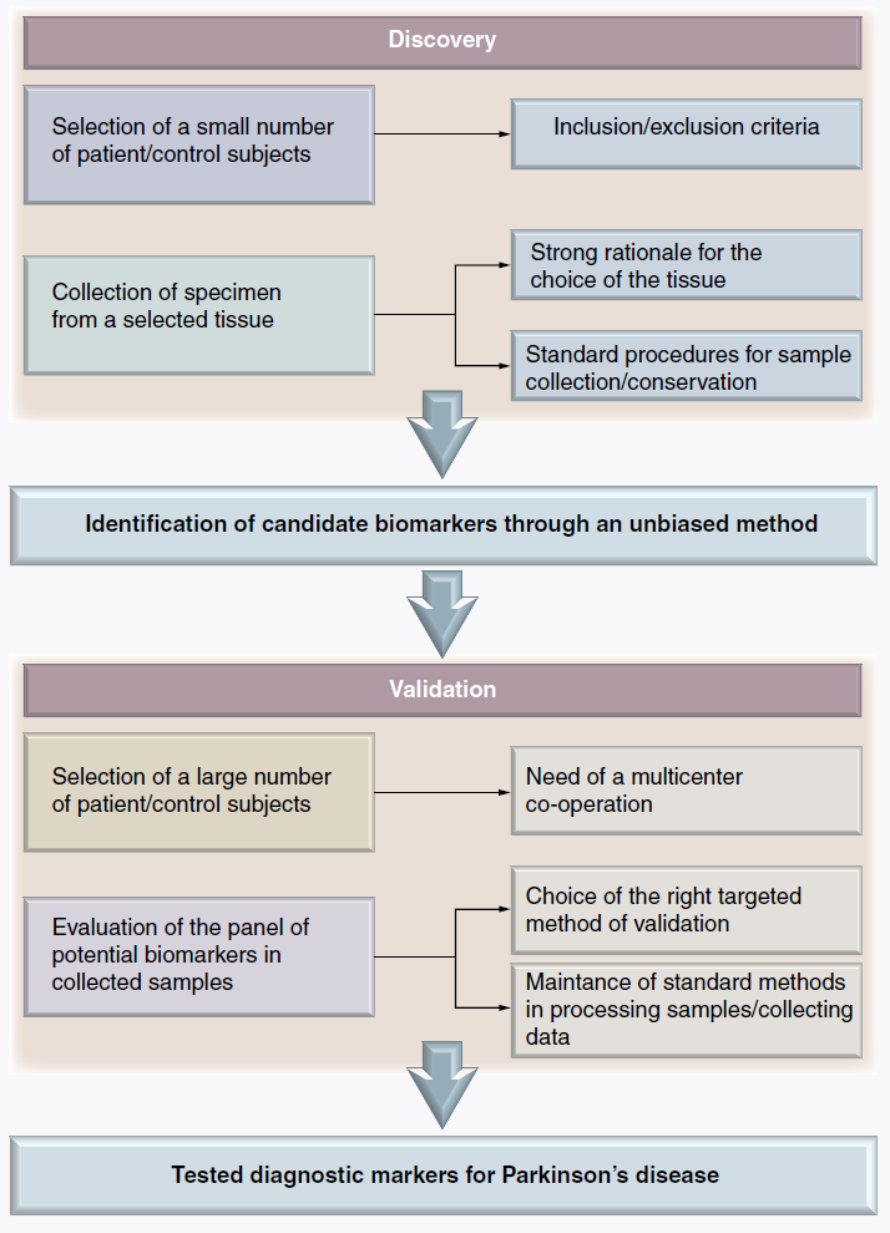

Fig. 33: Differences in methods and intents of the discovery and validation phases of a biomarker identification project.

Also standardization of sampling is necessary if enlargement of the collaboration network is planned. Unfortunately, collection of T lymphocytes from whole blood is a time and cost consuming procedure, so a further more accessible cell system in which to perform validation should be advisable. To this purpose, some experiments are in progress in our laboratory to test the possibility that the differences we found in T cells could be detected also in PBMC or PBL, also to verify a potential decrease in statistical significance.

If 2-DE is one of the techniques of choice for the discovery phase (see Introduction and Discussion), it would be advisable to use a different approach for the validation phase, due to the time required for each 2-DE analysis and the highly-specialized personnel it requires. In our cases, a technique able to discriminate different isoforms of the same protein is needed. In fact, some proteins showed a difference in volume of some isoforms that are not necessarily detected in others (e.g., transaldolase only changes in its higher molecular weight isoforms, Fig. 25), and a quantification of their total content would be unproductive for our purposes. For this reason, antibody-based approaches have to be excluded.

Mass spectrometry-based approaches are more suitable for the validation phase. In particular, the Selected reaction monitoring (SRM) method is especially suited for the high-throughput screening of a number of different targets, simultaneously (Wang et al., 2011). Briefly, it consists in the ionization of the samples in an electrospray source, selection of peptide precursors that are then isolated and fragmented so to obtain product ions whose signal abundances are indicative of the abundance of the peptide in the sample (de Hoffmann 1996). In this way, once peptides characteristic of proteins (and isoforms of proteins) to be quantified are individuated, the analysis consists in measuring abundance of such peptides in each sample, with the possibility to quantify several peptides (and consequently several proteins) in the same analysis. Difficulties in beginning this achievement are represented by the high costs of the instrument.

Concerned to the role of fibrinogen on T cells, it would be interesting to understand the reasons of the diminished amount that we observed in PD lymphocytes. Experiments addressed to establish if and how T lymphocytes (and/or other circulating cells) internalized it are, in my opinion, the most urgent. This could be reached both using cellular models and analyzing human samples. The cellular model of Jurkat cells, for example, that we showed to be fibrinogen free, could be treated with fibrinogen or plasma in order to detect the presence of FGB by Western Blot after a time course-treatment. In the case of a positive result, the process of internalization would be confirmed. We are also planning a cytofluorimetric analysis of freshly isolated PBMC from PD patients and control subjects, treated with FITC-labeled fibrinogen, in order to quantify the amount of internalized fibrinogen in the different cell populations.

7. HIGHLIGHTS

- T lymphocyte proteome changes have been shown to be a valid tool to recognize and classify PD patients. A biomarker discovery procedure has been conducted on the basis of common features between affected cells (dopaminergic neurons) and the probed system (T lymphocytes).

- We found 20 T cell proteins whose level was significantly different in PD patients and control subjects; their volumes were combined by LDA to calculate a PD likelihood score and classify each subjects as PD patient or control.

- Three predictive models were obtained, one combining all 20 changing spots, the second one combining only 14 spots, while the third is composed by only 9 spots. Models with 14 and 9 spots showed best parameters of sensitivity and specificity. Performance of the models was tested with the leave-one-out method.

- A total of 9 spots display linear correlation with parameters such as disease duration (years from onset) and disease progression (Hoehn and Yahr score). In particular, four spots correlate with duration, and 8 spots correlate with progression of symptoms; 3 of them correlate with both duration and progression. A panel of biomarkers able to track progression of the central disease at a peripheral level is expected to reasonably provide information on the effectiveness of drugs under development designed to interfere with specific cell death mechanisms targeting nigral neurons.

- Considering clinical manifestation and pathological features, subtypes of patients may be identified: we performed LDA in order to classify our patients in terms of age at onset, that is, in our opinion, the major factor of patients heterogeneity. We found 7 spots whose volumes statistically changed in the Early Onset (EO) and Late Onset (LO) PD groups, and a function able to correctly classify EO PD patients with the same "leave-one-out" procedure used for the predictive models.

- Specific stimulation of dopamine receptors has important effects on T-cell proteome in patients under long term treatment with dopamine agonists. In fact, the level of 2 proteins was modified by levodopa and the level of 7 spots was modified by dopamine agonists therapy: this demonstrates that these cells are sensitive to long term dopaminergic stimulation and that they are a valid tool to investigate dopaminergic imbalance at a peripheral level.

- In order to validate the results obtained by the proteomic approach with an independent technique, we conducted Western Blot quantifications on the same samples used for the 2-DE maps in order to clarify double identifications and verify those changes that seemed more significant. Two proteins of the model were chosen to this purpose: transaldolase and beta fibrinogen. Western blot confirmed the proteomic results and clarified how the isoform pattern changed in relation with PD.

- The presence of large amount of fibrinogen in T cells seemed so interesting, and spots corresponding to FGB were so important for the predictivity of the models (they also correlate with disease progression), that we decided to investigate this protein more deeply. FGB is not synthesized neither by T cells neither by other PBMC. Moreover, it is present inside the cells and it is not (exclusively) associated to the cell surface. It appears to be internalized from plasma, but the mechanism of internalization is not clear so far, neither the reasons why T cells from PD patients internalize it in a decreased amount.

- Next step of this research is leading the current finding about the predictive models to the clinical practice. This objective will be reached only through large collaborative networks, that will allow us to select large cohorts of subjects with high heterogeneity in terms of gender, age, ethnicity, clinical phenotype; the use of a different, less time consuming and high throughput technique in the clinical phase is advisable.

8. BIBLIOGRAPHY

Alberio T, Bossi AM, Milli A, Parma E, Gariboldi MB, Tosi G, Lopiano L, Fasano M. Proteomic analysis of dopamine and α-synuclein interplay in a cellular model of Parkinson's disease pathogenesis. FEBS J. **2010**; 277:4909-19.

Alberio T, Fasano M. Proteomics in Parkinson's disease: An unbiased approach towards peripheral biomarkers and new therapies. J Biotechnol. **2011**; 156:325-37.

Alberio T, Lopiano L, Fasano M. Cellular models to investigate biochemical pathways in Parkinson's disease. FEBS J. **2012a**; 279:1146-55.

Alberio T, Pippione AC, Comi C, Olgiati S, Cecconi D, Zibetti M, Lopiano L, Fasano M. Dopaminergic therapies modulate the T-CELL proteome of patients with Parkinson's disease. IUBMB Life. **2012b**; 64:846-52.

Albrecht D, Kniemeyer O, Brakhage AA, Guthke R. Missing values in gel-based proteomics. Proteomics. **2010**; 10:1202-11.

Amenta, F, Bronzetti, E, Cantalamessa, F, El-Assouad, D, Felici, L, Ricci, A, Tayebati, SK. Identification of dopamine plasma membrane and vesicular transporters in human peripheral blood lymphocytes. J. Neuroimmunol., **2001;** 117:133-42.

Balluff B, Schöne C, Höfler H, Walch A. MALDI imaging mass spectrometry for direct tissue analysis: technological advancements and recent applications. Histochem Cell Biol. **2011**; 136(3):227-44.

Banerjee R, Starkov AA, Beal MF, Thomas, B. Mitochondrial dysfunction in the limelight of Parkinson's disease pathogenesis. Biochim. Biophys. Acta. **2009;** 1792:651–63.

Barbanti P, Fabbrini G, Ricci A, Cerbo R, Bronzetti E, Caronti B, Calderaro C, Felici L, Stocchi F, Meco G, Amenta F, Lenzi GL. Increased expression of dopamine receptors on lymphocytes in Parkinson's disease. Mov. Disord. **1999;** 14:764-71.

Beaulieu JM, Gainetdinov RR. The physiology, signaling, and pharmacology of dopamine receptors. Pharmacol Rev **2011**; 63:182-217.

Benabou R, Waters C. Hepatotoxic profile of catechol-O-methyltransferase inhibitors in Parkinson's disease. Expert Opin Drug Saf. **2003**; 2:263-7.

Berggren K, Chernokalskaya E, Steinberg TH, Kemper C, Lopez MF, Diwu Z, Haugland RP, Patton WF. Background-free, high sensitivity staining of proteins in one- and two dimensional sodium dodecyl sulfate-polyacrylamide gels using a luminescent ruthenium complex. Electrophoresis. **2000**; 21:2509–21.

Bergquist J, Tarkowski A, Ekman R, Ewing A. Discovery of endogenous catecholamines in lymphocytes and evidence for catecholamine regulation of lymphocyte function *via* an autocrine loop. Proc. Natl. Acad. Sci. USA, **1994**; 91:12912-16.

Bergquist J, Silberring J. Identification of catecholamines in the immune system by electrospray ionization mass spectroscopy. Rapid Commun. Mass Spectrom. **1998**; 12:683-88.

Besser MJ, Ganor Y, Levite M. Dopamine by itself activates either D2, D3 or D1/D5 dopaminergic receptors in normal human T-cells and triggers the selective secretion of either IL-10, TNFalpha or both. J. Neuroimmunol. **2005;** 169:161-71.

Betarbet R, Sherer TB, MacKenzie G, Garcia-Osuna M, Panov AV, Greenamyre JT. Chronic systemic pesticide exposure reproduces features of Parkinson's disease. Nat Neurosci **2000**; 3:1301–06.

Biomarkers Definitions Working Group. Biomarkers and surrogate endpoints: preferred definitions and conceptual framework. Clin. Pharmacol. Ther. **2001**; 69:89–95.

Bisaglia M, Greggio E, Maric D, Miller DW, Cookson MR, Bubacco L. Alpha-synuclein overexpression increases dopamine toxicity in BE2-M17 cells. BMC Neurosci. **2010**; 11:41.

Boeve BF. Progressive supranuclear palsy. Parkinsonism Relat Disord. **2012**; 18 Suppl 1:S192-4.

Bogdanov M, Matson WR, Wang L, Matson T, Saunders-Pullman R, Bressman SS, Flint Beal M. Metabolomic profiling to develop blood biomarkers for Parkinson's disease. Brain. **2008**; 131:389–96.

Buttarelli FR, Fanciulli A, Pellicano C, Pontieri FE. The Dopaminergic System in Peripheral Blood Lymphocytes: From Physiology to Pharmacology and Potential Applications to Neuropsychiatric Disorders. Curr Neuropharmacol. **2011**; 9:278-88.

Candiano G, Bruschi M, Musante L, Santucci L, Ghiggeri GM, Carnemolla B, Orecchia P, Zardi L, Righetti PG. Blue silver: a very sensitive colloidal Coomassie G-250 staining for proteome analysis. Electrophoresis. **2004**; 25:1327-33.

Caronti B, Tanda G, Colosimo C, Ruggieri S, Calderaro C, Palladini G, Pontieri FE, Di Chiara G. Reduced dopamine in peripheral blood lymphocytes in Parkinson's disease. Neuroreport. **1999**; 10:2907-10.

Caudle WM, Bammler TK, Lin Y, Pan S, Zhang J.Using 'omics' to define pathogenesis and biomarkers of Parkinson's disease. Expert Rev Neurother. **2010**; 10:925-42.

Chiravuri M, Huber BT. Aminodipeptidase inhibitor-induced cell death in quiescent lymphocytes: a review. Apoptosis **2000;** 5:319-22.

Chung KK, Zhang Y, Lim KL, Tanaka Y, Huang H, Gao J, Ross CA, Dawson VL, Dawson TM. Parkin ubiquitinates the alpha-synuclein-interacting protein, synphilin-1: implications for Lewy-body formation in Parkinson disease. Nat Med. **2001**; 7:1144-50.

Colapinto M, Mila S, Giraudo S, Stefanazzi P, Molteni M, Rossetti C, Bergamasco B, Lopiano L, Fasano M. Alpha-synuclein protects SH-SY5Y cells from dopamine toxicity. Biochem Biophys Res Commun. **2006;** 349:1294–300.

Colvin RB, Johnson RA, Mihm MC Jr, Dvorak HF. Role of the clotting system in cell-mediated hypersensitivity I. Fibrin deposition in delayed skin reactions in man. J Exp Med. **1973;** 138:686-98.

Cookson MR. Hero versus antihero: the multiple roles of alpha-synuclein in neurodegeneration. Exp Neurol **2006;** 199:238–242.

Cordellini MF, Piazzetta G, Pinto KC, Delattre AM, Matheussi F, Carolino RO, Szawka RE, Anselmo-Franci JA, Ferraz AC. Effect of different doses of estrogen on the nigrostriatal dopaminergic system in two 6-hydroxydopamine-induced lesion models of Parkinson's disease. Neurochem Res. **2011**; 36:955-61.

Cosentino M, Fietta AM, Ferrari M, Rasini E, Bombelli R, Carcano E, Saporiti F, Meloni F, Marino F, Lecchini S. Human CD4+CD25+ regulatory T cells selectively express tyrosine hydroxylase and contain endogenous catecholamines subserving an autocrine/paracrine inhibitory functional loop. Blood. **2007**; 109:632-42.

Dahlan HM, Karsani SA, Rahman MA, Hamid NA, Top AG, Ngah WZ. Proteomic analysis reveals that treatment with tocotrienols reverses the effect of H(2)O(2) exposure on peroxiredoxin expression in human lymphocytes from young and old individuals J Nutr Biochem. **2012**; 23:741-51.

de Hoffmann E. Tandem mass spectrometry: A primer. Journal of Mass Spectrometry. **1996**; 31:129–37

de Lau LML, Breteler MMB. Epidemiology of Parkinson's disease. Lancet Neurol. **2006**; 5:525–35.

Fanciulli A, Misasi R, Campanelli D, Buttarelli FR, Pontieri FR. Dopaminergic drug-induced modulation of the expression of the dopamine transporter in peripheral blood lymphocytes in Parkinson's disease. Pharmacol Rep **2011**; 63:1056-60.

Faraj BA, Olkowski ZL, Jackson, RT. Binding of [3H]-dopamine to human lymphocytes: possible relationship to neurotransmitter uptake sites. Pharmacology. **1991;** 42:135-41.

Fasano M, Bergamasco B, Lopiano L. Modifications of the iron-neuromelanin system in Parkinson's disease. J Neurochem. **2006**; 96:909-16.

Fasano M and Lopiano L. Alpha-synuclein and Parkinson's disease: a proteomic view. Expert Rev Proteomics. **2008**; 5:239-48.

Fasano M, Alberio T, Lopiano L. Peripheral biomarkers of Parkinson's disease as early reporters of central neurodegeneration. Biomark. Med. **2008**; 2:465–478.

Flick MJ, Du X, Degen JL. Fibrin(ogen)-alpha M beta 2 interactions regulate leukocyte function and innate immunity in vivo. Exp Biol Med. **2004**; 229:1105-10.

Gasser T. Mendelian forms of Parkinson's disease. Biochim Biophys Acta. **2009;** 1792:587-96.

Gerlach M, Maetzler W, Broich K, Hampel H, Rems L, Reum T, Riederer P, Stöffler A, Streffer J, Berg D. Biomarker candidates of neurodegeneration in Parkinson's disease for the evaluation of disease-modifying therapeutics. J Neural Transm. **2012**; 119:39-52.

Gilman S, Wenning GK, Low PA, Brooks DJ, Mathias CJ, Trojanowski JQ, Wood NW, Colosimo C, Dürr A, Fowler CJ, Kaufmann H, Klockgether T, Lees A, Poewe W, Quinn N, Revesz T, Robertson D, Sandroni P, Seppi K, Vidailhet M. Second consensus statement on the diagnosis of multiple system atrophy. Neurology. **2008**; 71:670-6.

Giorelli M, Livrea P, Trojano M. Dopamine fails to regulate activation of peripheral blood lymphocytes from multiple sclerosis patients: effects of IFN-beta. J Interferon Cytokine Res**. 2005**; 25:395-406.

Goetz CG, Poewe W, Rascol O, Sampaio C, Stebbins GT, Counsell C, Giladi N, Holloway RG, Moore CG, Wenning GK, Yahr MD, Seidl L; Movement Disorder Society Task Force on Rating Scales for Parkinson's Disease.Mov Disord. Movement Disorder Society Task Force report on the Hoehn and Yahr staging scale: status and recommendations. **2004**; 19:1020-8.

Goetz CG, Fahn S, Martinez-Martin P, Poewe W, Sampaio C, Stebbins GT, Stern MB, et al. Movement Disorder Society-Sponsored Revision of the Unified Parkinson's Disease Rating Scale (MDS-UPDRS): Process, Format, and Clinimetric Testing Plan. Mov Disord. **2007**; 22:41-7.

Görg A, Weiss W, Dunn MJ. Current two-dimensional electrophoresis technology for proteomics. Proteomics **2004**; 4:3665–85.

Graeber MB. Biomarkers for Parkinson's disease. Exp Neurol. **2009**; 216:249-53.

Gromova I, Celis JE. Protein detection in gels by silver staining: A procedure compatible with mass-spectrometry. From: In Cell Biology: A Laboratory Handbook (Celis JE, Carter N, Hunter T, Simons K, Small JV, Shotton D) **2006**; 3rd ed., Elsevier, Academic Press, New York.

Grünblatt E, Zehetmayer S, Jacob CP, Muller T, Jost WH, Riederer P. Pilot study: peripheral biomarkers for diagnosing sporadic Parkinson's disease. J Neural Transm. **2010**; 117:1387-93.

Henchcliffe C, Beal MF. Mitochondrial biology and oxidative stress in Parkinson disease pathogenesis. Nat Clin Pract Neurol. **2008**; 4:600-9.

Ilani T, Strous RD, Fuchs S. Dopaminergic regulation of immune cells *via* D3 dopamine receptor: a pathway mediated by activated T cells. FASEB J. **2004**; 18:1600-2.

Jacob AM, Turck CW. Detection of post-translational modifications by fluorescent staining of two-dimensional gels. Methods Mol. Biol. **2008;** 446:21–32.

Jankovic J. Parkinson's disease: clinical features and diagnosis. J Neurol Neurosurg Psychiatry. **2008**; 79:368-76.

Jankovic J, Aguilar LG. Current approaches to the treatment of Parkinson's disease. Neuropsychiatr. Dis. Treat. **2008;** 4:743–757.

Jecmenica-Lukic M, Poewe W, Tolosa E, Wenning GK. Premotor signs and symptoms of multiple system atrophy. Lancet Neurol. **2012**; 11:361-8.

Jennewein C, Tran N, Paulus P, Ellinghaus P, Eble JA, Zacharowski K. Novel aspects of fibrin(ogen) fragments during inflammation. Mol Med. **2011**; 17:568-73.

Kirsch R, Jaffer MA, Woodburne VE, Sewell T, Kelly SL, Kirsch RE, Shephard EG. Fibrinogen is degraded and internalized during incubation with neutrophils, and fibrinogen products localize to electron lucent vesicles. Biochem J. **2002**; 364:403-12.

Kurlan R, Rubin AJ, Miller C, Rivera Calimlim L, Clarke A, Shoulson I. Duodenal delivery of levodopa for on-off fluctuations in parkinsonism: preliminary observations. Ann Neurol. **1986;** 20:262–65.

Lachaise F, Martin G, Drougard C, Perl A, Vuillaume M, Wegnez M, Sarasin A, Daya-Grosjean L. Relationship between posttranslational modification of transaldolase and catalase deficiency in UV-sensitive repair-deficient xeroderma pigmentosum fibroblasts and SV40-transformed human cells. Free Radic Biol Med. **2001**; 30:1365-73.

Languino LR, Duperray A, Joganic KJ, Fornaro M, Thornton GB, Altieri DC. Regulation of leukocyte-endothelium interaction and leukocyte transendothelial migration by intercellular adhesion molecule 1-fibrinogen recognition. Proc Natl Acad Sci U S A. **1995**; 92(5):1505-9.

Lishko VK, Podolnikova NP, Yakubenko VP, Yakovlev S, Medved L, Yadav SP, Ugarova TP. Multiple binding sites in fibrinogen for integrin alphaMbeta2 (Mac-1). J Biol Chem. **2004**; 279:44897-906.

Litvan I, Agid Y, Calne D, Campbell G, Dubois B, Duvoisin RC, Goetz CG, Golbe LI, Grafman J, Growdon JH, Hallett M, Jankovic J, Quinn NP, Tolosa E, Zee DS. Clinical research criteria for the diagnosis of progressive supranuclear palsy (Steele-Richardson-Olszewski syndrome): report of the NINDS-SPSP international workshop. Neurology. **1996**; 47:1-9.

Litvan I, Bhatia KP, Burn DJ, Goetz CG, Lang AE, McKeith I, Quinn N, Sethi KD, Shults C, Wenning GK; Movement Disorders Society Scientific Issues Committee. Movement Disorders Society Scientific Issues Committee report: SIC Task Force appraisal of clinical diagnostic criteria for Parkinsonian disorders. Mov Disord. **2003**; 18:467-86.

Lupi A, Tenni R, Rossi A, Cetta G, Forlino A. Human prolidase and prolidase deficiency: an overview on the characterization of the enzyme involved in proline recycling and on the effects of its mutations. Amino Acids **2008**; 35:739-52.

Manevich Y, Fisher AB. Peroxiredoxin 6, a 1-Cys peroxiredoxin, functions in antioxidant defense and lung phospholipid metabolism. Free Radic Biol Med. **2005**; 38:1422-32.

Marek K, Jennings D, Lasch S, Siderowf A, Tanner C, Simuni T, et al. The Parkinson Progression Marker Initiative (PPMI). Progress in Neurobiology. **2011**; 95:629-35.

McDonald JH. Handbook of Biological Statistics. **2009;** 2nd ed., Sparky House Publishing, Baltimore.

McKenna F, McLaughlin PJ, Lewis BJ, Sibbring GC, Cummerson JA, Bowen-Jones D, Moots RJ. Dopamine receptor expression on human T- and B-lymphocytes, monocytes, eosinophils and NK cells: a flow cytometric study. J Neuroimmunol. **2002**; 132:34-40.

McNaught KS, Olanow CW. Protein aggregation in the pathogenesis of familial and sporadic Parkinson's disease. Neurobiol Aging**. 2006**; 27:530-45.

Michell AW, Lewis SJG, Foltynie T, Barker RA: Biomarkers and Parkinson's disease. Brain. **2004**; 127:1693-705.

Miller I, Crawford J, Gianazza E. Protein stains for proteomic applications: which, when, why? Proteomics **2006**; 6:5385–408.

Mollenhauer B, Locascio JJ, Schulz-Schaeffer W, Sixel-Doering F, Trenkwalder C, Schlossmacher MG. alpha-Synuclein and tau concentrations in cerebrospinal fluid of patients presenting with parkinsonism: a cohort study. Lancet Neurol. **2011**; 10: 230-40.

Morgan JC, Mehta SH, Sethi KD. Biomarkers in Parkinson's disease. Curr.Neurol. Neurosci. Rep. **2010;** 10:423–30.

Mosesson MW. Fibrinogen and fibrin structure and functions. J Thromb Haemost. **2005**; 3:1894-904.

Musso NC, Brenci S, Setti M, Indiveri F, Lotti G. Catecholamine content and in vitro catecholamine synthesis in peripheral human lymphocytes. J Clin Endocrinol Metab. **1996;** 81:3553-57.

Nagai Y, Ueno S, Saeki Y, Soga F, Yanagihara T. Expression of D3 dopamine receptor gene and a novel variant transcript generated by alternative splicing in human peripheral blood lymphocytes. Biochem Biophys Res Commun. **1993**; 194:368-74.

Neuhoff V, Arold N, Taube D, Ehrhardt W. Improved staining of proteins in polyacrylamide gels including isoelectric focusing gels with clear background at nanogram sensitivity using Coomassie Brilliant Blue G-250 and R-250. Electrophoresis **1988**; 9:255–62.

Nyhlén J, Constantinescu R, Zetterberg H. Problems associated with fluid biomarkers for Parkinson's disease. Biomark. Med. **2010;** 4:671–81.

Obeso JA, Rodriguez-Oroz MC, Goetz CG, Marin C, Kordower JH, Rodriguez M, Hirsch EC, Farrer M, Schapira AH, Halliday G. Missing pieces in the Parkinson's disease puzzle. Nat Med. **2010;** 16:653-61.

Oli RG, Fazeli G, Kuhn W, Walitza S, Gerlach M, Stopper H. No increased chromosomal damage in L-DOPA-treated patients with Parkinson's disease: a pilot study. J Neural Transm. **2010;** 117:737-46.

Ong SE, Blagoev B, Kratchmarova I, Kristensen DB, Steen H, Pandey A, et al. Stable Isotope Labeling by Amino Acids in Cell Culture, SILAC, as a Simple and Accurate Approach to Expression Proteomics. Mol Cell Proteomics. **2002**; 1:376–86.

Pacheco R, Prado CE, Barrientos MJ, Bernales S. Role of dopamine in the physiology of T-cells and dendritic cells. J. Neuroimmunol. **2009;** 216:8–19.

Payami H, Zareparsi S, James D, Nutt J. Familial aggregation of Parkinson disease: a comparative study of early-onset and late-onset disease. Arch Neurol. **2002**; 59:848-50.

Pavon JM, Whitson HE, Okun MS. Parkinson's disease in women: A call for improved clinical studies and for comparative effectiveness research. Maturitas. **2010**; 65:352-8.

Petrak J, Ivanek R, Toman O, Cmejla R, Cmejlova J, Vyoral D, et al. Déjà vu in proteomics. A hit parade of repeatedly identified differentially expressed proteins. Proteomics. **2008;** 8:1744-9.

Petrovitch H, Ross GW, Abbott RD, Sanderson WT, Sharp DS, Tanner CM, Masaki KH, Blanchette PL, Popper JS, Foley D, Launer L, White LR. Plantation work and risk of Parkinson disease in a population-based longitudinal study. Arch Neurol**. 2002**; 59:1787-92.

Qiu YH, Peng YP, Jiang JM, Wang JJ. Expression of tyrosine hydroxylase in lymphocytes and effect of endogenous catecholamines on lymphocyte function. Neuroimmunomodulation. **2004;** 11:75-83.

Rabilloud T, Strub JM, Luche S, van Dorsselaer A, Lunardi J. A comparison between Sypro Ruby and ruthenium II tris (bathophenanthroline disulfonate) as fluorescent stains for protein detection in gels. Proteomics. **2001**; 1:699-704.

Rascol O, Lozano A, Stern M, Poewe W. Milestones in Parkinson's disease therapeutics. Mov Disord. **2011**; 26:1072-82.

R Development Core Team. R: A language and environment for statistical computing. **2009;** R Foundation for Statistical Computing, Vienna.

Robinson PA. Understanding the molecular basis of Parkinson's disease, identification of biomarkers and routes to therapy. Expert Rev. Proteomics. **2010**; 7:565–78.

Ross PL, Huang YN, Marchese JN, Williamson B, Parker K, Hattan S, Khainovski N, Pillai S, Dey S, Daniels S, Purkayastha S, Juhasz P, Martin S, Bartlet-Jones M, He F, Jacobson A, Pappin DJ. Multiplexed protein quantitation in Saccharomyces cerevisiae using amine-reactive isobaric tagging reagents. Mol. Cell. Proteomics **2004;** 3:1154–69.

Rotilio D, Della Corte A, D'Imperio M, Coletta W, Marcone S, Silvestri C, Giordano L, Di Michele M, Donati MB. Proteomics: bases for protein complexity understanding. Thromb Res. **2012**; 129:257-62.

Samland AK, Sprenger GA. Transaldolase: from biochemistry to human disease. Int J Biochem Cell Biol. **2009**; 41:1482-94.

Sapra R. The use of difference in-gel electrophoresis for quantitation of protein expression. Methods Mol Biol **2009**; 492:93–112.

Sarah L. Rowland-Jones and Andrew J. McMichael. Lymphocytes: A Practical Approach. **2000**; Oxford University Press, New York.

Sarkar C, Basu B, Chakroborty D, Dasgupta PS, Basu S. The immunoregulatory role of dopamine: an update. Brain Behav Immun. **2010;** 24:525–28.

Saunders-Pullman R. Estrogens and Parkinson disease: neuroprotective, symptomatic, neither, or both? Endocrine **2003**; 21**:**81–7.

Schapira AH, Cooper JM, Dexter D, Clark JB, Jenner P, Marsden CD. Mitochondrial complex I deficiency in Parkinson's disease. J Neurochem. **1990**; 54:823-7.

Schapira AH. Mitochondrial pathology in Parkinson's disease. Mt Sinai J Med. **2011**; 78:872-81.

Shevchenko A, Wilm M, Vorm O, Mann M. Mass Spectrometric Sequencing of Proteins from Silver-Stained Polyacrylamide Gels. Anal Chem **1996**; 68:850–8.

Shulman JM, De Jager PL, Feany MB. Parkinson's disease: genetics and pathogenesis. Annu Rev Pathol. **2011**; 6:193-222.

Schulze WX, Usadel B. Quantitation in mass-spectrometry-based proteomics. Annu Rev Plant Biol. **2010;** 61:491–516.

Sørensen B, Larsen OH, Rea CJ, Tang M, Foley JH, Fenger-Eriksen C. Fibrinogen as a hemostatic agent. Semin Thromb Hemost. **2012**; 38:268-73.

Spillantini MG, Goedert M. The alpha-synucleinopathies: Parkinson's disease, dementia with Lewy bodies, and multiple system atrophy. Ann N Y Acad Sci**. 2000**; 920:16-27.

Steen H, Mann M. The ABC's (and XYZ's) of peptide sequencing. Nat Rev Mol Cell Biol **2004**; 5:699–711.

Stoessl AJ. Neuroimaging in Parkinson’s disease: from pathology to diagnosis. Parkinsonism Relat Disord. **2012**; 18 Suppl 1:S55-9.

Surinova S, Schiess R, Hüttenhain R, Cerciello F, Wollscheid B, Aebersold R. On the development of plasma protein biomarkers. J Proteome Res. **2011**; 10: 5-16.

Surmeier DJ, Guzman JN, Sanchez-Padilla J, Goldberg JA. What causes the death of dopaminergic neurons in Parkinson’s disease? Prog Brain Res. **2010**; 183:59-77.

Tang L, Eaton JW. Fibrin(ogen) mediates acute inflammatory responses to biomaterials. J Exp Med. **1993;** 178:2147–56.

Thomas B, Beal MF Parkinson’s disease. Hum Mol Genet. **2007;** 16:R183–R194.

Tolosa E, Wenning G, Poewe W. The diagnosis of Parkinson's disease. Lancet Neurol. **2006**; 5:75-86.

Tousoulis D, Papageorgiou N, Androulakis E, Briasoulis A, Antoniades C, Stefanadis C. Fibrinogen and cardiovascular disease: genetics and biomarkers. Blood Rev. **2011**; 25:239-45.

Unlu M, Morgan ME, Minden JS. Difference gel electrophoresis. A single gel method for detecting changes in protein extracts. Electrophoresis **1997**; 18:2071–7.

Ugarova TP, Yakubenko VP. Recognition of fibrinogen by leukocyte integrins. Ann N Y Acad Sci. **2001**; 936:368-85.

Valastro B, Dekundy A, Krogh M, Lundblad M, James P, Danysz W, et al. Proteomic analysis of striatal proteins in the rat model of L-DOPA-induced dyskinesia. J Neurochem **2007**; 102:1395-409.

Van Den Eeden SK, Tanner CM, Bernstein AL, Fross RD, Leimpeter A, Bloch DA, Nelson LM. Incidence of Parkinson's Disease: Variation by Age, Gender, and Race/Ethnicity. Am J Epidemiol **2003**; 157:1015–22.

Villoslada P, Steinman L, Baranzini SE. Systems biology and its application to the understanding of neurological diseases. Ann Neurol. **2009**; 65:124–39.

Wang Q, Chaerkady R, Wu J, Hwang HJ, Papadopoulos N, Kopelovich L, Maitra A, Matthaei H, Eshleman JR, Hruban RH, Kinzler KW, Pandey A, Vogelstein B. Mutant proteins as cancer-specific biomarkers. Proc Natl Acad Sci U S A. **2011**; 108:2444-9.

Wieser A, Schneider L, Jung J, Schubert S. MALDI-TOF MS in microbiological diagnostics-identification of microorganisms and beyond (mini review). Appl Microbiol Biotechnol. **2012**; 93:965-74.

Wilkins MR. Hares and tortoises: the high- versus low-throughput proteomic race. Electrophoresis. **2009;** 30:S150-5.

Wu WW, Wang G, Baek SJ, Shen RF. Comparative study of three proteomic quantitative methods, DIGE, cICAT, and iTRAQ, using 2D gel- or LC-MALDI TOF/TOF. J Proteome Res **2006**; 5:651–8.

Wu X, Helfrich MH, Horton MA, Feigen LP, Lefkowith JB. Fibrinogen mediates platelet-polymorphonuclear leukocyte cooperation during immune-complex glomerulonephritis in rats. J Clin Invest. **1994**; 94:928-36.

Yates JR, Ruse CI, Nakorchevsky A. Proteomics by Mass Spectrometry: Approaches, Advances, and Applications. Annu Rev Biomed Eng **2009**; 11:49–79.

Zibetti M, Merola A, Rizzi L, Ricchi V, Angrisano S, Azzaro C, Artusi CA, Arduino N, Marchisio A, Lanotte M, Rizzone M, Lopiano L. Beyond nine years of continuous subthalamic nucleus deep brain stimulation in Parkinson's disease. Mov Disord. **2011**; 26:2327-34.

Publications on international ISI journals

Alberio T, Pippione AC, Comi C, Olgiati S, Cecconi D, Lopiano L, Fasano M. Dopaminergic therapies modulate the T-cell proteome of patients with Parkinson's disease. IUBMB Life. **2012**; 64:846-52.

Alberio T, Pippione AC, Zibetti M, Olgiati S, Cecconi D, Comi C, Lopiano L, Fasano M. Discovery and verification of panels of T-lymphocyte proteins as biomarkers of Parkinson's disease. Sci. Rep. **2012;** 2:953; DOI:10.1038/srep00953.